

RANK-L EXPRESSION IN *STAPHYLOCOCCUS AUREUS*-INDUCED
OSTEOMYELITIS, THERAPEUTIC INTERVENTION USING
NANOTECHNOLOGY AND USE OF UV-KILLED BACTERIA AS AN
OSTEOCONDUCTIVE COATING FOR BIOMATERIALS

by

Shankari Narasimha Somayaji

A dissertation submitted to the faculty of
The University of North Carolina at Charlotte
in partial fulfillment of the requirements
for the degree of Doctor of Philosophy in
Biology

Charlotte

2009

Approved by:

Dr. Michael C. Hudson

Dr. Kenneth L. Bost

Dr. Ian Marriott

Dr. Laura W. Schrum

Dr. Yvette M. Huet

Dr. Craig A. Ogle

ABSTRACT

SHANKARI NARASIMHA SOMAYAJI. RANK-L expression in *Staphylococcus aureus*- induced osteomyelitis, therapeutic intervention using nanotechnology and use of UV-killed bacteria as an osteoconductive coating for biomaterials. (Under the direction of DR. MICHAEL C. HUDSON)

Staphylococcus aureus is responsible for approximately 80% of all cases of human osteomyelitis. RANK-L is an essential signal produced by osteoblasts and is required for full osteoclastic differentiation. PGE₂ - induced bone resorption involves both inducible cyclooxygenase (COX-2), as well as RANK-L. Our studies show that during infection with *S. aureus*, osteoblasts increase RANK-L and PGE₂ secretion. Through the use of NS-398, a specific COX-2 inhibitor, we show that when PGE₂ production is inhibited, RANK-L production is decreased. In the current study, we also demonstrate that effective killing of intracellular *S. aureus* is possible by treating the infected osteoblasts with nanoparticles loaded with nafcillin antibiotic.

While titanium alloys are the preferred material of choice for orthopaedic implants, they do not mediate osseointegration (intimate apposition of bone to the implant surface). Enhancement of titanium (Ti) based biomaterials is therefore necessary to increase the functional lifespan of an implant. *S. aureus* can bind to biomaterials directly and also attach efficiently to osteoblasts. Moreover, as UV-killed *S. aureus* does not stimulate immune modulator expression, we investigated whether UV-killed bacteria could serve as a novel osteoconductive coating on Ti alloy surfaces. Our in vitro data demonstrate that osteoblast adhesion and matrix synthesis was enhanced on Ti surfaces coated with bacteria compared to uncoated surfaces. In vivo, the osteoconductivity of *S. aureus*-coated implants was increased at 8 weeks compared to the uncoated implants.

ACKNOWLEDGMENTS

First, I would like to acknowledge my advisor, Dr. Michael Hudson for his patience, guidance and support throughout my graduate career. I appreciate the opportunity he has provided me as a member of his research lab. I would also like to thank members of my Committee; Dr. Kenneth Bost, Dr. Ian Marriott, Dr. Laura Schrum, Dr. Yvette Huet and Dr. Craig Ogle for their constant encouragement and valuable suggestions towards the project. I am extremely grateful to Dr. Yvette Huet for performing my animal surgeries with great care and expertise. I am indebted to Dr. Helen Gruber at Carolinas Medical Center for graciously offering the use of her lab resources and for taking the time and effort to help me interpret the in vivo data. Many thanks are due to members of her lab, Jane Ingram and Natalia Zinchenko for their assistance in bone histology studies. I am immensely grateful to members of the electron microscopy lab at Carolinas Medical Center; Daisy Ridings, Pat McCoy, David Radoff for generously helping me out with transmission electron microscopy analysis. I also acknowledge Dr. Kent Ellington for help in designing the animal model for in vivo implant studies. I am grateful to the following people who helped me with various aspects of this dissertation: John Hudak for biomaterial preparation, Cynthia Petty for typhoon analysis, Dr. Alyssa Gullledge for animal perfusion, David Gray for confocal microscopy, and Bob Riffie for donating the implant material. I thank Dr. Kenneth Gonsalves and members of his lab for their collaboration with the nanoparticle studies. Members of Hudson lab, Jay and Tasha, provided an affable lab environment and gave me pleasant company during the unpleasant task of bone harvesting and sectioning. I also appreciate the members of Marriott and Bost lab who were generous in sharing their lab resources. Finally, I would

like to thank the National Institutes of Health for providing the necessary funds for my research.

I could not have completed this body of work without the support of my family and friends. I am especially grateful to Vinita, Anusha, Namrata and Sameer who have cheered me often and have fed me generously on many occasions. I would like to dedicate this work to my parents who have supported me unconditionally in all my endeavours. I thank my husband, Rama, for his love, support and understanding through the years despite my occasional crankiness! I am extremely fortunate to have sisters, brothers & sisters-in-law and nieces who have comforted and humored me often.

INTRODUCTION

Staphylococcus aureus is a gram-positive bacterium that causes serious community-acquired and nosocomial infections (33). The range of disease caused by *S. aureus* is broad and includes septic shock, skin infections, endocarditis and osteomyelitis (3). *S. aureus* is the most common nosocomial pathogen encountered in the United States and the incidence of nosocomial *S. aureus*-induced disease has increased dramatically in recent years (3, 6, 22). Diseases caused by antibiotic-resistant strains of *S. aureus* are a worldwide epidemic and are necessitating the development of novel therapies for their treatment (4, 33). Once considered an extracellular pathogen, recent evidence, both in vitro and in vivo, indicates that *S. aureus* has the ability to invade osteoblasts and persist intracellularly, therefore escaping host humoral immune responses (3, 33). Additional studies have shown that *S. aureus*, once internalized, can escape the host endosome and gain access to the cytoplasm (8). The persistence of intracellular *S. aureus* is the first indication that the survival of these bacteria inside the osteoblasts could be involved in bone infection.

Staphylococcus aureus and osteomyelitis.

S. aureus is responsible for approximately 80% of all osteomyelitis cases (50). Osteomyelitis is an infection of bone that results from hematogenous seeding, spread of infection from a contiguous area such as the skin adjacent to the wound, or surgical or traumatic inoculation of bacteria into bone (26). The disease can be acute or chronic with sporadic recurrence (3, 59). The current treatment for osteomyelitis is often traumatic, expensive, and leads to further selection of antibiotic-resistant strains of *S. aureus*. In many cases it is necessary that infected bone is debrided, tissues are reconstructed and

long-term antibiotic therapy is used (59). The pathogenesis of *S. aureus*-induced osteomyelitis is poorly understood. Elucidating the mechanisms by which *S. aureus* induces osteomyelitis could lead to a better understanding of the disease, its progression, and development of new treatments.

Role of MSCRAMMs in mediating cell adherence and internalization.

Staphylococcus aureus is an extremely capable bone pathogen and is a common cause of bone and joint infections in humans because it possesses several cell-surface adhesion molecules that facilitate its binding to bone matrix. Binding involves a family of adhesins that interact with extracellular matrix components and these adhesins have been termed microbial surface components recognizing adhesive matrix molecules (MSCRAMMs). MSCRAMMs recognizing proteins such as collagen, bone sialoprotein, fibronectin, and fibrinogen mediate adherence of *S. aureus* to bone and biomaterials coated with host proteins (39). *S. aureus* can bind to cells either directly by utilizing MSCRAMMs or via bridging ligands, proteins which have affinity for both host cell receptors and MSCRAMMs (24, 62). Amongst all MSCRAMMs, Fibronectin-binding proteins (FnBPs) are critically important for adherence and invasion of *S. aureus* of osteoblasts. A bridging model has been proposed to explain interaction of *S. aureus* with osteoblasts where fibronectin is bound by FnBPs as well as host cell integrins. Integrins are $\alpha\beta$ -heterodimeric cell membrane receptors which mediate adhesion between cells and components of extracellular matrix which is subsequently known to induce signal transduction, tyrosine kinase activity, and cytoskeletal rearrangement (23, 24). Specifically, distinct peptide sequences such as Arg-Gly-Asp motif (RGD) from adhesive proteins interact with integrin cell membrane receptors (30). At least six bone- related

proteins; fibronectin, bone sialoprotein, collagen, osteopontin, thrombospondin and vitronectin are known to contain the RGD adhesive sequence (60). $\alpha_5\beta_1$ integrin, the most predominant integrin found on osteoblasts, binds to Fibronectin (Fn) with high specificity while $\alpha_2\beta_1$ integrin binds to collagen and laminin in addition to binding to Fn (18).

Bone remodeling and regulatory factors involved in the process.

Skeletal structure is continually adapting to metabolic and mechanical demands (79). Bone remodeling is a continuous, coordinated equilibrium between bone synthesis and bone resorption (71), and two principal cell populations are responsible for the continual process. Osteoclasts derive from myeloid precursors and drive the resorption of bone by acidification and release of lysosomal enzymes. Conversely, osteoblasts derive from a mesenchymal bone marrow precursor and produce components of bone, principally type I collagen. Osteoblasts also catalyze the calcification process and produce factors which serve to modulate the activity or formation of osteoclasts (11). Perturbations in inflammatory cytokines, growth factors, and hormones cause an imbalance between osteoblast and osteoclasts activities and result in skeletal abnormalities such as decreased bone mineral density, reduced bone strength, fractures, hypercalcemia, osteopetrosis, and osteoporosis (9, 78).

Receptor Activator of NF- κ B Ligand: Recent studies have revealed key molecules involved in the communication between osteoblasts and osteoclasts. Receptor Activator of NF- κ B Ligand (RANK-L) is a transmembrane molecule belonging to the TNF ligand superfamily that is expressed in lymphoid tissue and trabecular bone (56). Murine RANK-L is a 316 amino acid, 45kDa protein that shares 83% sequence homology with human RANK-L. The protein contains a ligand-binding region in its C-terminal half, and

has a transmembrane domain. It has also been proposed that RANK-L can be cleaved into a soluble form. Binding of RANK-L to RANK, found on osteoclasts, triggers intricate and distinct signaling cascades that control lineage commitment and activation of osteoclasts (78). RANK-L is thought to be the essential and final common signal required both in vitro and in vivo for full osteoclastic differentiation from multipotential hematopoietic precursor cells into mature multi-nucleated bone-resorptive osteoclasts (43, 44).

Osteoprotegerin and Tumor Necrosis Factor-Related Apoptosis-Inducing Ligand:

Osteoprotegerin (OPG), produced and secreted by osteoblasts, is a negative regulator of osteoclast formation (64, 83). OPG is a member of the TNF receptor superfamily and is secreted as a disulfide-linked 110 kDa homodimer (47, 64, 77). The expression of OPG is positively (e.g. TGF β , IL-1, TNF, estrogen) and negatively (e.g. PGE₂ and glucocorticoids) regulated by a wide array of factors. OPG represents an endogenous receptor antagonist that can bind to RANK-L and neutralize the biologic effects of RANK-L. Tumor Necrosis Factor-Related Apoptosis-Inducing Ligand [TRAIL] (64), is another key molecule produced by osteoblasts. Alexander et al demonstrated that when osteoblasts are infected with *S. aureus*, TRAIL expression is increased (2). TRAIL has numerous receptors including, R1, R2, R3, R4, and OPG. Since TRAIL expression is increased by *S. aureus*-infected osteoblasts and OPG is known to bind both TRAIL and RANK-L, competition may limit the amount of OPG available to block the interaction between RANK-L and RANK during infection of osteoblasts by *S. aureus*.

Okahashi et al demonstrated that normal mouse osteoblasts infected with *Streptococcus pyogenes* increase expression of RANK-L mRNA and protein (56). These

data indicate that when challenged with intracellular bacteria, osteoblasts increase RANK-L expression, suggesting one possible mechanism whereby *S. aureus*-infected bone tissue undergoes altered remodeling. **We therefore hypothesize that RANK-L mRNA and protein expression is induced during normal mouse osteoblast infection with *S. aureus* at increasing Multiplicities of Infection (MOI) and at various time points.**

Role of prostaglandin E₂ in RANK-L production: RANK-L expression in osteoblasts is up-regulated by pro-resorptive hormones and cytokines, such as $1\alpha, 25\text{-dihydroxyvitamin D}_3$ ($1\alpha, 25(\text{OH})_2\text{D}_3$), parathyroid hormone (PTH), prostaglandin E₂ (PGE₂), and interleukin (IL)-1 (37, 38, 80, 83). Prostaglandin E₂ (PGE₂) is produced in bone mainly by osteoblasts and acts as a potent stimulator of bone resorption (58, 61, 70). It has also been reported that PGE₂ induces osteoclast formation in mouse bone marrow cultures and stimulated bone resorption in mouse calvarial cultures (1, 15, 73). PGE₂ synthesis is regulated by three metabolic steps: the release of arachidonic acid from the membranous phospholipids by phospholipase A₂ (PLA₂), the conversion of arachidonic acid to PGH₂ by cyclooxygenase (COX), and the synthesis of PGE₂ by PGE synthase (16, 41, 46, 54, 63, 65, 75). Although both constitutive COX (COX-1) and inducible COX (COX-2) are expressed in mouse osteoblasts, the expression of COX-2 is markedly induced by several bone-resorbing factors such as IL-1 and IL-6. Bost et al. (13, 25) reported that *S. aureus* infection induces IL-6 and IL-12 production by osteoblasts. Stimulation of RANK-L, IL-6, and IL-12, are important events in bone destruction (43-45, 70, 74, 76). IL-6 can directly or indirectly modulate the activity of bone-resorptive osteoclasts (42, 69),

possibly through the induction of PGE₂, and in turn RANK-L. The addition of NS-398, a selective inhibitor of COX-2, was shown to inhibit IL-1-induced PGE₂ synthesis (15, 73).

Since it has been determined that PGE₂ can up-regulate RANK-L (37, 38, 80, 83), we propose that PGE₂ production by *S. aureus*-infected osteoblasts will be increased and that inhibition of PGE₂ by the specific COX-2 inhibitor, NS-398 will result in decreased levels of PGE₂ and RANK-L by infected osteoblasts. Based on the results of these proposed studies, agents that inhibit COX-2 or block RANK-L production could potentially ameliorate bone loss.

Treatment of osteomyelitis.

Surgical intervention as well as antibiotic therapy using cephalosporins and penicillins remains the most effective means of treatment for this disease (51). However, osteomyelitis cases caused by *S. aureus* are especially chronic in nature and recalcitrant to therapy. In addition, the effectiveness of traditional antibacterial agents is becoming increasingly limited as the prevalence of methicillin-resistant *S. aureus* (MRSA), has increased sharply in recent years. The wide array of virulence factors in *S. aureus*, including secreted products for host damage and immune avoidance, coupled with its ability to invade and reside inside osteoblasts using cell surface adherence factors, can protect these bacteria from host defence mechanisms and antibiotics which can account for the persistence of disease despite what may be considered adequate surgical and antibiotic management (19).

Poly (lactide-co-glycolide) (PLGA) based nanoparticles for antibiotic delivery: The biodegradability and biocompatibility of polymers such as poly (lactic acid) (PLA), poly (lactide-co-glycolide) (PLGA), and polyanhydrides (PAH) as well as their use as drug

delivery systems have been clearly demonstrated (28, 29, 66, 67). One of the advantages of these systems for drug delivery is reduction in systemic complications and allergic reactions due to the feasibility of delivering the drug locally (14). In addition, no follow-up surgical interference is required once the drug supply is depleted (53). Lastly, biodegradation occurs by simple hydrolysis of the ester backbone in aqueous environments such as body fluids and the degradation products are then metabolized to carbon dioxide and water. **We propose to use biodegradable polymer nanoparticles loaded with nafcillin that can penetrate osteoblasts infected with *S. aureus* and deliver the antibiotic intracellularly.** Nafcillin is an amphiphillic penicillin (32) which can effectively kill *S. aureus* but cannot enter eukaryotic cells in its native form. A novel approach of using polymer nanoparticles loaded with an antibiotic would ensure that these particles diffuse across the osteoblast cell membrane thereby effectively delivering the drug that can target both intracellular and extracellular bacteria. In addition, the drug can be delivered topically rather than systemically which would reduce the emergence of antibiotic resistant strains.

Composition of bone.

Bone is an anisotropic and dynamic tissue consisting of cells (osteoblasts and osteoclasts), connective tissue (primarily type 1 collagen), and minerals (hydroxyapatite). Osteoblasts form a bone matrix (the osteoid) that later becomes mineralized. The extracellular matrix (ECM) secreted by osteoblasts is approximately 90% collagen and 10% non-collagenic proteins such as osteocalcin, osteonectin, sialoproteins, proteoglycans, osteopontin, and fibronectin (68). These extracellular matrix proteins can contribute to both bone formation and homeostasis. For instance, fibronectin is important

for cell attachment whereas osteocalcin and osteopontin serve as foci for deposition of mineral component. Successful communication between cells and the ECM is mediated by the family of cell surface receptors called integrins that stimulate signal transduction pathways and mediate osteoblast adhesion, spreading, cell differentiation and bone morphogenesis (31, 34, 57). Specifically, integrin activation induces expression of osteoblast specific transcripts such as osteocalcin and type I collagen and is required for differentiation of osteoblast precursors (82).

Bone-associated biomaterials and osseointegration.

Artificial joints and orthopedic implants are used to repair or restore function to damaged and diseased tissue. Following insertion, the host response to implants involves a series of events, both at a cellular and molecular level, which ideally should result in osseointegration. Osseointegration is desirable because it represents formation of an appropriate interface and provides a functional connection between the implant and bone (5). Of the various implant materials, titanium (Ti) and cobalt-chromium (Co-Cr) alloys as well as bioactive ceramics such as calcium phosphate, principally hydroxyapatite, and bioglass are most commonly used (49). However, Titanium alloys such as Ti-6Al-4V are the preferred material of choice for orthopedic applications as it offers excellent biocompatibility on account of the interaction of its spontaneously formed oxide layer with the biologic fluids, resistance to corrosion and excellent mechanical properties (52). However, a major disadvantage of titanium alloys as a biomaterial is that they are relatively bio-inert and do not facilitate or mediate osseointegration which is intimate apposition of bone to the implant surface (20). As a result, the functional lifespan of artificial prostheses is estimated at about 15 years which makes them unsuitable for

active and younger patients (52). Enhancement of biomaterials is therefore necessary in order to increase the implant success rate and extend their functional lifespan.

Modification of implant surfaces to enhance osseointegration.

A number of techniques have been employed to enhance such biomaterials, including alteration of surface roughness, wettability, porosity, and hydrophobicity in an attempt to enhance osseointegration and mediate proper interface formation (5, 52, 81). Some of these strategies include modulating the implant surface by applying coatings of either extracellular matrix (ECM) components such as fibronectin, collagen, hydroxyapatite (HAP), bone sialoprotein (BSP) or cell adhesion peptides; Arg-Gly-Asp (RGD) or osteotropic growth factors such as Bone morphogenetic proteins; BMPs and Transforming growth factor-beta; TGF- β (17, 21, 27, 48, 55). However, there are still long-term complications and limitations associated with these methods such as high temperatures needed for coating in case of HAP which in turn alter both mineral as well as metal structure, variable thickness of deposited coatings and their subsequent dissolution from the substrates (7, 10, 27, 72). In addition, short half-life of osteoinductive growth factors along with their high concentrations locally can cause ectopic bone formation which is concerning in their applications. Lastly, while the coating treatments enhanced binding of osteoblasts to implant surfaces, cellular functions of osteoblasts failed to increase subsequently.

Binding of *S. aureus* to biomaterials.

For the clinical success of implants, anchorage-dependent cells such as osteoblasts must first successfully adhere to the implant surface in order to perform subsequent cellular functions such as proliferation and deposition of a mineralized

extracellular matrix (ECM) (5). In this context, it has been shown extensively that *S. aureus* can bind to biomaterials directly (35, 36). Following insertion, bacteria adhere to biomaterials coated immediately with host plasma constituents including fibronectin and fibrinogen and this adherence is mediated by MSCRAMMs, particularly FnBPs (39). As described earlier, *S. aureus*, both live and UV-killed, can also bind efficiently to osteoblasts and then induce signal transduction, tyrosine kinase activity, and cytoskeletal rearrangement (23, 24, 40). Lastly, while viable *S. aureus* cells are potent inducers of immune modulator expression by osteoblasts such as interleukin (IL)-6, IL-12 and monocyte chemoattractant protein (MCP-1), UV-killed *S. aureus* does not induce significant expression of such molecules (11-13). All of the above present an intriguing combination of properties that can be utilized in a novel coating of implant materials which can solicit osteoblast adhesion specifically around an implant. Potentially, an increase in osteoblast recruitment, a necessary pre-requisite for subsequent cell functions on biomaterials, can result in enhanced synthesis of an extracellular matrix on bone-biomaterial interface which can lead to enhanced osseointegration. **Therefore, as UV-killed *S. aureus* can tenaciously bind biomaterials and effectively colonize bone which can initiate cell-signaling cascades that can potentiate osteogenesis, we propose to examine the use of *S. aureus* as an effective osteoconductive coating for bone-associated biomaterials.**

In summary, the current study investigates the expression of RANK-L and PGE₂ by *S. aureus*- infected osteoblasts and also evaluates the therapeutic use of nafcillin-loaded nanoparticles in targeting both intracellular and extracellular bacteria in an in vitro model of osteomyelitis. We also examined the use of UV-killed *S. aureus* as a bioactive

coating for implants both in vitro and in vivo. The dissertation is divided into four sections with one section dedicated to the data relevant to each corresponding objective as described above. Each section is in turn comprised of an introduction, materials and methods, results, and discussion chapter. A summary section on the entirety of this research is presented at the end of the dissertation.

TABLE OF CONTENTS

PROJECT I: RANK-L EXPRESSION IN *STAPHYLOCOCCUS AUREUS*-
INDUCED OSTEOMYELITIS

CHAPTER 1: INTRODUCTION	1
CHAPTER 2: MATERIALS AND METHODS	4
CHAPTER 3: RESULTS	9
CHAPTER 4: DISCUSSION	12
FIGURES	17

PROJECT II: THERAPEUTIC INTERVENTION USING
NANOTECHNOLOGY

CHAPTER 5: INTRODUCTION	22
CHAPTER 6: MATERIALS AND METHODS	25
CHAPTER 7: RESULTS	32
CHAPTER 8: DISCUSSION	34
FIGURES	38

PROJECT III: IN VITRO USE OF UV-KILLED BACTERIA AS AN
OSTEOCONDUCTIVE COATING FOR BIOMATERIALS

CHAPTER 9: INTRODUCTION	42
CHAPTER 10: MATERIALS AND METHODS	45
CHAPTER 11: RESULTS	52
CHAPTER 12: DISCUSSION	56
FIGURES	63

PROJECT IV: IN VIVO USE OF UV-KILLED BACTERIA AS AN
OSTEOCONDUCTIVE COATING FOR BIOMATERIALS

CHAPTER 13: INTRODUCTION	71
CHAPTER 14: MATERIALS AND METHODS	75
CHAPTER 15: RESULTS	83
CHAPTER 16: DISCUSSION	88
FIGURES	97
SUMMARY	105
REFERENCES	107

CHAPTER 1: INTRODUCTION

Osteomyelitis is a severe infection of bone tissue that results in progressive inflammatory destruction of bone (40). The gram-positive organism, *Staphylococcus aureus*, is the most common causative agent of osteomyelitis, accounting for approximately 80% of all human cases (25). It is often necessary that infected bone be debrided, tissues reconstructed and long-term antibiotic therapy utilized (17). The current treatment for osteomyelitis is often traumatic, expensive, and leads to further selection of antibiotic-resistant strains of *S. aureus*. The growing incidence of antibiotic-resistant *S. aureus* strains can explain the recurrent attacks of osteomyelitis in patients undergoing therapy. In addition, the pathogenesis of *S. aureus*-induced osteomyelitis is poorly understood. Elucidating the mechanisms by which *S. aureus* induces osteomyelitis could therefore lead to a better understanding of the disease, its progression, and development of new treatments.

Bone remodeling is a continuous, coordinated equilibrium between bone synthesis and bone resorption and two cell populations are responsible for the continual process (21). Osteoclasts drive the resorption of bone by acidification and release of lysosomal enzymes while osteoblasts produce components of the bone matrix, principally type I collagen. Osteoblasts also produce factors which serve to modulate the activity or formation of osteoclasts (1). One such key molecule produced by osteoblasts is receptor activator of NF- κ B ligand (RANK-L), which on binding to RANK, found on osteoclast

precursors, triggers intricate and distinct signaling cascades that control lineage commitment and activation of osteoclasts (52). RANK-L is therefore thought to be the essential and final common signal required both in vitro and in vivo for full osteoclastic differentiation from multipotential hematopoietic precursor cells into mature multinucleated bone-resorptive osteoclasts (22, 23). Thus, osteoblasts can regulate both net bone formation as well as resorption.

Prostaglandin E₂ (PGE₂) is produced in bone mainly by osteoblasts and acts as a potent stimulator of bone resorption by inducing osteoclast formation in both mouse bone marrow cultures and calvarial cultures (1, 7, 35, 39, 45, 47). PGE₂ synthesis is regulated by three metabolic steps: the release of arachidonic acid from the membranous phospholipids by phospholipase A₂ (PLA₂), the conversion of arachidonic acid to PGH₂ by cyclooxygenase (COX), and the synthesis of PGE₂ catalyzed by PGE synthase (9, 19, 24, 32, 41, 43, 49). Although both constitutive COX (COX-1) and inducible COX (COX-2) are expressed in mouse osteoblasts, the expression of COX-2 is markedly induced by several proinflammatory cytokines such as IL-6. Bost et al. (5, 11) have reported that *S. aureus*-infected osteoblasts produce high levels of IL-6 which have been shown to modulate the activity of bone-resorptive osteoclasts either directly or indirectly (20, 44). It has also been determined that PGE₂ can up-regulate RANK-L expression in osteoblasts (15, 16, 53, 56).

Bacterial pathogens can stimulate osteoclastogenesis which can potentiate bone resorption leading to bone destruction (29). Okahashi et al (34) have also demonstrated that normal mouse osteoblasts infected with *Streptococcus pyogenes* increase expression of RANK-L mRNA and protein. In addition, elevated levels of RANK-L have been

detected in the bone lesions of mandibular osteomyelitis (31). We therefore propose that following an intracellular challenge with *S. aureus*, osteoblasts can increase RANK-L expression which could stimulate osteoclast activity and thereby potentiate the bone loss that occurs in *S. aureus*-infected bone tissue. The current study investigates RANK-L mRNA and protein expression during normal mouse osteoblast infection with *S. aureus*. Such a proposed upregulation of RANK-L from infected osteoblasts could be mediated either directly or indirectly. Since it has been determined that PGE₂ can up-regulate RANK-L, we propose in the current study that PGE₂ production by *S. aureus*-infected osteoblasts will be increased and that inhibition of PGE₂ by the specific COX-2 inhibitor, NS-398 will result in decreased levels of PGE₂ and RANK-L by infected osteoblasts.

CHAPTER 2: MATERIALS AND METHODS

Bacterial strains:

Staphylococcus aureus strain UAMS-1 (ATCC 49230) is a human osteomyelitis clinical isolate (14). *Staphylococcus carnosus* (ATCC 51365) is a nonpathogenic species with reduced ability to invade osteoblasts (11). Strains N1, N2, N3, N4 and N5 are *Staphylococcus aureus* nasopharyngeal isolates kindly provided by Dr. Vance G. Fowler, Jr. (Duke University Medical Center).

Normal mouse osteoblast cell culture:

Primary osteoblasts were isolated from mouse neonatal calvariae by sequential digestion with collagenase and protease according to a method previously described for chick embryos (37). The periosteum were removed, the frontal bones were harvested free of the suture regions, and the bones were incubated for 10 min at 37°C in 10 ml of digestion medium containing collagenase (375 U/ml, type VII; Sigma Chemical Company, St. Louis, MO) and protease (7.5U/ml; Sigma). Cells released during an initial 7 min digestion were discarded. Ten milliliters of fresh digestion medium was added, and incubation continued for another 20 min. Cells were harvested by centrifugation and rinsed three times in 25 mM HEPES- buffered Hanks' balanced salt solution (pH 7.4; HBSS). The digestion step was repeated twice, and the three cell isolates were pooled in mouse osteoblast growth medium (OBGM) consisting of Dulbecco's modified eagle medium containing 25 mM HEPES, 10% fetal bovine serum (Atlanta Biologicals, GA), 2

g of sodium bicarbonate per liter, 75 mg of glycine/ml, 100 mg of ascorbic acid, 40 ng of vitamin B₁₂/ml, 2 mg of *p*-aminobenzoic acid/ml, 200 ng of biotin/ml, and penicillin (100 U/ml)-streptomycin (100 µg/ml)-amphotericin B (25 µg/ml) (pH 7.4) (36). Osteoblasts were seeded in six-well polystyrene dishes and incubated at 37°C in a 5% CO₂ atmosphere until they reached confluence (6-7 days).

Invasion assay:

The invasion assay with live or UV-killed *S. aureus* strain UAMS-1, live *S. carnosus*, or live nasopharyngeal isolates was performed as previously described (11, 12). Bacteria were grown overnight (16 h) in 5 ml of tryptic soy broth in a shaking water bath at 37°C. The bacteria were harvested by centrifugation for 10 min at 4,300 × *g* at 4°C and washed twice. The pellets were then resuspended in 5 ml of growth medium lacking antibiotics/antimycotics (Abx-Amx). Confluent cell layers of osteoblasts were washed three times to remove the growth medium. The cultures were then infected at a multiplicity of infection (MOI) of 25:1 or 75:1 with *S. aureus* strain UAMS-1, or with *S. carnosus*, UV-killed *S. aureus* or the nasopharyngeal isolates at a MOI of 25:1 in 4 ml of growth medium lacking Abx-Amx. Following a 45-minute infection period, infected cell cultures were washed three times and incubated for 1 h in growth medium containing 25 µg of gentamicin/ml to kill the remaining extracellular bacterial cells. The osteoblast cultures were washed and subsequently lysed at different time points by the addition of 1.2 ml of 0.1% Triton X-100 (Fisher Biotech, N.J.) with incubation for 5 min at 37°C.

Quantitative real-time polymerase chain reaction:

To quantify RANK-L mRNA, real-time PCR was performed using a Roche LightCycler 2.0 with SYBR Green reagent (QIAGEN, CA) according to the

manufacturer's instructions. Amplicons of RANK-L and G3PDH were used to develop a standard curve. Samples were subjected to 40 cycles of amplification consisting of 95°C for 15 s followed by 53°C for 20 s. Each assay was normalized to G3PDH mRNA. PCR primers were derived from published sequences (IDT, IA.) (34). Positive and negative strand primers were as follows:

RANK-L (89 bp)

5'-TACTTTTCGAGCGCAGATGGAT-3'

5'-ACCTGCGTTTTTCATGGAGTCT-3'

G3PDH (63 bp)

5'-AACTACATGGTCTACATGTTCCA-3'

5'-CCATTCTCGGCCTTGACTGT-3'

Protein isolation:

Osteoblasts were isolated and seeded at 10^6 cells per well in six-well plates and infected once the cells had reached confluence (6-8 days). Following a 45-minute incubation +/- bacteria and 1 hour treatment with 25 µg/ml gentamicin sulfate, total protein was isolated from the osteoblasts at 0, 6, and 24 hours using Tissue Protein Extraction Reagent (T-PER) (PIERCE, IL) with additional protease inhibitors, aprotinin (2 µg/ml) and lupeptin (2.5 µg/ml) (Sigma Chemical Company, MO). Two hundred µl of T-PER was added to each well at the appropriate time point and cells were removed from the culture plates with a cell scraper (Costar). Samples were collected in 1.5 ml microcentrifuge tubes and then centrifuged at 10,000 x g for 2 minutes to pellet cell debris. Supernatants were collected and placed in fresh tubes and stored at -80°C.

Inhibitor study:

Osteoblasts were isolated and cultured in six-well plates as previously described. Forty-eight hours prior to infection, cells were either treated with 0.025% dimethylsulfoxide (DMSO) or 20 μ M NS-398 (Cayman Chemicals, MI), a specific COX-2 inhibitor, dissolved in DMSO at an optimal dose that was previously determined to provide inhibition of COX-2 (6, 57). Following the 48 hour treatment, cells were rinsed one time with osteoblast growth medium (OBGM) containing no Gentamicin Sulfate or Amphotericin B. One ml of OBGM, containing no Gentamicin Sulfate or Amphotericin B and containing either DMSO or NS-398, was then added to each appropriate well. The osteoblasts were either uninfected (MOI 0) or were infected with the bacterial strains noted above using the method previously described. Following the 45-minute incubation +/- bacteria, each well was rinsed one time with OBGM. One ml of fresh media, containing either DMSO or NS-398 and 25 μ g/ml of Gentamicin, was then added to each well. Cells were then incubated for 1 hour at 37°C in a 5% CO₂ atmosphere to allow remaining extracellular bacteria to be killed. Following the 1 hour incubation period, protein samples were isolated as previously described (time 0). Samples were also isolated at 6 hours and 24 hours following time 0. In addition, culture supernatants were collected and stored at -80°C.

Quantification of RANK-L protein and prostaglandin E₂:

Using protein samples collected as previously described, mouse TRANCE/TNSF11/RANK ligand ELISA (R&D Systems, Minneapolis, MN) was used to detect the levels of RANK-L in osteoblast whole cell extracts. Prostaglandin E₂ correlate-

enzyme immunoassay (EIA) (Assay Designs, MI) was performed on the cell culture supernatants following the manufacturer's instructions.

Statistical analysis:

Data were analyzed using a two-way analysis of variance followed by the Tukey-Kramer multiple comparison analysis. Results are presented as the mean \pm standard error. For all tests $p < 0.05$ was considered significant.

CHAPTER 3: RESULTS

Induction of RANK-L mRNA expression in osteoblasts following exposure to bacteria:

Staphylococcal osteomyelitis is associated with increased osteoclast activity and RANK-L is a key factor required for osteoclastogenesis (22, 23, 45, 56). Therefore, it is important to determine whether osteoblasts infected with *S. aureus* produce RANK-L and if the levels of RANK-L increase in a time- and dose-dependent manner. Quantitative analysis by real-time RT-PCR demonstrated that the RANK-L expression in osteoblasts infected with *S. aureus* strain UAMS-1 (75:1 MOI) was tenfold greater than RANK-L expression in uninfected cells at 4 hours following infection (Figure 1). RANK-L mRNA expression by osteoblasts also increases in a dose-dependent manner. In addition, we show that there was a time-dependent increase in RANK-L mRNA in Figure 1 with the expression of RANK-L mRNA by infected cells being tenfold greater than the expression in the uninfected controls at 4 hours.

To confirm that the changes in RANK-L mRNA result in corresponding protein expression, cell associated RANK-L was measured by specific capture ELISA. As shown in Figure 2, there was a time- and dose-dependent response to *S. aureus* strain UAMS-1. At 24 hours and an MOI of 75:1, there was a 2.5 fold increase in RANK-L protein compared to the control. Although the documented effects of RANK-L have been shown to be mediated by the membrane-bound form, we also measured the levels of soluble

RANK-L as well and found its levels to be undetectable (data not shown). Osteoblasts infected with *S. carnosus* and UV-killed *S. aureus* strain UAMS-1 demonstrate the same levels of RANK-L protein expression as uninfected osteoblasts (Fig 2). Additionally, osteoblasts infected with *S. aureus* nasopharyngeal isolates N3 and N4 induce RANK-L production at levels similar to strain UAMS-1 at 0 hour. Strains N4 and N3 sustain this increased RANK-L expression following 6 and 24 hours of incubation, respectively.

Induction of prostaglandin E₂ expression by osteoblasts following exposure to S. aureus:

Choi et al (8) demonstrated that PGE₂ is a main mediator in RANK-L dependent osteoclastogenesis induced by several periodontal pathogens. Therefore, it is possible that RANK-L production in osteoblasts infected with *S. aureus* involves a PGE₂-dependent mechanism. The current study examined levels of PGE₂ following infection of osteoblasts by *S. aureus*. Figure 3 demonstrates that PGE₂ is up-regulated by *S. aureus* strain UAMS-1-infected osteoblasts at all time points examined. Although there is no significant difference between infection at the 25:1 and 75:1 MOI, there is a significant difference in PGE₂ expression between *S. aureus* strain UAMS-1-infected and uninfected osteoblasts. Figure 3 also shows that the increase in levels of PGE₂ occurs early following *S. aureus* infection and remains at an elevated level throughout the 24 hour duration of the experiment. PGE₂ expression in response to UV-killed *S. aureus* strain UAMS-1- or *S. carnosus*-infected osteoblasts is not significantly different than that observed from uninfected osteoblasts (Fig 3). Although *S. aureus* nasopharyngeal isolates N1-N5 significantly increase PGE₂ expression at time 0, PGE₂ levels following 6 and 24 hours of infection are comparable to uninfected osteoblasts.

Prostaglandin E₂ production mediates S. aureus-induced increases in RANK-L production by osteoblasts:

One of the steps in the PGE₂ synthesis pathway involves the conversion of arachidonic acid to PGH₂, which is then metabolized to PGE₂, by cyclooxygenase enzyme (COX). The addition of NS-398, a selective inhibitor of COX-2, inhibits IL-1-induced PGE₂ synthesis (7, 47). Therefore, in the current study, it is hypothesized that inhibition of COX-2 by NS-398 will result in decreased levels of PGE₂ production by *S. aureus*-infected osteoblasts. Figure 4 demonstrates that NS-398 significantly attenuates PGE₂ production in both uninfected and *S. aureus*-infected osteoblasts. Infected control cells treated with DMSO show the same dose-response to *S. aureus* strain UAMS-1 seen in Figure 3.

Since it is known that PGE₂ up-regulates RANK-L, we also examined the effects of NS-398 on RANK-L expression by *S. aureus*-infected osteoblasts. When infected osteoblasts were treated with NS-398, RANK-L levels were attenuated; indicating *S. aureus*-induced PGE₂ plays a role in RANK-L expression by infected cells (Figure 5).

CHAPTER 4: DISCUSSION

Osteomyelitis is a disease associated with abnormal bone remodeling and bone resorption. The mechanisms responsible for such bone loss are largely unclear. The generation of proinflammatory cytokines and chemokines helps recruit immune cells, such as leukocytes, which could alter the balance between bone resorption and formation. Recent studies in our lab have demonstrated *S. aureus*-infected osteoblasts as a hitherto unrecognized source of soluble immune modulators both in vivo and in vitro (3-5, 27, 28). Osteoblasts can also produce other soluble factors that can modulate the activity or formation of osteoclasts. RANK-L is one such key molecule that stimulates differentiation in osteoclasts and is an inducing agent involved in bone destruction (22, 23, 45, 48, 56). Following the binding of RANK-L to its receptor RANK on osteoclast precursors, the signal transduction can diverge into diverse pathways that can regulate distinct aspects of osteoclast functions (10, 17, 33, 38, 55).

Bacterial pathogens can stimulate osteoclastogenesis, either directly or indirectly, which can potentiate bone resorption leading to bone destruction (29, 34). Ishida et al have recently shown elevated RANK-L expression in *S. aureus*-infected NRG cells, which is a fibroblast cell line that has osteoblast like features (18). Based on these findings, we undertook this study to evaluate the production of RANK-L from *S. aureus*-infected primary osteoblasts. Results outlined in Figures 1-2 demonstrate that viable *S. aureus* strain UAMS-1 is a potent inducer of membrane-bound, and not secreted, RANK-

L mRNA and protein production by osteoblasts. In addition, UV-killed *S. aureus* strain UAMS-1 did not induce RANK-L expression, thus indicating that active bacterial gene expression may be required for maximal RANK-L production. Similarly, *S. carnosus*, an invasion-deficient species, did not stimulate increased RANK-L expression. Although osteoblasts infected with *S. aureus* nasopharyngeal isolates N3 and N4 induce RANK-L expression comparable to expression from osteoblasts infected with the osteomyelitis clinical isolate UAMS-1 at time 0, and the strains maintain induction at 6 hours in one case and at 24 hours in the other, it is possible that strains N3 and N4 are capable of inducing osteomyelitis if they gain access to the bloodstream and subsequently to bone. The majority of the nasopharyngeal isolates are not capable of inducing RANK-L production. Taken together, these findings substantiate that live *S. aureus* is required for maximal RANK-L production from infected osteoblasts. An increase in RANK-L production by infected osteoblasts can further osteoclast differentiation and activation which can potentiate the exacerbated bone destruction observed during osteomyelitis.

While RANK-L potentiates osteoclastogenesis, Osteoprotegerin (OPG), produced and secreted by osteoblasts, is a negative regulator of osteoclast formation. Tumor Necrosis Factor-Related Apoptosis-Inducing Ligand (TRAIL) (42), is another key molecule produced by osteoblasts which can bind to OPG. Alexander et al (2) have demonstrated that when osteoblasts are infected with *S. aureus*, TRAIL expression is increased. Since OPG is known to bind both TRAIL and RANK-L, competition may limit the amount of OPG available to block the interaction between RANK-L and RANK during infection of osteoblasts by *S. aureus*. Taken together, it is highly likely that the

increased levels of RANK-L contributes to the massive bone loss and aberrant bone remodeling associated with the pathology of staphylococcal osteomyelitis.

We next attempted to delineate the mechanism involved in up-regulation of RANK-L expression in osteoblasts following exposure to *S. aureus*. Prostaglandin E₂ (PGE₂) is produced in bone mainly by osteoblasts and acts as a potent stimulator of bone resorption (35, 39, 45). It has been demonstrated that PGE₂ can mediate RANK-L-dependent osteoclastogenesis in periodontal diseases (8). Furthermore, the production of PGE₂ by osteoblasts is regulated by several cytokines and is also reported to induce osteoclast formation in mouse bone marrow cultures and stimulate bone resorption in mouse calvarial cultures (1, 7, 47). We therefore hypothesized that increased RANK-L expression in infected osteoblasts occurs as a result of PGE₂ activation upstream in the RANK-L pathway. The current study demonstrates that live *S. aureus* strain UAMS-1 induces significant PGE₂ production in infected osteoblasts (Figure 3). However, UV-killed *S. aureus* strain UAMS-1 and *S. carnosus* do not induce PGE₂ production by osteoblasts. Osteoblasts infected with *S. aureus* nasopharyngeal isolates N1-N5 demonstrate increased PGE₂ expression initially and decreased expression subsequently comparable to uninfected osteoblasts. Increased and sustained levels of PGE₂ production are only induced by live osteomyelitis clinical isolate UAMS-1, indicating the strain is capable of potentiating the bone damage observed in osteomyelitis. These results along with the RANK-L data are consistent with our previous findings that live *S. aureus* strain UAMS-1 is more effective at eliciting immune modulator production by cultured osteoblasts compared to UV-killed bacteria or non-pathogenic species (3-5, 11).

The functions of PGE₂ in target cells are mediated by four different G protein-coupled receptor subtypes, EP1, EP2, EP3, and EP4 (26, 46). Among these PGE₂ receptor subtypes, EP4 is the main receptor expressed on osteoblasts and is responsible for mediating PGE₂-induced RANK-L expression by osteoblasts (13, 46, 51). In addition, PGE₂ synergistically promotes the differentiation of bone marrow macrophages into osteoclasts induced by RANK-L and M-CSF (50, 54). Thus, PGE₂ stimulates osteoclastic bone resorption through the following two different pathways: the induction of RANK-L expression in osteoblasts, and the direct enhancement of RANK-L induced differentiation of osteoclast precursor cells into osteoclasts. The mechanism of the synergistic effect of PGE₂ on the RANK-L-induced osteoclastic differentiation of precursor cells has not yet been explained (21).

PGE₂ synthesis is regulated by three metabolic steps: the release of arachidonic acid from the membranous phospholipids by phospholipase A₂ (PLA₂), the conversion of arachidonic acid to PGH₂ by cyclooxygenase (COX), and the synthesis of PGE₂ by PGE synthase (24, 32, 43). Both constitutive COX (COX-1) and inducible COX (COX-2) are expressed in mouse osteoblasts with COX-2 being markedly induced by several bone-resorbing, inflammatory factors, including IL-1 and IL-6 in osteoblasts (30, 46). To establish the role of COX-2 with respect to production of PGE₂ during infection of osteoblasts with *S. aureus*, we used NS-398 to inhibit COX-2 and examined its effect on PGE₂ expression. When osteoblasts were treated with NS-398, PGE₂ levels were significantly attenuated in both un-infected and *S. aureus*-infected osteoblasts (Figure 4). These results indicate that COX-2 is important in the regulation of PGE₂ production during *S. aureus* infection of osteoblasts.

We next examined the effects of NS-398 on the production of RANK-L. Although NS-398 significantly reduced the RANK-L produced by *S. aureus*-infected osteoblasts, levels of RANK-L still remained detectable and were still responsive to *S. aureus* infection (Figure 5). These data suggest that COX-2 and PGE₂ play a significant role in potentiating RANK-L production by *S. aureus*-infected osteoblasts.

The increasing incidence in bacterial infections caused by *S. aureus*, and the emergence of antibiotic-resistant strains of this organism has made it imperative that we understand the mechanisms of initiation and maintenance of inflammation, as well as bone loss observed in sites of infection in order to develop safe and effective therapies. Data presented here clearly outline a mechanism by which RANK-L, an essential factor for osteoclastogenesis, is up-regulated by *S. aureus* strain UAMS-1-infected osteoblasts, further substantiating the role that osteoblasts may have in the aberrant bone remodeling observed in staphylococcal osteomyelitis. In addition, this up-regulation of RANK-L appears to involve a COX-2 mediated PGE₂-dependent pathway. Potentially, agents that inhibit COX-2 or block RANK-L production could ameliorate bone loss. Further studies are warranted to investigate the in vivo significance of RANK-L in *S. aureus*-induced osteomyelitis.

FIGURES

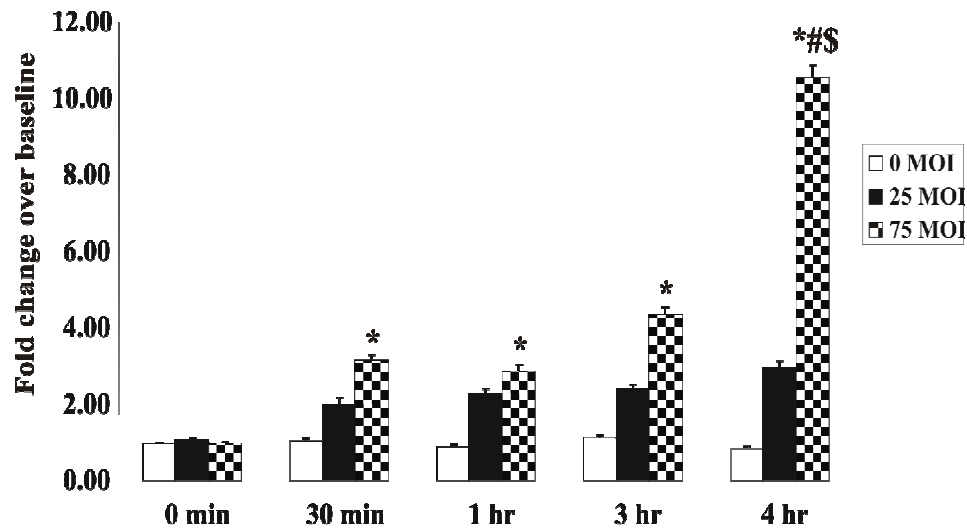


Figure 1. Expression of RANK-L mRNA by osteoblasts. Primary mouse osteoblasts were either uninfected (MOI 0) or were infected with *S. aureus* strain UAMS-1 (MOI 25:1 or 75:1). Following a 45-minute incubation +/- bacteria (time 0 hours), total RNA was extracted at various time points and subjected to Quantitative Real-time RT-PCR analysis for RANK-L mRNA. All values were normalized to G3PDH and are expressed in fold change over baseline (0 hours, 0 MOI). Data are expressed as the means \pm SEM of three separate osteoblast cultures. *, $P < 0.05$ versus 75:1 MOI at 0 min; #, $P < 0.05$ versus 0 MOI at time 0 min; \$, $P < 0.05$ versus 25:1 at 4hrs.

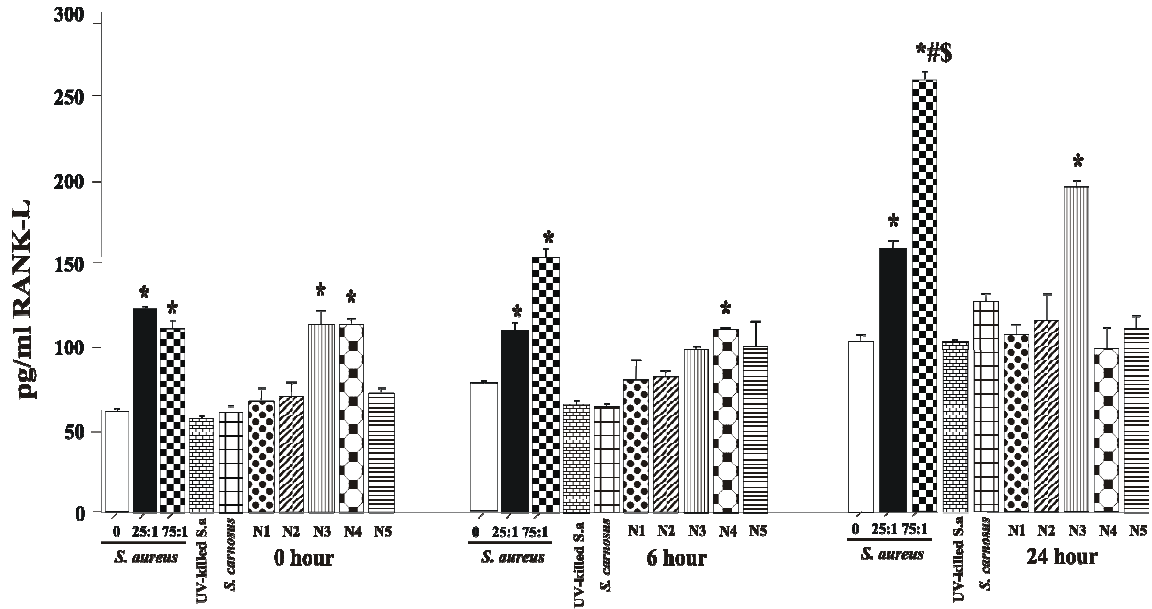


Figure 2. Expression of RANK-L protein by osteoblasts. Primary mouse osteoblasts were either uninfected (MOI 0) or were infected with either *S. aureus* strain UAMS-1 (MOI 25:1 or 75:1), UV-killed strain UAMS-1 (MOI 25:1), *S. carnosus* (MOI 25:1) or with *S. aureus* nasopharyngeal isolates N1, N2, N3, N4 and N5 (MOI 25:1). Following a 45-minute incubation +/- bacteria and 1 hour treatment with 25 µg/ml Gentamicin Sulfate, whole cell extracts were taken at time 0 hours, 6 hours, and 24 hours. RANK-L concentrations were determined by an ELISA and the results are displayed in pg/ml. Data are expressed as the means \pm SEM of three separate osteoblast cultures. *, $P < 0.05$ versus 0 MOI at all time points; #, $P < 0.05$ versus 75:1 MOI at 0h and 6h; \$, $P < 0.05$ versus 25:1 at 6h and 24h.

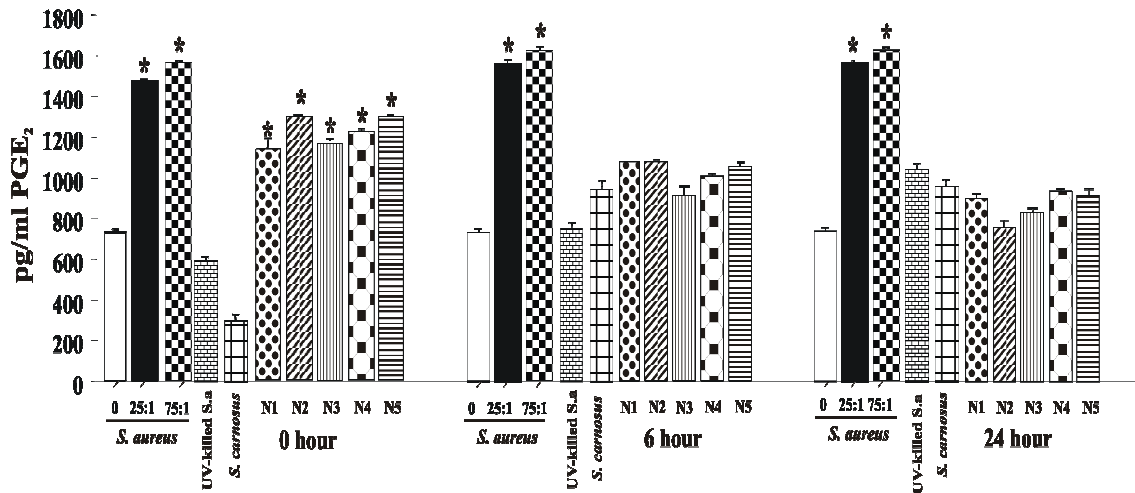


Figure 3. Expression of Prostaglandin E₂ by osteoblasts. Primary mouse osteoblasts were either uninfected (MOI 0) or were infected with either *S. aureus* strain UAMS-1 (MOI 25:1 or 75:1), UV-killed strain UAMS-1 (MOI 25:1), *S. carnosus* (MOI 25:1) or with *S. aureus* nasopharyngeal isolates N1, N2, N3, N4 and N5 (MOI 25:1). Following a 45-minute incubation +/- bacteria and 1 hour treatment with 25µg/ml Gentamicin Sulfate, supernatants were collected at time 0 hours, 6 hours, and 24 hours. Prostaglandin E₂ concentrations were determined by an EIA and are expressed in pg/ml. Data are expressed as the means ± SEM of three separate osteoblast cultures. *, P < 0.05 versus 0 MOI at 0, 6h, and 24h.

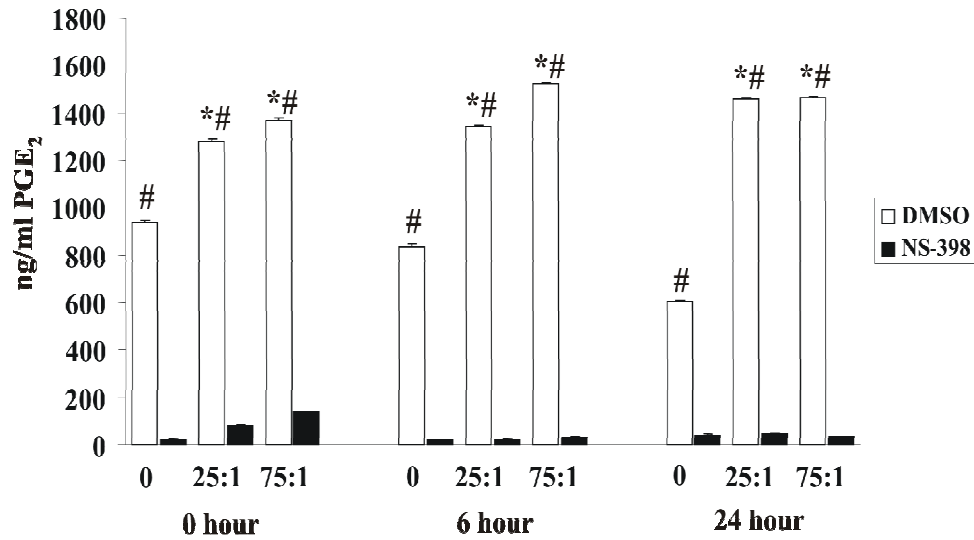


Figure 4. Expression of Prostaglandin E₂ and the Effects of NS-398. Primary mouse osteoblasts were cultured in the presence of 0.025% DMSO or 20 μ M NS-398 in DMSO, 48 hours prior to infection. Osteoblasts were either uninfected (MOI 0) or were infected with *S. aureus* strain UAMS-1 (MOI 25:1, or 75:1). Following a 45-minute incubation +/- bacteria and 1 hour treatment with 25 μ g/ml Gentamicin Sulfate, supernatants were collected at time 0 hours, 6 hours and 24 hours. Prostaglandin E₂ concentrations were determined by an EIA and are expressed in ng/ml. Data are expressed as the means \pm SEM of three separate osteoblast cultures. *, $P < 0.05$ versus 0 MOI treated with DMSO; #, $P < 0.05$ versus all groups treated with NS-398 at all time points.

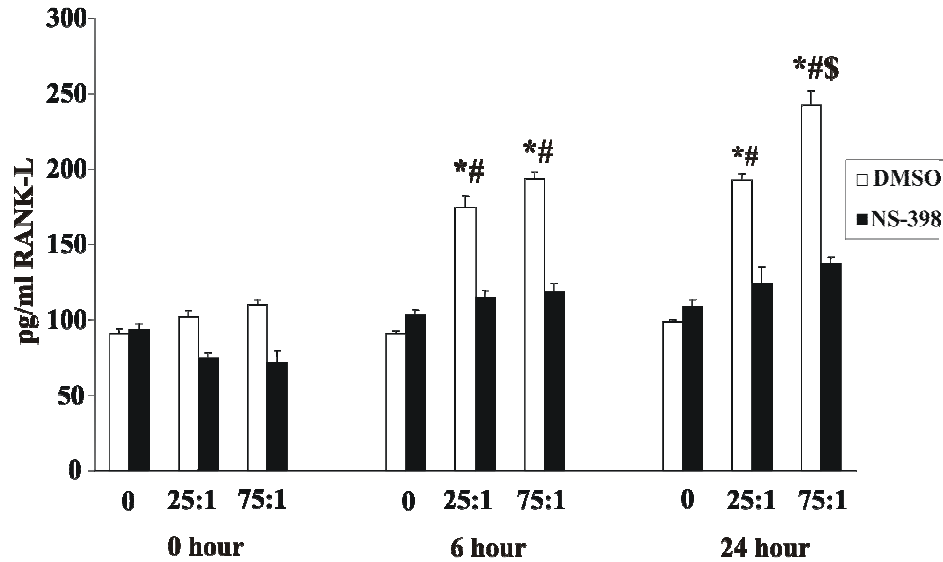


Figure 5. Expression of RANK-L and the Effects of NS-398. Primary mouse osteoblasts were cultured in the presence of 0.025% DMSO or 20 μ M NS-398 in DMSO, 48 hours prior to infection. Osteoblasts were either uninfected (MOI 0) or were infected with *S. aureus* strain UAMS-1 (MOI 25:1, or 75:1). Following a 45-minute incubation +/- bacteria and 1 hour treatment with 25 μ g/ml Gentamicin Sulfate, whole cell extracts were collected at time 0 hours, 6 hours and 24 hours. RANK-L concentrations were determined by an ELISA and are expressed in pg/ml. Data are expressed as the means \pm SEM of three separate osteoblast cultures. *, $P < 0.05$ versus 0 MOI treated with DMSO at 0h, 6h, and 24h; #, $P < 0.05$ versus all groups treated with NS-398 at all time points; \$, $P < 0.05$ versus 25:1 MOI at 24h.

CHAPTER 5: INTRODUCTION

Osteomyelitis is a severe infection of bone tissue that results in progressive inflammatory destruction of bone. It is often necessary that infected bone be debrided, tissues reconstructed, and long-term antibiotic therapy utilized. The gram-positive organism *Staphylococcus aureus* is the most common causative agent of osteomyelitis, accounting for approximately 80% of all human cases (8). These bacteria are characterized by their high affinity to bone, rapid induction of osteonecrosis (bone death) and resorption of bone matrix (20). While *S. aureus* is generally considered to be an extracellular pathogen, previous studies from our lab have demonstrated that *S. aureus* has the ability to adhere to and persist within osteoblasts (bone-forming cells) (1, 9, 14). The ability of *S. aureus* to invade and survive within osteoblasts is critical to the observation that greater than 80% of all cases of chronic osteomyelitis are caused by *S. aureus*. Therefore, it is possible that the ability of bacteria to persist intracellularly offers the bacteria a route to evade antibiotic treatment, which could subsequently lead to recurrent infections.

Biodegradable biocompatible polymer nanoparticles are effective drug delivery systems (35, 36). The biodegradability and biocompatibility of poly (lactic acid) PLA and poly(lactide-co-glycolide) PLGA has been well documented (10, 11). One of the advantages of these systems for drug delivery is reduction in systemic complications and allergic reactions due to the feasibility of delivering the drug locally (6). In addition, no

follow-up surgical interference is required once the drug supply is depleted (21). Lastly, biodegradation occurs by simple hydrolysis of the ester backbone in aqueous environments such as body fluids and the degradation products are then metabolized to carbon dioxide and water. Biodegradation of these polymers offers potential use in drug delivery, either as drug delivery systems alone or in combination with other medical devices. Drug (the active agent) can be incorporated within the polymer matrix (the carrier), which later degrades in the body releasing the drug in a controlled way (22). Some controlled release devices include microspheres (5, 24), rods (28), films (19) and nanoparticles (18). Several techniques such as single emulsion-solvent evaporation technique have been developed to prepare nanoparticles loaded with a broad variety of drugs using PLGA (3, 12, 17, 32).

The goal of this study was to develop PLGA based nanoparticles for the delivery of antibiotics such as nafcillin, an amphiphilic penicillin (13), to intracellular bacteria inside osteoblasts. Polyvinyl alcohol (PVA) was used as a copolymer because nanoparticles using this emulsifier are relatively uniform and smaller in size, and are easy to redisperse in aqueous medium (26). As proof of concept, PLGA nanoparticles were first linked to quantum dots to model the diffusion of antibiotic-nanoparticles into osteoblasts and subsequently loaded with nafcillin to evaluate the viability of intracellular *S. aureus* inside infected osteoblasts.

Quantum dots (QDs) are a new class of fluorophores excitable over a broad wavelength range stretching from the UV up to slightly less than their emission peak. They have narrow, size-tunable emission bands, and are resistant to photobleaching. Their biological applications in a variety of in vitro and in vivo procedures including

methods of labeling cells with them have been reported (4, 16, 33). In this investigation In/Ga/P amine functionalized QDs were used to model the diffusion of the nanoparticles within the osteoblasts by adding PLGA-encapsulated InGaP/ZnS nanoparticles to confluent cultures of primary mouse osteoblasts. Following Prefer fixation, cultures were examined via confocal microscopy. Fluorescent confocal microscopy results verified that PLGA loaded nanoparticles tagged to quantum dots diffused inside osteoblasts and were located in the periphery of the nucleus (29).

Subsequently, PLGA particles loaded with nafcillin were constructed and characterization and drug-loading studies were performed by UV-Visible spectrophotometry, dynamic light scattering and scanning electron microscopy (SEM). In addition, viability studies were conducted in primary osteoblasts intracellularly-infected with *S. aureus*. Following 24 and 48 h of incubation, all formulations of nanoparticles loaded with nafcillin either killed or significantly reduced all of the intracellular bacteria. Our data thereby demonstrate that effective killing of intracellular *S. aureus* is possible by treating the infected osteoblasts with nanoparticles loaded with nafcillin (27).

CHAPTER 6: MATERIALS AND METHODS

PLGA Nanoparticles preparation

Materials:

Poly(*dl*-lactide-co-glycolide) MW. 12,000-16,000, (PLGA) (50:50), poly(*dl*-lactide-co-glycolide) MW 20,000, (75:25) and poly(vinyl alcohol) MW 6000, (PVA) (80 mol% hydrolyzed) were purchased from PolySciences, Inc (Warrington, PA). Nafcillin Sodium was obtained from Sandoz Inc (Broomfield, CO). Quantum dots (QD), T2-MP InGaP/ZnS Amine Macoun Red, 650nm was obtained from Evident Technologies. Sodium Chloride, potassium chloride, sodium phosphate, dibasic, potassium phosphate, monobasic and dimethyl sulfoxide (DMSO) were purchased from VWR international (West Chester, PA), SpectraPor 1 dialysis tubing (MWCO 6-8 kDa) and SpectraPor 2 dialysis tubing (MWCO 12-14 kDa) (Spectrum Laboratories, Inc) were used. Collagenase (375 *microgram/ml*, type VII), protease (7.5 *microgram/ml*), Dulbecco's modified Eagle's medium, glycine, ascorbic acid, vitamin B12, *p*-amino benzoic acid, penicillin, streptomycin and amphotericin B were obtained from Sigma Chemical Co (St. louis, MO). Fetal bovine serum was purchased from Atlanta Biologicals (GA). Accugene Molecular Biology Grade Water (Lonza, Rockland, ME) was used for all preparations. All reagents were either American Chemical Society Analytical Grade Reagents or HPLC grade.

Emulsion- solvent evaporation technique:

In this study PLGA nanoparticles using several copolymer molecular weights were prepared by the single emulsion-solvent evaporation technique (3, 35). The lactide content of the copolymers varied from 50, 75 to 100%. The effect of the stabilizer in the nanoparticle size was studied by using different amounts of polyvinyl alcohol (0, 0.5, 1, 2, and 2.5%). Poly (vinyl alcohol) (PVA) was used as surfactant because nanoparticles using this emulsifier are relatively uniform and smaller in size, and are easy to redisperse in aqueous medium (26). Also, nanoparticles loaded with amine functionalized quantum dots composed of an In/Ga/P core surrounded by a ZnS shell and a PEG lipid coating functionalized with an amine linker group were prepared.

For nanoparticles loaded with quantum dots (QD), 3 ml of QD solution in double distilled ionized water at a concentration of 9×10^4 nmol/ ml was prepared and added to the PLGA organic phase and vortexed for 3 min. PLGA organic phase was prepared by dissolving 300 mg PLGA in 10ml dichloromethane and acetone mixture (8:2, v/v) by vortexing. 20 mL of aqueous PVA solution was prepared at concentrations of 0.5, 1, 2, and 2.5% w/v. The oil-water (O/W) emulsion was obtained by pouring the organic phase into the aqueous phase, vortexing for a min and then sonicating with a probe at 90W for 15 minutes over an ice bath. The organic solvents were allowed to evaporate while being stirred at atmospheric pressure. The solidified nanoparticles were collected by ultracentrifugation at 10000 rpm for 15 min to eliminate the big nanoparticles, and then washed three times with double distilled ionized water at 35,000 rpm for 30 minutes. The final product was dried by lyophilization.

For nanoparticles loaded with nafcillin, 300 mg PLGA was dissolved in 10 ml dichloromethane and acetone mixture (8:2, v/v) by vortexing. 100 mg of Nafcillin sodium was dissolved in 10 ml of the co-solvent, acetone and 18 drops of water were added. These two organic phases were mixed together by vortexing and added to 20 ml 0.5% PVA solution. Then the mixture was sonicated for 15 minutes (amplitude 75) (Vibracell, VCX 130PB, Sonics and Materials, Inc., Newtown, CT) over an ice bath. An oil in water (o/w) emulsion was formed. The organic solvents were evaporated at atmospheric pressure for 72 hours under constant stirring (250 rpm). The precipitated nanoparticles were collected by ultracentrifugation (20,000 rpm, 30 min). Nanoparticles were washed 3 times with water followed by ultracentrifugation to remove excess PVA and nafcillin sodium. Purified nanoparticles were dried by lyophilization. Unloaded PLGA nanoparticles (nanoparticles without nafcillin) were also prepared by single emulsion/solvent evaporation method.

Characterization of nanoparticles:

Particle Size, Zeta potential and Morphology:

0.1 mg of nanoparticles were suspended in 5 ml of double distilled ionized water and the suspension was sonicated for 5 min. The particle size and Zeta potential of the nanoparticles were then determined by dynamic light scattering (Zeta Pals, Brookhaven Instruments corp., Holtsville, NY). The morphology of the nanoparticles was studied by scanning electron microscope (Raith 150, Raith USA, Ronkonkoma, NY) by spreading the particles over an aluminum holder.

Drug loading measurements:

Drug loading of nanoparticles was determined by UV-Vis spectroscopy (Cary 300 Bio, Varian Australia PTY Ltd, Australia). Nafcillin-loaded nanoparticles were dissolved in DMSO and the absorbance was measured at 325 nm and 335nm (37). The drug concentration was determined by using calibration curves obtained from standard solutions of nafcillin in DMSO.

$$\text{Drug loading (\%, w/w)} = \frac{\text{mass of drug in nanoparticles}}{\text{mass of nanoparticles}} \times 100$$

In vitro drug release:

The *in vitro* degradation studies as well as the early stages of the drug release profile have been studied using phosphate buffer saline (PBS, pH 7.4), as the release medium. In vitro drug release studies of nanoparticles were conducted in an incubator shaker (Lab line, Labline Instruments Inc, Melrose Park, ILL) in phosphate buffer saline (PBS) (pH 7.4, 0.15M). The temperature of the system was maintained at 37°C. SpectraPor dialysis tubing was used for the study. The dialysis tubing was first activated by treating with sodium bicarbonate and sodium EDTA. Fifty mg of nafcillin loaded nanoparticles were suspended in 5 ml phosphate buffer saline and placed in dialysis bag and both ends were sealed with clips. SpectraPor (MWCO 6000) dialysis tubing was used for PLGA 50:50 and SpectraPor (MWCO 12,000-14,000) dialysis tubing was used for PLGA 75:25. The bag was immersed into a glass bottle containing 100 ml of release media (PBS) and closed tightly. The system was kept under constant shaking at 100 rpm to keep the concentration of drug in the buffer uniform. One ml of the buffer solution was sampled periodically at predetermined intervals and was replaced with one ml of fresh

PBS. The drug concentration was measured using UV-Vis spectroscopy at 325 nm and 335 nm using calibration curves obtained from standard solutions. The experiment was repeated with nafcillin sodium without polymer nanoparticles. Nafcillin sodium was dissolved in 5 ml PBS and loaded in a dialysis bag and the release of drug was determined. These results were compared with that of release from drug loaded PLGA nanoparticles in PBS solution.

Viability study

Normal mouse osteoblast cell culture:

Primary osteoblasts were isolated from mouse neonatal calvariae by sequential digestion with collagenase and protease according to a method previously described for chick embryos (30, 31). The periosteum were removed, the frontal bones were harvested free of the suture regions, and the bones were incubated for 10 min at 37°C in 10 ml of digestion medium containing collagenase (375 U/ml, type VII; Sigma Chemical Company, St. Louis, MO) and protease (7.5U/ml; Sigma). Cells released during an initial 7 min digestion were discarded. Ten milliliters of fresh digestion medium was added, and incubation continued for another 20 min. Cells were harvested by centrifugation and rinsed three times in 25 mM HEPES- buffered Hanks' balanced salt solution (pH 7.4; HBSS). The digestion step was repeated twice, and the three cell isolates were pooled in mouse osteoblast growth medium (OBGM) consisting of Dulbecco's modified eagle medium containing 25 mM HEPES, 10% fetal bovine serum (Atlanta Biologicals, GA), 2 g of sodium bicarbonate per liter, 75 mg of glycine/ml, 100 mg of ascorbic acid, 40 ng of vitamin B₁₂/ml, 2 mg of *p*-aminobenzoic acid/ml, 200 ng of biotin/ml, and penicillin (100 U/ml)-streptomycin (100 µg/ml)-amphotericin B (25 µg/ml) (pH 7.4) (30). Osteoblasts

were seeded on a coverslip in 24-well culture dishes (for confocal microscopy) or 6-well culture dishes (for viability studies) and incubated at 37°C in a 5% CO₂ atmosphere until they reached confluence (2-7 days).

Confocal microscopy analysis:

Once the cells reached confluency, cells were washed once with Hank's balanced salt solution (HBSS) and were treated with quantum dots alone or quantum dots tagged to nanoparticles suspended in 1X phosphate-buffered saline (PBS). Following different time periods of incubation, the quantum dots with and without nanoparticles were removed and rinsed twice with 1X PBS. Cell layers were rinsed twice with 1X PBS and were fixed using prefer fixative (Anatech Ltd, MI) for 20 minutes. The fixative was then removed and the cells were washed twice with 1X PBS. Cells were counterstained with 4'-6-diamidino-2-phenylindole (DAPI) for 10 minutes to visualize the nucleus, which stains blue with DAPI. The excess DAPI stain was then removed and cells were washed twice with 1X PBS. Finally, the extent of fluorescence present in the cells was visualized using a FLUOVIEW FV500 confocal laser scanning biological microscope (Olympus America Inc., Melville, NY).

Bacterial strain and growth conditions:

Staphylococcus aureus strain UAMS-1 (ATCC 49230) is a human osteomyelitis clinical isolate, and was grown overnight with aeration in 75 ml of Tryptic soy broth (TSB) at 37°C. The bacteria were harvested by centrifugation at 4300 x g for 10 minutes at 4°C and the cell pellet was resuspended in osteoblast growth medium (OBGM) lacking antibiotics. Following resuspension of bacteria in OBGM, bacterial cell density was determined via spectrophotometric analysis.

Invasion assay and *S. aureus* viability:

PLGA (50:50) and PLGA (75:25) loaded with nafcillin were used for the study. Samples G1 (PLGA 50:50, unloaded), G2 (PLGA 75:25, unloaded), G1.1 (PLGA 50:50, loaded), G1.2 (PLGA 50:50, loaded), G2.1 (PLGA 75:25, loaded) and G2.2 (PLGA 75:25, loaded) were used in these experiments. Nafcillin loaded particles were suspended in the growth medium at a concentration of 100 µg/ml. Once the osteoblasts reached confluency, cells were washed with OBGM lacking antibiotics and treated with 75 µl of the *S. aureus* suspension (approximately 2×10^9 colony forming units) in OBGM lacking antibiotics. Following a 45 min infection at 37°C, bacteria were removed and cell cultures were washed once with OBGM lacking antibiotics. Cells were then incubated for 1 hour at 37°C in OBGM containing either gentamicin (25 µg /ml) (to kill remaining extracellular bacteria) and unloaded nanoparticles or OBGM containing gentamicin and nafcillin loaded nanoparticles. Following 1 hour incubation period (time 0 hour), OBGM containing nanoparticles were removed and the cells were either lysed by treating with 0.1% triton X 100 for 5 minutes at 37°C or the cells were incubated for an additional 24-48 hours and then lysed. Serial dilutions of the cell lysates were plated on to tryptic soy agar plates (TSA) and the numbers of viable intracellular bacteria were quantified following an overnight incubation of the plates at 37°C.

Statistical analysis:

Data are all expressed as mean \pm S.E.M utilizing three independent osteoblast cultures. The statistical significance of results was analyzed using a student t-test (Sigmastat, SPSS Inc.) and a p value of less than 0.05 was considered significant.

CHAPTER 7: RESULTS

Intracellular diffusion of quantum dots tagged to nanoparticles into osteoblasts:

In the present study, we tested the ability of nanoparticles loaded with nafcillin to cross the osteoblast cell membrane to ensure better drug delivery to intracellular bacteria. To provide proof of concept, we first examined the ability of nanoparticles tagged to quantum dots to be incorporated inside osteoblasts. Nanoparticles of poly (lactide-co-glycolide) were prepared by single emulsion solvent evaporation technique. Three different copolymer compositions were used and the amount of the emulsifier, polyvinyl alcohol (PVA), was also varied. The particle size of nanoparticle suspensions was determined and results are summarized in Table 1. Primary mouse osteoblasts were then treated with these quantum dots tagged to PLGA nanoparticles. After incubation periods of 1 and 2 h followed by Prefer fixation, the cultures were examined via confocal microscopy to observe the extent of fluorescence present in the cells. As shown in Fig. 1, the tagged particles were internalized by osteoblasts and were located adjacent to the osteoblast nuclei.

Characterization of nanoparticles loaded with nafcillin:

Nanoparticles were then loaded with nafcillin and the particle size of nanoparticle suspensions along with the drug loading of the dry nanoparticles was determined and results are summarized in Table 2. Scannin electron microscopy imaging of nanoparticles

shows that they are spherical in shape with a smooth surface (Fig. 2). The zeta potential of plain PLGA nanoparticles was measured to be -45 mV. The release of nafcillin from nafcillin-PBS solution loaded in a dialysis bag is shown in Figs. 3a and 3b. The release of nafcillin from nafcillin-PBS solution without polymer nanoparticles followed a rapid profile with 97% of the drug being released within the first 9 h. Figs. 4 and 5 show the release of nafcillin from PLGA 75:25 and PLGA 50:50 respectively. The drug release followed a biphasic profile with 42-47% of the drug being released within 48 h of study (burst release) and the entire drug released within 35-40 days.

Viability of *S. aureus* inside osteoblasts exposed to nafcillin loaded nanoparticles:

As detailed in Fig. 6, following 24 and 48 hours of incubation, all formulations of nanoparticles loaded with nafcillin significantly reduced the numbers of intracellular bacteria. G1.2 and G2.2 formulations of nanoparticles loaded with nafcillin killed all of the intracellular bacteria. Other loaded formulations of particles, G1.1 and G2.1, caused a significant decrease in the viability of intracellular *S. aureus* inside infected osteoblasts. For all time points, the numbers of intracellular bacteria from osteoblasts infected with *S. aureus*, in the absence of any further treatment, were comparable to the numbers of bacteria obtained from infected osteoblasts treated with the unloaded nanoparticles formulations (G1 and G2).

CHAPTER 8: DISCUSSION

Osteomyelitis is an inflammatory disease of the bone that is characterized by extensive bone destruction and its primary causative bacterium is *Staphylococcus aureus*. The organism is a capable bone pathogen, with adhesins that facilitate its binding to bone matrix and toxin secretion capable of stimulating bone resorption via increasing osteoclast activity (23, 25). Previous studies in our lab have shown that *S. aureus* can be internalized by osteoblasts (14). Intracellular invasion provides protection from the humoral immune response and several classes of antibiotics. These factors, coupled with the fact that antibiotics cannot effectively penetrate intracellularly-infected eukaryotic cells could explain the recalcitrant nature of this disease despite what can be considered adequate surgical and antibiotic management (7). We have successfully demonstrated the use of nafcillin-loaded nanoparticles to target intracellular *S. aureus*. Nafcillin was chosen in these studies, since *S. aureus* clinical isolate UAMS-1 is sensitive to the drug, nafcillin is often prescribed for *S. aureus* infections, and nafcillin does not have the ability to enter eukaryotic cells in its native form.

Poly(lactide-co-glycolide) [PLGA] particles were first tagged to quantum dots (In/Ga/P amine functionalized QDs) in order to model the diffusion of the nanoparticles across the osteoblast cell membrane. The QD was composed of an In/Ga/P core surrounded by a ZnS shell and a lipid coating to make it water soluble. Other biomolecules such as antibiotics can be potentially conjugated to the amine linker group

functionalized to the lipid coat. PLGA nanoparticles were prepared by single-emulsion solvent evaporation technique and the lactide content of the copolymers varied from 50, 75 to 100%. The effect of the stabilizer in the nanoparticle size was studied by using different amounts of polyvinyl alcohol (0, 0.5, 1, 2, and 2.5%). For all copolymer compositions, optimum results in terms of particle size and nafcillin loading was obtained when 0.5% of PVA was used to prepare the PLGA nanoparticles (data not shown) and was henceforth chosen as the optimum stabilizer concentration for preparation of PLGA particles loaded with nafcillin. An interesting phenomenon observed was the reduction in the particle size of nanoparticles upon loading of nafcillin compared to that of unloaded PLGA nanoparticles (Table 2). As observed in other studies, a hydrophobic drug such as nafcillin with its aromatic rings in its molecular structure, might decrease the interfacial tension between the aqueous phase and the organic phase, which results in an increase of the area to volume ratio which results in a reduction of particle size (38). The PLGA nanoparticles prepared in these studies were spherical in shape, with particle size in the range of 200 nm (Fig. 2). The negative zeta potential of these particles, due the presence of free carboxyl groups on the polymer surface, was in agreement with previous studies (15). Fluorescent confocal microscopy verified that PLGA nanoparticles loaded with QDs diffused inside osteoblasts and were located in the periphery of the nucleus (Fig. 1) (29).

We then evaluated the drug release profiles of nafcillin loaded PLGA nanoparticles. Firstly, the drug release profile of nafcillin solution in PBS across dialysis tubing was measured and the majority of the drug was rapidly released within the first 9 hours (Fig. 3). This shows that the transport of drug through the dialysis membrane is not

a rate-limiting factor. Drug release measured from nafcillin-loaded PLGA nanoparticles followed a biphasic profile with an initial rapid release followed by a more controlled release as shown in Figs. 4 and 5. Biodegradable polymers can be arbitrarily classified into two groups - bulk eroding (homogeneous) and surface eroding (heterogeneous) polymers. In the case of surface-eroding polymers, polymer degradation is much faster than water intrusion into the polymer bulk and hence, the erosion affects only the surface and not the inner parts of the matrix. In bulk eroding polymers, water uptake by the system is much faster than polymer degradation which results in the hydration of entire polymer and cleavage of polymer chains inside the polymer. The erosion process is therefore not confined to the outer surface alone. PLGA is documented to be a bulk eroding polymer (2, 34) as corroborated by the release profile observed here. The initial burst release was probably due to the drug that was present close to the surface and the second phase of slow release was due to simultaneous polymer degradation and drug diffusion. Such a release profile is important because an initial burst release may help control the rapid growth of the organism in osteoblasts.

Lastly, we investigated the effects of nafcillin-loaded PLGA nanoparticles on the viability of intracellular *S. aureus* in infected osteoblasts. Our viability study data demonstrate that effective killing of intracellular *S. aureus* is possible by treating the infected osteoblasts with nanoparticles loaded with nafcillin. These particles released the drug and eliminated all of the intracellular bacteria following an incubation period of 24-48 h (27).

In summary, we have provided compelling data substantiating a novel approach using antibiotic-loaded nanoparticles to enter inside infected osteoblasts which results in

killing of all intracellular bacteria. One of the potential applications of such a unique approach can be the development of a spray device that can be used to immediately treat injured patients, target extracellular and intracellular bacterial pathogens and be a topical application replacing systemic antibiotic therapy with the associated risk of selection for resistant bacteria.

FIGURES

PLGA Composition	PLGA (mg)	PVA (mg, %)	Particle size / PD, (nm)	QD Loading (%)
50:50	313	116, 0.5	263 (0.13)	9×10^{-4} nmol/mL
75:25	304	107, 0.5	301 (0.20)	9×10^{-4} nmol/mL
100:0	305	107, 0.5	228 (0.18)	9×10^{-4} nmol/mL

Table 1: Characterization of poly(lactide-co-glycolide) [PLGA] nanoparticles tagged to Quantum dots (QD) prepared by emulsion solvent evaporation technique.

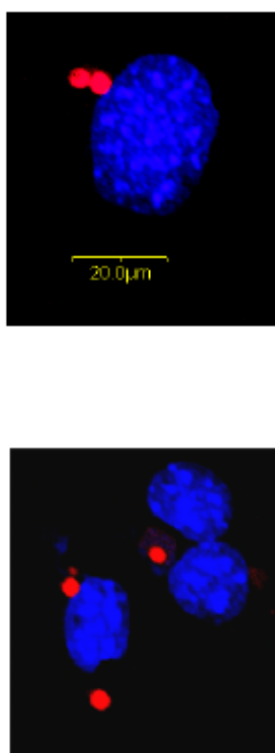


Figure 1: Confocal microscopy images of poly(lactide-co-glycolide) [PLGA] nanoparticles tagged to quantum dots (QD) (50:50; upper panel, 75:25; lower panel) inside primary mouse osteoblasts. Quantum dots fluoresce red while osteoblast nuclei fluoresce blue.

Sample number	Type of polymer	Weight of PLGA (mg)	Weight of PVA (mg)	Weight of Nafcillin (mg)	Particle Size (nm)	Zeta Pot (mV)	Drug Loading (% , w/w)
G1	PLGA 50:50	900	305	Nil	373	- 45	-----
G1.1	PLGA 50:50	910	306	310	140	- 78	10
G1.2	PLGA 50:50	908	305	300	168	- 77	09
G1.3	PLGA 50:50	300	100	100	160	- 66	10
G2	PLGA 75: 25	905	102	Nil	280	- 45	-----
G2.1	PLGA 75:25	905	300	305	162	- 84	07
G2.2	PLGA 75:25	903	300	305	207	- 82	11
G2.3	PLGA 75:25	302	101	100	180	- 73	12

Table 2: Characterization of poly(lactide-co-glycolide) [PLGA] unloaded and nafcillin loaded nanoparticles prepared by emulsion solvent evaporation technique.

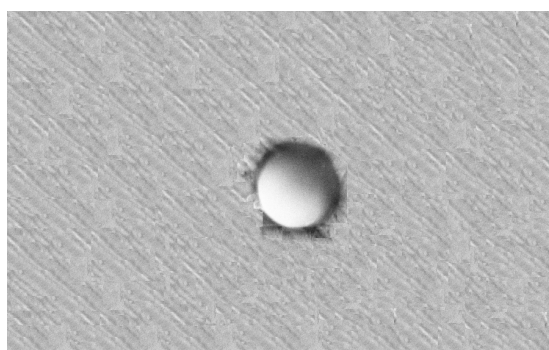


Figure 2: Scanning electron micrograph (SEM) of a PLGA nanoparticle

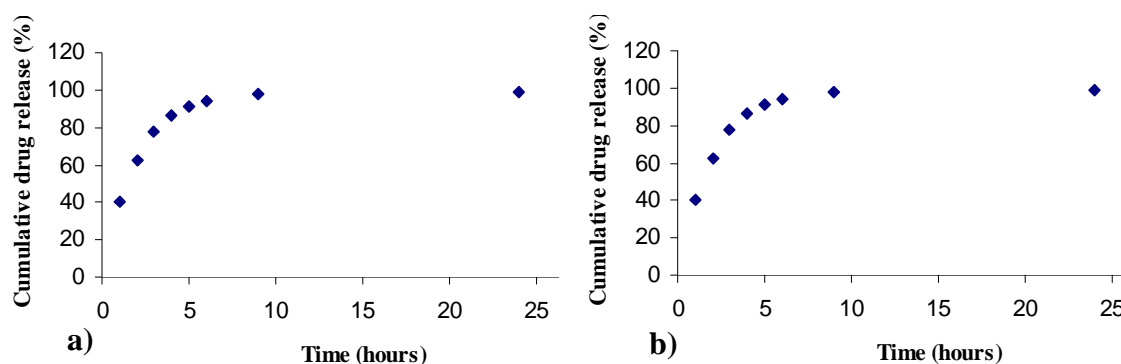


Figure 3: Release of drug from nafcillin-PBS solution loaded in a dialysis bag at 37°C. a) MWCO 6 kDa; b) MWCO 12-14 kDa.

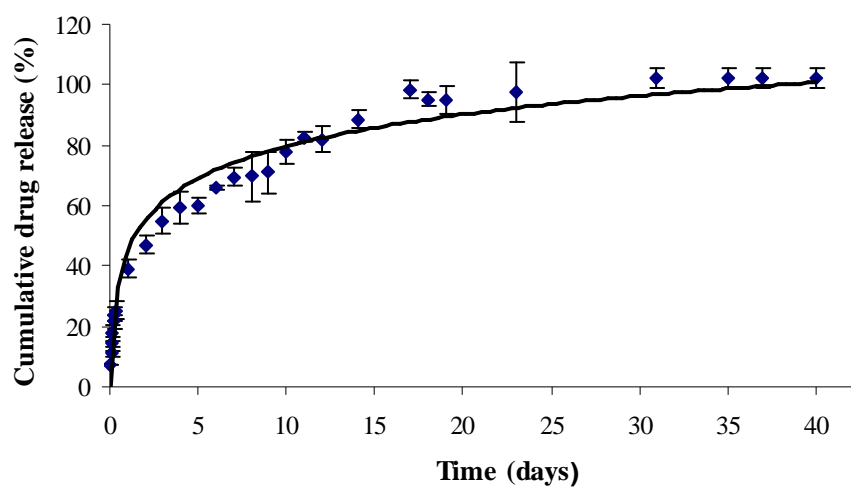


Figure 4: Release of nafcillin from PLGA 75:25 nanoparticles in PBS at 37°C.

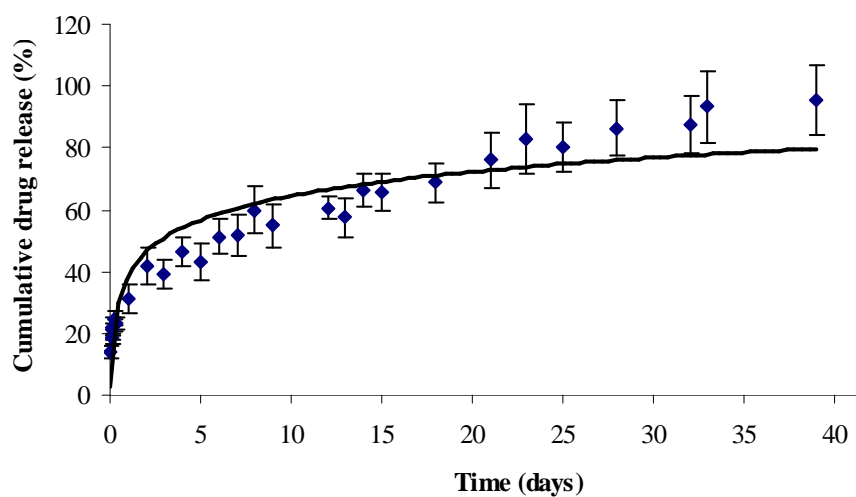


Figure 5: Release of nafcillin from PLGA 50:50 nanoparticles in PBS at 37°C

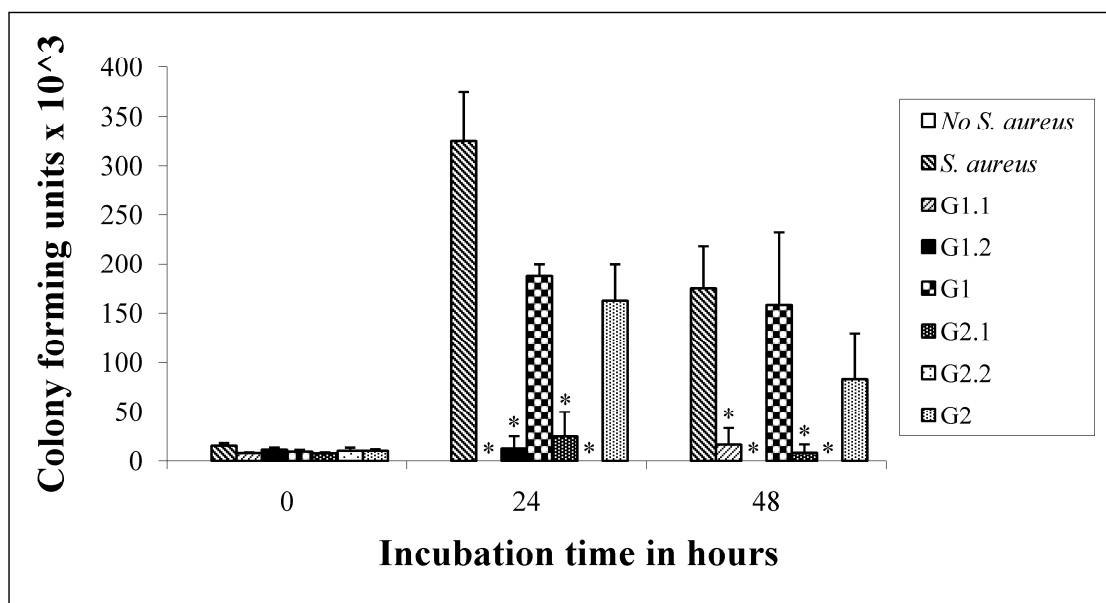


Figure 6: Viability of intracellular *S. aureus* from osteoblasts treated with nanoparticles or nanoparticles loaded with nafcillin. Primary mouse osteoblasts were infected intracellularly with *S. aureus* and were subsequently treated with unloaded nanoparticles (G1 and G2) or nanoparticles loaded with nafcillin (G1.1, 1.2, 2.1 and 2.2) for 1 (0 hour), 24 and 48 hours. Osteoblasts were subsequently lysed at these time intervals with a solution containing 0.1% triton X-100 and serial dilutions of the lysates were plated on tryptic soy agar (TSA). Following an overnight incubation at 37°C, the numbers of intracellular bacteria were enumerated. *, $P < 0.05$ versus *S. aureus*- treated osteoblasts at the same time point.

CHAPTER 9: INTRODUCTION

Artificial joints and orthopedic implants are used to repair or restore function to damaged and diseased tissue. Conventionally, such devices are constructed of metals such as titanium and cobalt-chromium which are relatively non-immunogenic, non-toxic, and resist corrosion when placed in contact with host tissues (34). However, the most significant problem encountered with such biomaterials is inadequate osseointegration, or intimate apposition of bone to the implant surface (11). As a result, the functional lifespan of artificial prostheses is estimated at about 15 years which makes them unsuitable for active and younger patients (34). Implant failure can be caused by various factors, but tends to be the result of mechanical fatigue or loosening of the device. Enhancement of biomaterials is therefore necessary in order to increase the implant success rate and extend their functional lifespan.

Osseointegration is desirable for the clinical success of implants because it provides a functional connection between the implant and bone by strong bonding of the surrounding bone tissue on implant-material surfaces. Formation of a proper interface requires immediate and rigid immobilization of the implant as any implant motion can also cause release of particle debris which can initiate a deleterious inflammatory response (19). At the cellular level, a proper interface formation requires osteoblast adhesion and subsequent functions pertinent to osteogenesis (2).

Bone is an anisotropic and dynamic tissue consisting of cells (osteoblasts and osteoclasts), connective tissue (primarily type 1 collagen), and minerals (hydroxyapatite). Osteoblasts form a bone matrix (the osteoid) that later becomes mineralized. The extracellular matrix (ECM) secreted by osteoblasts is approximately 90% collagen and 10% non-collagenic proteins such as osteocalcin, osteonectin, sialoproteins, proteoglycans, osteopontin, and fibronectin (50). Successful communication between cells and the ECM is mediated by a family of cell surface receptors called integrins that stimulate signal transduction pathways and mediate osteoblast adhesion, spreading, cell differentiation and bone morphogenesis (21, 23, 37). Specifically, integrin activation induces expression of osteoblast specific transcripts such as osteocalcin and type I collagen and is required for differentiation of osteoblast precursors (55).

Staphylococcus aureus is a gram-positive bacterium capable of binding to and colonizing tissues via a collection of cell-surface adhesins referred to as microbial surface components recognizing adhesive matrix molecules (MSCRAMMs). MSCRAMMs recognizing collagen, bone sialoprotein, fibronectin, and fibrinogen mediate adherence of *S. aureus* to bone and biomaterials coated with host proteins (28). There is evidence that *S. aureus* can bind to cells (16, 48) and biomaterials (25, 26) directly. Interaction of *S. aureus* with host cells via MSCRAMMs can induce signal transduction, tyrosine kinase activity, and cytoskeletal rearrangement (15, 16). UV-killed *S. aureus* is also able to attach efficiently osteoblasts (29). Although viable *S. aureus* cells are potent inducers of immune modulator expression by osteoblasts, UV-killed *S. aureus* does not induce significant expression of such molecules (4-6). In summary, UV-killed *S. aureus* can tenaciously bind biomaterials and effectively colonize bone which can initiate cell-

signaling cascades that can potentiate osteogenesis. These are an intriguing combination of properties with respect to bone-implant interfaces and the current proposal addresses the efficacy of *S. aureus* as a novel osteoconductive coating for bone-associated biomaterials.

Here, we investigated the effects of coating Ti surfaces with dead bacteria on osteoblast functions pertinent to new bone formation. For this purpose, cell adhesion, proliferation as well as synthesis and mineralization of the extracellular matrix were examined using mouse calvarial osteoblasts, a well-characterized, cell culture model. Osteoblast differentiation on Ti-6Al-4V alloy coated with fibronectin (Ti-Fn) surfaces was compared to Ti-Fn surfaces coated with UV-killed *S. aureus* (Ti-Fn-SA). Fibronectin was chosen to pre-coat the polymer surface as it is pre-adsorbed on all biomaterials following insertion and is considered to be the model host protein that promotes *S. aureus* attachment to biomaterial surfaces (2, 52). Results of these studies demonstrate that compared to the Ti-Fn surface, osteoblast attachment and adhesion was enhanced on Ti-Fn surfaces coated with bacteria. On both substrates, cell proliferation was sustained at comparable levels while markers of osteoblast differentiation such as collagen, osteocalcin, alkaline phosphatase and mineralized nodule formation were increased on Ti-Fn-SA alloys compared to Ti-Fn surfaces. A productive interaction of bone-associated biomaterials with osteoblasts, aided by *S. aureus*, thus suggests a unique role for *S. aureus* to increase apposition of bone to implant surfaces.

CHAPTER 10: MATERIALS AND METHODS

Normal mouse osteoblast cell culture:

Primary osteoblasts were isolated from mouse neonatal calvariae by sequential digestion with collagenase and protease according to a method previously described for chick embryos (43). The periosteum were removed, the frontal bones were harvested free of the suture regions, and the bones were incubated for 10 min at 37°C in 10 ml of digestion medium containing collagenase (375 U/ml, type VII; Sigma Chemical Company, St. Louis, MO) and protease (7.5U/ml; Sigma). Cells released during an initial 7 min digestion were discarded. Ten milliliters of fresh digestion medium was added, and incubation continued for another 20 min. Cells were harvested by centrifugation and rinsed three times in 25 mM HEPES- buffered Hanks' balanced salt solution (pH 7.4; HBSS). The digestion step was repeated twice, and the three cell isolates were pooled in mouse osteoblast growth medium (OBGM) consisting of Dulbecco's modified eagle medium containing 25 mM HEPES, 10% fetal bovine serum (Atlanta Biologicals, GA), 2 g of sodium bicarbonate per liter, 75 mg of glycine/ml, 100 mg of ascorbic acid, 40 ng of vitamin B₁₂/ml, 2 mg of *p*-aminobenzoic acid/ml, 200 ng of biotin/ml, and penicillin (100 U/ml)-streptomycin (100 µg/ml)-amphotericin B (25 µg/ml) (pH 7.4) (42). Osteoblasts were seeded in 25 cm² flasks and incubated at 37°C in a 5% CO₂ atmosphere until they reached confluence (6-7 days). Cells were then washed with 10 ml of HBSS, treated with

5 ml of trypsin (Sigma) for 5 min at 37°C. Following centrifugation, osteoblasts were seeded on to the biomaterial surfaces as described below.

Biomaterial preparation:

12- well polystyrene tissue culture dishes were coated with the titanium alloy Ti-6Al-4V (hereby abbreviated as Ti) (Teledyne Allvac/Vasco, NC) using electron beam deposition (Varian 3125 electron beam evaporator). Ti-coated dishes were then treated with osteoblast growth medium (OBGM) supplemented with mouse Fibronectin (hereby abbreviated as Fn) (Affiland Company, Belgium) at a concentration of 2 µg/ml for 24 hr at 37° C. Following incubation, plates were rinsed with Hank's balanced salt solution (HBSS) to remove unbound Fn. Selected plates were incubated an additional 24 hr with different doses of UV-killed *S. aureus* - 1×10^6 , 10^7 and 10^8 numbers of bacteria per well. For all experiments, Ti-Fn coated plates with no bacteria (hereby abbreviated as Ti-Fn) served as controls for comparison with bacteria-coated surfaces (hereby abbreviated as Ti-Fn-SA). Following incubation, plates were rinsed with HBSS to remove unbound bacteria. Osteoblasts subcultured from tissue culture flasks (as described above) were seeded into Ti-Fn +/- dead *S. aureus*-coated 12 well dishes at a density of 2×10^4 cells/cm² and incubated at 37°C at 5% CO₂ for various time points.

Bacterial strain, growth conditions and UV-killing:

S. aureus strain UAMS-4 is a co-isogenic mutant of osteomyelitis-clinical isolate UAMS-1 (ATCC 49230) with an inactivated *agr* (accessory gene regulator) locus (20). The *agr* locus encodes a trans-activator of multiple *S. aureus* virulence-associated genes and is also responsible for growth-phase-dependent expression of cell surface and secreted virulence factors. The *agr* locus is inactive during exponential growth where cell

surface adhesins are maximally expressed (38). Entry into stationary phase results in activation of *agr*, down-regulation of cell surface adhesins, and up-regulation of secreted proteins. Therefore, *agr* mutants retain the ability to colonize host tissue, but demonstrate decreased virulence (20, 38). UAMS-4 was grown overnight in 15 ml of tryptic soy broth (TSB) supplemented with erythromycin (5 µg/ml) (Em5) at 37°C with aeration. Ten ml of this overnight culture was then transferred to 1 liter of TSB-Em5 and grown for 3 hr in conditions as described above. Bacteria were harvested in the resulting exponential phase to ensure maximal expression of cell surface adhesions. Cells were harvested by centrifugation at 4300 x *g* at 4°C for 10 min and washed in HBSS. Bacteria were killed by exposure to short-wave (254 nm) ultraviolet radiation for 5 min and centrifuged at conditions described above. Subsequently, bacteria were suspended in OBGM to give the final concentration of 1 to 5 x 10⁸ colony-forming units (CFU/ml). To verify successful killing, aliquots of the cell suspension were plated on tryptic soy agar (TSA) supplemented with erythromycin (10 µg/ml) (Em10), followed by incubation for 24 h at 37°C.

Osteoblast attachment:

Attachment of osteoblasts to Ti in the presence and absence of UV-killed *S. aureus* was analyzed using phosphor-screen autoradiography (10). Before subculturing onto Ti-Fn +/- *S. aureus* surfaces, osteoblasts were incubated with methionine-free DMEM supplemented with 5 µCi/ml ³⁵S-methionine. Following 18 h incubation with the labeling medium, cells were removed from flasks using 0.05% trypsin/0.01% EDTA, washed in OBGM, and seeded into culture dishes prepared as described above. Osteoblasts suspended in the labeling medium were seeded onto Ti-Fn and Ti-Fn-SA

coated plates and cell attachment was assessed at 1 and 36 h. At the indicated time points, culture plates were rinsed 3 times with HBSS, air dried, and exposed to a phosphor screen for 2 hrs. Following exposure, the screen was analyzed using a Typhoon 8600 Variable Mode Phosphor Imager and the pixel intensities, indicative of the relative number of attached osteoblasts, were measured using appropriate software (Molecular Dynamics, CA).

Osteoblast adhesion:

Cell adhesion was assessed by reduction of the yellow tetrazolium salt 3-(4,5-dimethylthiazol-2-yl)-5-(3-carboxymethoxyphenyl)-2-(4-sulfophenyl)-2H-tetrazolium (MTS) to the blue formazan product (Promega, WI) (18). Osteoblasts were incubated on Ti-Fn and Ti-Fn-SA surfaces for 1, 3, 7 and 10 days. At the indicated time points, culture medium was removed; the wells were washed with HBSS and replaced with OBGm without phenol red (Hyclone labs, UT). Twenty μ l of MTS reagent was added to each well and incubated overnight at 37 °C in a humidified atmosphere with 5% CO₂. The extent of osteoblast adhesion was determined by measuring the absorbance of the culture media at 540 nm in a plate reader.

Osteoblast proliferation:

Osteoblast proliferation was assessed by measuring incorporation of ³H-thymidine into osteoblasts (13). Briefly, osteoblasts were seeded onto Ti-Fn and Ti-Fn-SA-coated dishes as described earlier. Cells were incubated at 37°C in 5% CO₂ in OBGm containing 0.5 μ Ci/ml tritiated thymidine (methyl-³H) (Amersham, MA). At 24, 48, and 72 h, labeling media were removed from individual plates, and the wells were rinsed once with PBS to remove unincorporated tritiated thymidine. Adherent cells were then lysed in 0.5

ml of a 5 mM Tris (pH 8.0), 20 mM EDTA, 0.5% Triton X-100 solution. Samples were treated with NaOH (2.0 N), followed by HCl (2.0 N), and then incubated overnight at 4°C in 0.6 N perchloric acid. Cell lysates were centrifuged, the supernatant discarded, and the pellet resuspended in 100 uL of Tris-EDTA buffer. Liquid scintillation analysis was then used to quantify the amount of tritiated thymidine present in each sample. Radioactivity levels (disintegrations/minute, dpm) serve as an indicator of cell proliferation on a particular substrate.

Insoluble matrix collagen synthesis assay:

To determine the bone-matrix forming ability of osteoblasts, production of insoluble collagen was measured to assess the bone matrix- forming ability of osteoblasts as described (49). Osteoblasts suspended in OBGm were plated on Ti-Fn and Ti-Fn-SA-coated surfaces and incubated at 37°C in 5% CO₂ for 3, 6 and 9 days. Following incubation at the different time points, media was aspirated and cell layers were fixed for 1 hour in picric acid: 37% formaldehyde containing 4.8% acetic acid (3:1). Cell layers were then air dried and stained for 1 hr with 0.1% Sirius red F3B in picric acid (Sigma) , a dye that binds to the [gly-x-y] helical structure found in all collagens without staining other components of the extracellular matrix (33, 51). The stained cell layers were washed with 0.01N HCl and the bound dye was released using 0.1 NaOH. The absorbance of the released dye was measured spectrophotometrically at 540 nm.

Osteocalcin production:

Osteoblasts were cultured in growth medium (OBGM) on Ti-Fn and Ti-Fn-SA-coated dishes for 7, 14 and 21 days. Cell culture media was collected at the indicated time points and osteocalcin production was measured in the culture media using a

commercially available osteocalcin enzyme linked immuno assay (ELISA) kit (Biomedical Technologies, Inc., MA) as described previously (53). The measurement sensitivity was 1 ng/ml.

Measurement of alkaline phosphatase activity:

Alkaline phosphatase activity was measured using an assay based on the hydrolysis of p-nitrophenyl phosphate (p-NPP) to p-nitrophenol (p-NP) (17). Briefly, cells suspended in OBGm were seeded in 12-well plates coated with Ti-Fn and Ti-Fn-SA coated surfaces and incubated for 3, 6 and 9 days. At the indicated time points, cell culture media was decanted, cell layers washed once with HBSS and then lysed with 1% triton X-100. Enzyme activity in the cell lysate was spectrophotometrically measured at 410 nm as released p-nitrophenol (p-NP) over a 5-minute period. Nmol product/minute was calculated assuming $1A_{410} = 64 \text{ nMol p-NP}$ (36). Measurement of total protein content in each sample using the BCA protein assay kit (PIERCE, IL) was performed to allow a determination of alkaline phosphatase specific activities for osteoblasts attached to the different substrates. Alkaline phosphatase specific activity was expressed as nanomoles of product (p-nitrophenol) produced per milligram of protein.

Osteoblast mineralization:

The degree of mineralization was determined using Alizarin Red S staining as described (1). Osteoblasts were suspended in mineralization media (DMEM supplemented with 10% FBS, 10 mM β -glycerophosphate (β -GP) and 50 μ g/ml ascorbic acid), plated on Ti-Fn and Ti-Fn-SA-coated surfaces and incubated for 7, 14 and 21 days. Following the indicated times of culture, media was removed and the cells were fixed for 1 hr with ice-cold 70% ethanol. Following fixation, cell layers were rinsed twice with

deionized water and stained with 40 mM Alizarin Red S solution (pH 4.2) for 10 minutes at room temperature. The dye was aspirated; cells were rinsed three times with deionized water and then washed with PBS for 10 min to remove nonspecific staining. After removal of the PBS, the cells were destained from the cell matrix by incubation in 10% cetyl-pyridinium chloride (Sigma) in 10 mM sodium phosphate (pH-7.0) for 15 minutes. Finally, the absorbance of the extracted stain was measured at 570nm with a spectrophotometer.

Statistical analysis:

Data are reported as mean \pm SEM of triplicate values from a single experiment. All experiments were repeated three times and yielded similar results. The statistical significance of results was analyzed using a one way analysis of variance (ANOVA) with one repeated measure, followed by a Dunnett's test for a *post hoc* comparison (Sigmastat, SPSS Inc.). A p value of less than 0.05 was considered significant.

CHAPTER 11: RESULTS

Osteoblast attachment, adhesion and proliferation:

Ti-6Al-4V alloy was deposited on to tissue culture plastic and coated with mouse fibronectin alone (Ti-Fn surface) or with fibronectin followed by UV-killed *S. aureus* (Ti-Fn-SA). Osteoblasts were incubated on these Ti surfaces for different time periods. Osteoblast attachment to Ti-Fn +/- *S. aureus* surfaces was measured by phosphor-screen autoradiography following 1 and 36 hours of incubation. Results from these studies (Fig.1) demonstrate that using dead *S. aureus* enhances osteoblast attachment in a dose dependent manner to thin films of titanium alloy, following 1 and 36 hours of incubation. The magnitude of attachment, as estimated by the average pixel intensity, is dependent on the numbers of bacteria added. When pixel intensity was quantitated by the image phosphor, a significant increase in attachment was noted in osteoblasts cultured in the presence of the 10^7 and 10^8 doses of bacteria, following 36 hours of incubation (Fig.2).

Especially in the field of biomaterials, attachment refers to an initial physicochemical interaction between two surfaces mediated by ionic and van der Waals forces while adhesion is a more complex cellular process that involves activation of transcription factors, altered gene expression, and formation of focal adhesion points (2). Therefore, we tested if increased cell attachment in the presence of dead bacteria also resulted in corresponding increase in cell adhesion. Osteoblast adhesion on both surfaces was indirectly estimated by measuring the absorbance of the end product of MTS dye

degradation, formazan. Figure 3 shows a dose-dependent as well as kinetic increase in the number of osteoblasts that adhere on to Ti-Fn surfaces coated with dead *S. aureus* compared to those incubated on Ti-Fn surfaces. There is a significant increase in osteoblast adhesion in the presence of highest dose of bacteria following 1, 3 and 10 days of incubation.

The proliferation of osteoblasts on Ti-Fn and Ti-Fn-SA surfaces was measured by liquid scintillation analysis following 24, 48 and 72 hours of incubation. The relative cell proliferation rate was determined by measuring the amount of ^3H -thymidine incorporated. Data are reported as the number of disintegrations per minutes (dpm) per well. There were no significant differences in the proliferation rate of osteoblasts on Ti-Fn surfaces compared to Ti-Fn surfaces coated with different numbers of dead *S. aureus* bacteria at any time point studied (Fig.4).

Extracellular matrix synthesis and mineralization:

Primary mouse osteoblasts undergo an ordered sequence of differentiation which results in the formation of a mineralized extracellular matrix that consists of type I collagen, alkaline phosphatase and specialized noncollagenous proteins (50). Presence of a collagen matrix is required for mineralization to occur as the bone cells mineralize collagen by surrounding it with the hard mineral component, hydroxyapatite (HAP) which consists of calcium phosphate primarily (39). Osteocalcin is the second most abundant protein in bone after collagen and binds to both collagen and HAP. Moreover, it is believed to assist in the deposition of HAP onto collagen and therefore renders the matrix competent for mineralization to occur. Therefore, synthesis of the total insoluble collagen as well as osteocalcin production was determined as an index of extracellular

matrix synthesis on both Ti-Fn and Ti-Fn-SA surfaces. As shown in Figure 5, the kinetics of total collagen synthesis, as measured by staining with a dye specific for collagen, Sirius red F3B, is similar when osteoblasts were cultured for time periods of 3 and 6 days. After 9 days of incubation, however, collagen production was markedly increased in the presence of 10^7 and 10^8 doses of bacteria.

The synthesis of osteocalcin protein was measured by osteoblasts on Ti-Fn and Ti-Fn-SA surfaces following 7, 14 and 21 days of incubation. As shown in Table 1, there is an at least 25-fold increase in the amount of osteocalcin produced from osteoblasts grown on Ti-Fn coated with the highest dose of *S. aureus* versus osteoblasts grown on Ti-Fn coated dishes. Osteocalcin secretion from osteoblasts incubated on Ti-Fn alone and Ti-Fn surface with 10^6 or 10^7 bacteria remained below the detection limits of the assay.

Having verified increased deposition of extracellular matrix by osteoblasts cultured on Ti-Fn-SA, the ability of dead bacteria to induce successful mineralization activity from the osteoblasts was examined. Alkaline phosphatase (ALP) is an enzyme that is involved in the bone mineralization process and hydrolyzes organic phosphates to release inorganic phosphate which is incorporated at the site of mineralization (3). Therefore, ALP activity was measured as an index of mineralization activity in osteoblasts on Ti-Fn and Ti-Fn-SA surfaces following 3, 6 and 9 days of incubation. As shown in Figure 6, ALP activity of osteoblasts added on both Ti-Fn and Ti-Fn-SA-coated dishes increased in a time-dependent manner. However, significantly greater enzyme activity was observed in osteoblasts incubated on the Ti-Fn surface coated with 10^7 numbers of bacteria at day 6 compared with the Ti-Fn surface.

When osteoblast cultures are maintained in mineralizing conditions (mouse osteoblast growth medium supplemented with β -glycerophosphate), calcium and phosphate are incorporated into the cell layers to form the mineral component (HAP). Alizarin red-S stains the calcium incorporated in the matrix and we can indirectly estimate the extent of mineralization activity by measuring the amount of calcium extracted from the matrix. As shown in Figure 7, there is a dose-dependent increase in mineralization activity in osteoblasts grown on Ti-Fn-SA-coated surfaces compared to Ti-Fn group following 7, 14 and 21 days of incubation in the culture media. At all time periods, the highest dose of bacteria induces a significant increase in mineralization from osteoblasts grown on Ti-Fn-SA surface.

CHAPTER 12: DISCUSSION

Titanium alloys, such as Ti-6Al-4V, are the most common orthopedic implant materials because they offer excellent mechanical properties such as resistance to wear and corrosion (34). However, a major disadvantage of titanium alloys as a biomaterial is that they are relatively inert biologically and do not facilitate or mediate osseointegration which is intimate apposition of bone to the implant surface (11). Osseointegration is desirable because it represents formation of an appropriate interface and provides a functional connection between the implant and bone. A number of techniques have been employed to enhance such biomaterials, including alteration of surface roughness, wettability, porosity, and hydrophobicity in an attempt to enhance osseointegration and mediate proper interface formation (2, 34, 54). Recently, techniques have focused on coating implants with biological materials such as cell surface receptors and extracellular matrix (ECM) components (e.g., collagen, fibronectin, and vitronectin) (9, 12, 32, 34, 35, 41). Some of these techniques have enhanced binding of osteoblasts to implant surfaces, but have failed to enhance cellular functions and formation of a proper interface between implant and bone. Therefore, any implant surface that would promote osseointegration would need to facilitate osteoblast adhesion as well as proliferation and demonstrate production of a mineralized extracellular matrix (ECM).

Staphylococcus aureus is a gram-positive bacterium capable of binding to host cells (16, 48) and biomaterials (25, 26) directly. A collection of cell-surface adhesins

referred to as microbial surface components recognizing adhesive matrix molecules (MSCRAMMs) (28, 29) are responsible for localization of *S. aureus* both to bone tissue as well as biomaterials coated with host proteins and include adhesins such as fibronectin binding proteins (FnBPs), fibrinogen binding proteins, collagen-binding adhesin and bone sialoprotein-binding adhesin (28). MSCRAMM-mediated interaction of *S. aureus* with ECM or with osteoblasts, via integrin receptors on their surface, can induce tyrosine kinase activity, cytoskeletal rearrangement and signal transduction (15, 16).

Previous studies from our lab have demonstrated that UV-killed *S. aureus* retain the ability to attach efficiently to osteoblasts but, in contrast to live bacteria, do not induce the expression of immune modulators such as interleukin (IL)-6, IL-12 and monocyte chemoattractant protein (MCP-1) (4-6, 29). Therefore, as *S. aureus* can tenaciously bind biomaterials, effectively colonize bone, and stimulate signal transduction in host cells, we examined the efficacy of UV-killed *S. aureus* as an osteoconductive coating for titanium alloy in the current study. For all experiments, the ability of dead *S. aureus* to enhance osteoblast adhesion, proliferation and matrix synthesis was compared to fibronectin (Fn)-coated Ti surfaces (Ti-Fn). Fn is a component of plasma that coats virtually any device implanted within the body and more importantly, osteoblasts have been demonstrated to bind Fn preferentially when compared to other serum proteins (2, 52).

Osteoblast attachment and adhesion to the implant interface is a crucial pre-requisite for successful osseointegration of the implant (31, 40). Our results show that osteoblasts effectively attach to Ti-Fn surfaces, both coated and uncoated, within 1 h in vitro. However, osteoblasts attach significantly more on Ti surfaces coated with dead

bacteria especially after 36 h of incubation (Fig. 1,2). Osteoblast adhesion, in contrast to osteoblast attachment, involves activation of transcription factors and formation of focal adhesion points which involves the cell membrane as well as proteins associated with the cytoskeleton (vinculin, talin) and ECM (fibronectin, type I collagen) (2). As indicated in Fig. 3, we have demonstrated that osteoblasts adhere better on Ti-Fn-SA surfaces compared to Ti-Fn surfaces alone and sustain increased adherence up to 10 days in culture. This increase in osteoblast attachment and adherence can be explained by enhanced hydrophilicity of the Ti-Fn surface coated with *S. aureus* as it has been established that surface hydrophilicity of a biomaterial surface greatly facilitates cell adhesion (2, 24). Metals, such as Ti alloy, have an oxide layer that is spontaneously deposited on all their surfaces and are therefore hydrophilic due to presence of hydroxyl groups present on the oxide layer (56). However, it is possible that the surface hydrophilicity is compromised by coating with fibronectin as would be the case in both Ti-Fn as well as Ti-Fn-SA substrates. However, coating the Ti-Fn alloy with bacteria renders the surface more hydrophilic because bacterial surfaces in aqueous solutions are always ionized (27). Moreover, the cell wall of *S. aureus* is slightly more negatively charged because of the presence of teichoic acids in their cell walls (22). As a result, Ti-Fn-SA surfaces by being considerably more hydrophilic than Ti-Fn alone substrate facilitate enhanced binding of osteoblasts.

The strength of the ECM and osteoblast interactions in the presence and absence of dead *S. aureus* can also be a contributing factor for observed differences in cell adhesion on both substrates. Successful formation of bone requires continued dialogue between osteoblasts and components of the extracellular matrix (ECM), such as

fibronectin, type I collagen etc. Such communication between cells and the ECM is mediated by a family of cell surface receptors called integrins (21, 23). It is known that the affinity of Fn binding to the $\alpha_5\beta_1$ - integrin receptor, present on the osteoblast surface, is much lower with a $K_d = 8 \times 10^{-7}$ M compared to binding of *S. aureus* to fibronectin. Through its fibronectin-binding receptor (FnBP), there is an irreversible interaction with a dissociation constant of $K_d = 1.8 \times 10^{-9}$ M (16). Also, in addition to FnBP, other MSCRAMMs present on the *S. aureus* surface may subsequently interact with other ligands of the extracellular matrix as the matrix production ensues, further ‘cementing’ the osteoblasts in a cohort of multivalent ECM-cell interactions as outlined in Figure 8. Therefore, single process interaction of fibronectin (Fn) with integrin on the osteoblast surface is weaker in strength than the array of processes possible between osteoblasts and ECM are potentiated by the surface receptors of the interlying bacteria.

The developmental phase of an osteoblast involves three stages- proliferation, extracellular matrix synthesis and mineralization. Therefore, a temporal sequence of events in osteoblast differentiation is characterized by a) active proliferation of osteoblasts, which is accompanied by the onset of expression of the enzyme alkaline phosphatase b) synthesis of high levels of several collagens (type I primarily) and other non collagenous proteins such as osteocalcin and osteopontin, and c) deposition of the mineral component, hydroxyapatite (CaPO_4) in the extracellular matrix (50). We measured rates of proliferation of osteoblasts cultured on both Ti-Fn+/- *S. aureus* by liquid scintillation analysis. In spite of increase in cell attachment and adhesion on Ti-Fn-SA surfaces compared to Ti-Fn alone, osteoblast proliferation occurred equally well on both substrates, revealing no significant differences at all times of incubation. One

possible explanation is that osteoblasts on Ti-Fn-SA surface, which demonstrate increase in all indices of bone formation (Figs. 5-7, table 1), may auto-regulate their proliferation rates to prevent aberrant bone deposition which is a likely scenario if there is increased cell proliferation. Also, Stein *et al* have discussed the existence of a restriction point in the developmental sequence of an osteoblast where a decrease in osteoblast proliferation is coupled with the subsequent induction of genes associated with matrix maturation and mineralization (50). Therefore, proliferation of osteoblasts grown on Ti-Fn-SA may be down-regulated following the onset of a more differentiated phenotype on the alloy surface (Figs. 5-7).

We next examined the synthesis of collagen and osteocalcin which are the key proteinaceous constituents of the extracellular matrix synthesized by osteoblasts. In this study, osteoblasts grown on Ti-Fn surfaces coated with dead *S. aureus* were found to express insoluble collagen at similar levels when compared to the uncoated levels up to 6 days in culture, followed by a significant increase at later time points (Fig. 5). Osteocalcin production is also significantly upregulated on bacteria-coated alloy compared to Ti-Fn surface up to 3 weeks of culture (Table 1). These results suggest that osteoblasts cultured on dead *S. aureus*-coated titanium alloy demonstrate a more differentiated phenotype compared to their counterparts grown on Ti-Fn alone. Given that cell adhesion, a necessary pre-requisite for subsequent cell functions on biomaterials was enhanced in the presence of the bacteria, it is corroborative that synthesis of an extracellular matrix on bone-biomaterial interface is increased on the Ti-Fn-SA surface.

It is well documented that osteoblast differentiation and responses during osseointegration are affected by implant surface topography and that increasing surface

roughness of implants is greatly beneficial to their biological performance as osteoblast differentiation is enhanced on rougher biomaterial surfaces (7, 30, 44-46). Compared to smoother surfaces, osteoblast proliferation on rough surfaces is impaired and phenotypes of cells cultured on rough surfaces shows attributes of more differentiated osteoblasts, such as increased osteocalcin, ALP production and mineralization activity (8, 44-46). These findings suggest that coating the Ti surfaces with dead bacteria could render the surface 'rougher' compared to Ti alloy alone which can explain the enhanced differentiation of osteoblasts on bacterial-coated surfaces versus uncoated surfaces.

Another aspect of osteoblast differentiation is the mineralization of bone matrix which occurs by deposition of apatite (CaPO_4) component along the collagen framework. Alkaline phosphatase (ALP), an enzyme characteristic of the bone phenotype, is essential for matrix mineralization as it cleaves α -glycerophosphate to release inorganic phosphate that comprises the phosphate phase of the apatite component. Non-collagenous proteins such as osteocalcin also support the deposition of the mineral phase. Our findings demonstrate that the difference in ALP activity between Ti-Fn-SA and Ti-Fn alloy was maximal on day 6 and is insignificant at later time points (Fig. 6). These results are consistent with earlier findings where increased osteocalcin together with enhanced cell layer alkaline phosphatase activity have also been demonstrated on osteoblasts cultured on Ti surfaces with high surface energy (56), as is the case with Ti-Fn-SA alloy. As shown in Fig. 7, osteoblasts also showed a dose-dependent and kinetic increase of apatite deposition on surfaces coated with dead bacteria as early as day 7. Bellows *et al* have demonstrated that initiation and progression of mineralization are separate phenomena and that alkaline phosphatase is critical for the former but the progression of matrix

mineralization is ALP-independent (3). Given the sustained mineralization activity demonstrated by osteoblasts on both surfaces at day 14 and 21, and the especially enhanced mineral deposition in the presence of dead bacteria, there must be other ALP-independent phenomena that facilitate mineral deposition on the Ti-Fn-SA surface. One possible explanation is that the presence of both hydroxyl groups and an overall negative charge on *S. aureus* cell walls facilitate the deposition of calcium and phosphate ions on Ti-Fn-SA surfaces.

It is possible that the above changes in gene expression, following the interaction of the osteoblasts with the extracellular matrix components on the Ti-Fn-SA implant surface, occur as a result of differences in integrin-mediated cell adhesion and shape, which in turn can influence regulation of downstream signaling cascades as demonstrated in other studies (47). One potential downstream target molecule could be Runx2/ Cbfa1 (Core binding factor $\alpha 1$), a DNA-binding transcription factor that is critical for regulation of osteoblast differentiation and for the development of a mineralized phenotype. It can positively upregulate genes responsible for matrix synthesis (type I collagen, osteocalcin, osteopontin) by binding to the promoter of major osteoblast genes (14, 55).

In conclusion, Ti-Fn alloy coated with dead *S. aureus* has been shown here to promote osteoblast adhesion, sustain cell proliferation and enhance the expression of a mineralized extracellular matrix. Collectively, these findings support our hypothesis that inactivated *S. aureus* enhances osseointegration on implant surfaces. Thus, further investigations are warranted to determine the biocompatibility and osseointegration of Ti-Fn-SA alloy in animal models.

FIGURES

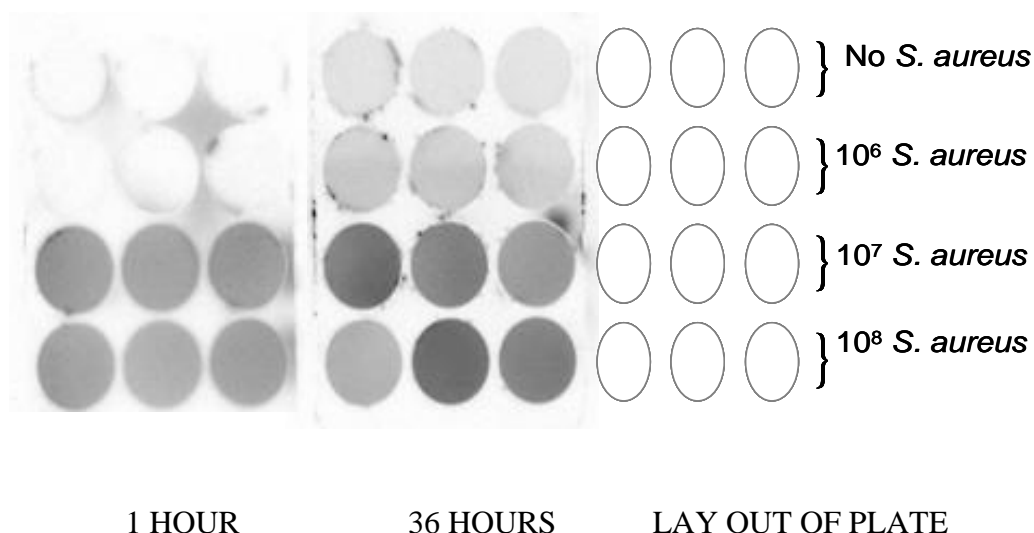


Figure 1. Osteoblast attachment to Ti-Fn and Ti-Fn-*S. aureus*-coated culture dishes at 1 and 36 hours of incubation. Cells were cultured in standard osteoblast growth medium supplemented with 5 $\mu\text{Ci/ml}$ ^{35}S -methionine. The emission density, indicative of relative number of osteoblasts attaching to each substrate, was detected using phosphor-screen autoradiography. The data are representative of three separate experiments performed in triplicate.

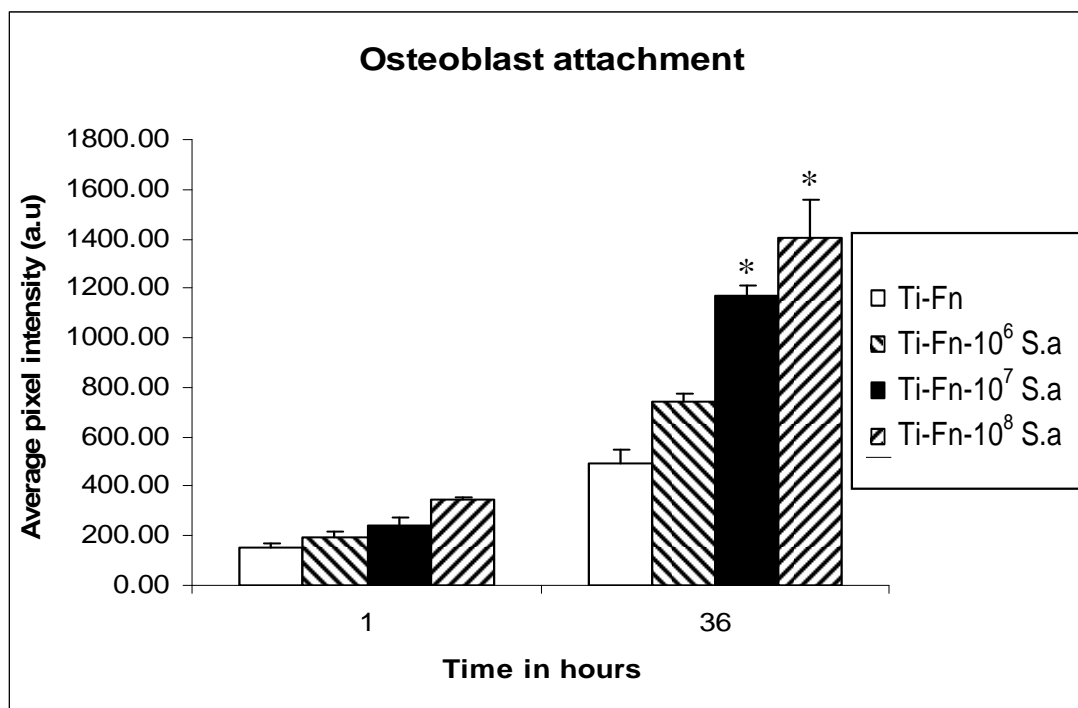


Figure 2. Average pixel intensity, an index of osteoblast attachment, as measured from Ti-Fn and Ti-Fn-*S. aureus*-coated culture dishes following 1 and 36 hours of incubation. Pixel intensity was calculated using the appropriate image phosphor software. Results are expressed as means \pm SEM. The data are representative of three separate experiments performed in triplicate. * $p < 0.05$ compared to Ti-Fn at 36 hr.

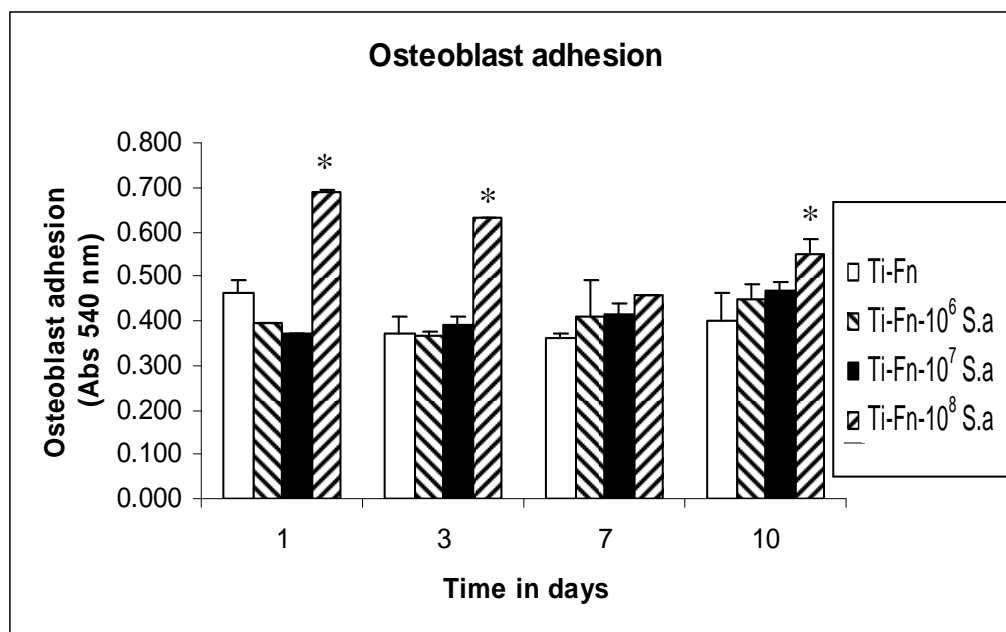


Figure 3. Osteoblast adhesion to Ti-Fn and Ti-Fn-*S. aureus*-coated culture dishes at 1 and 36 hours of incubation. Cells were treated with MTS dye and formation of formazan product, proportional to the number of adherent cells, was spectrophotometrically measured at 540 nm. Results are expressed as means \pm SEM. The data are representative of three separate experiments performed in triplicate. * $p < 0.05$ compared to Ti-Fn at all time points.

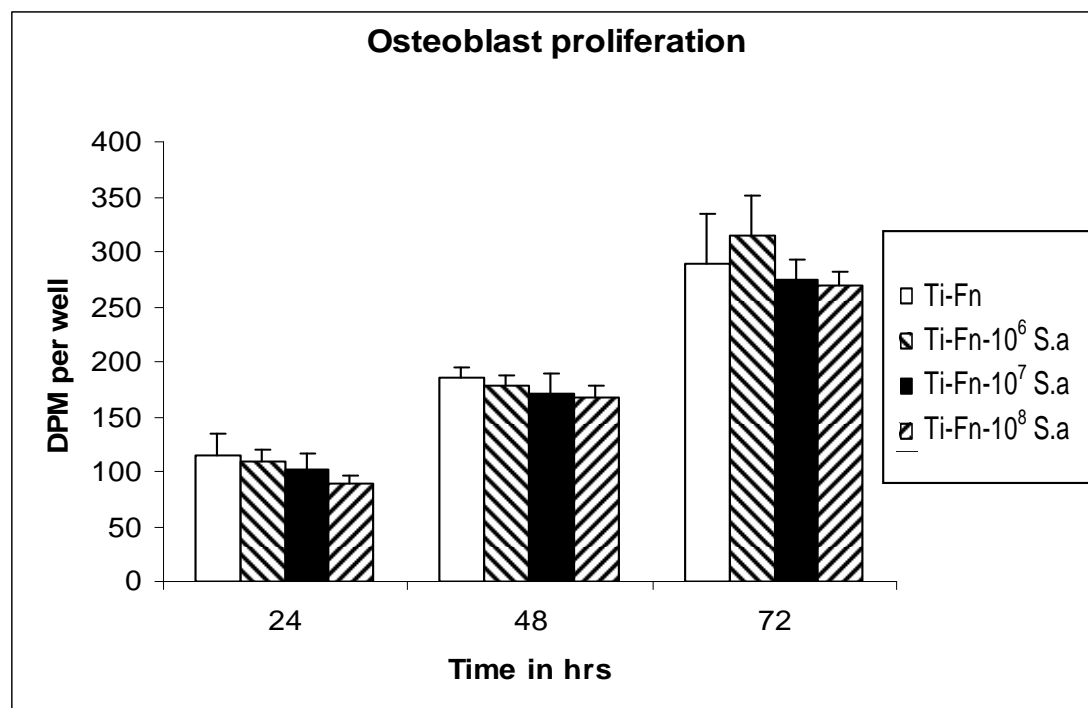


Figure 4. Osteoblast proliferation rate as measured from Ti-Fn and Ti-Fn-*S. aureus*-coated culture dishes following 24, 48 and 72 hours of incubation. Cells were cultured in standard osteoblast growth medium supplemented with 0.5 $\mu\text{Ci/ml}$ tritiated thymidine (^3H). Disintegrations per minute were determined by measuring ^3H incorporation. Results are expressed as means \pm SEM. The data are representative of three separate experiments performed in triplicate.

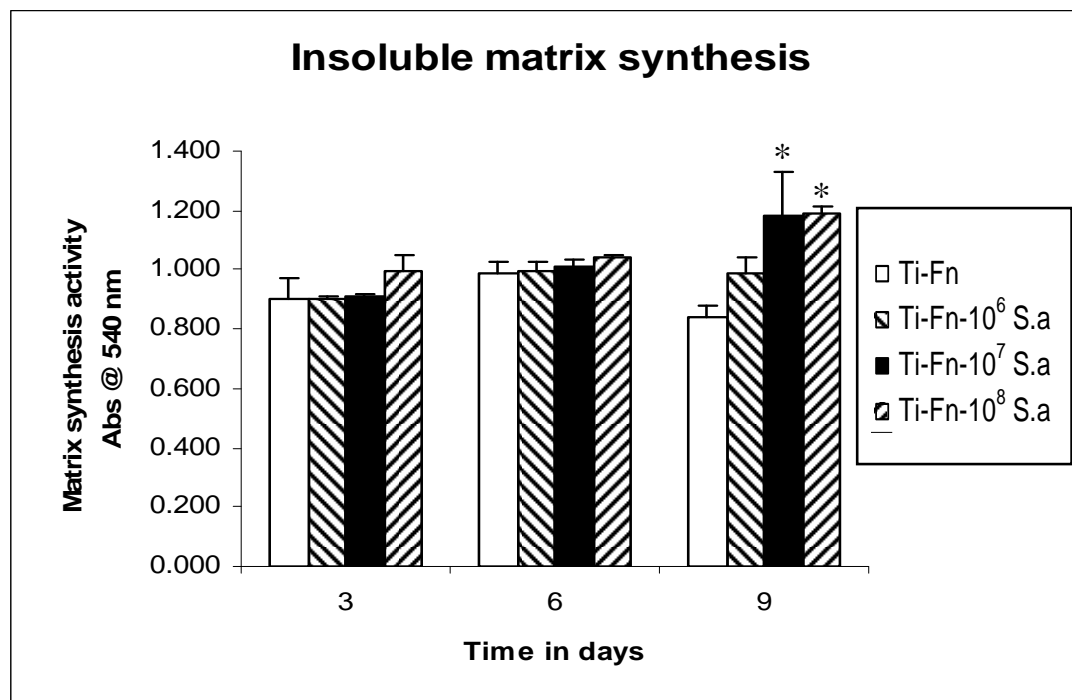


Figure 5. Insoluble collagen matrix synthesis activity by osteoblasts on Ti-Fn and Ti-Fn-*S. aureus*-coated culture dishes following 3, 6 and 9 days of incubation.. Cells were cultured and stained with Sirius red F3B to quantify total collagen synthesis. After elution with NaOH, total absorbance of the released dye was measured spectrophotometrically at 540 nm. Results are expressed as means \pm SEM. The data are representative of three separate experiments performed in triplicate. * $p < 0.05$ compared to Ti-Fn at day 9.

Amount of osteocalcin secreted (ng/ml)	No <i>S. aureus</i>	10 ⁶ / well	10 ⁷ / well	10 ⁸ / well
7 days	< 1ng/ml	< 1ng/ml	< 1ng/ml	> 25 ng/ ml (*)
14 days	< 1ng/ml	< 1ng/ml	< 1ng/ml	> 25 ng/ ml (*)
21 days	< 1ng/ml	< 1ng/ml	< 1ng/ml	> 25 ng/ ml (*)

Table 1. Osteocalcin synthesis from osteoblasts on Ti-Fn and Ti-Fn-*S. aureus*-coated culture dishes following 7, 14 and 21 days of incubation. Concentration of osteocalcin in the cell culture supernatants was measured by ELISA. The data are representative of three separate experiments performed in triplicate. * p < 0.05 compared to Ti-Fn at the respective time points.

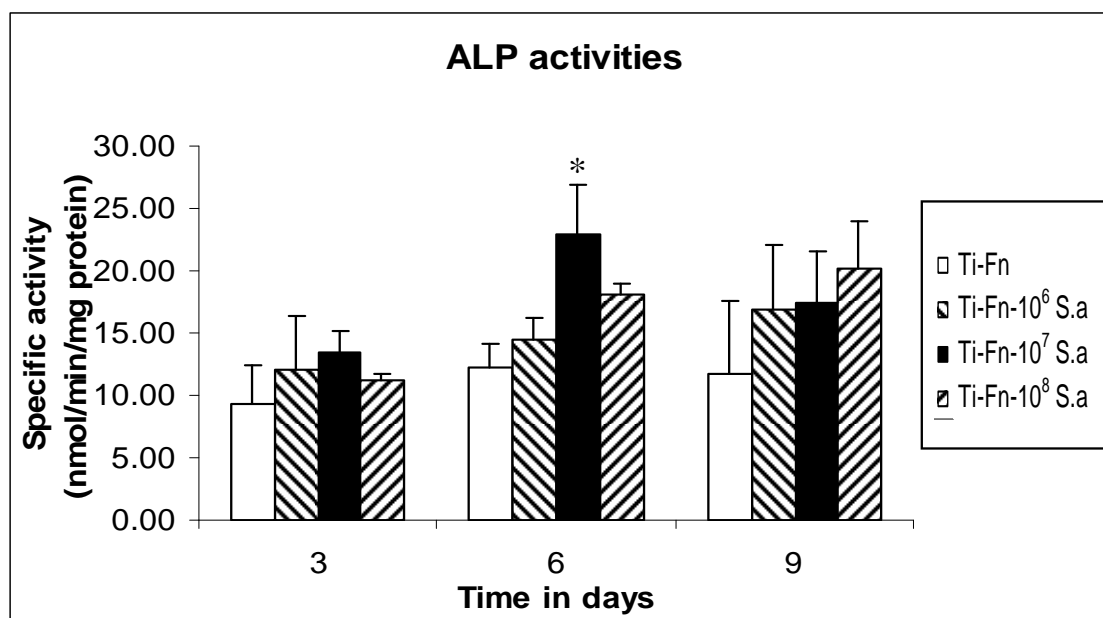


Figure 6. Alkaline phosphatase specific activity, on Ti-Fn and Ti-Fn-*S. aureus*-coated culture dishes following 3, 6 and 9 days of incubation. Cells were cultured and enzyme activity was measured by conversion of a p-Nitrophenol Phosphate (p-NPP) substrate to p-Nitrophenol (p-NP). Specific activities are expressed as nmol of p-Nitrophenol produced per minute per milligram of protein. Results are expressed as means \pm SEM. The data are representative of three separate experiments performed in triplicate. * p < 0.05 compared to Ti-Fn at day 6.

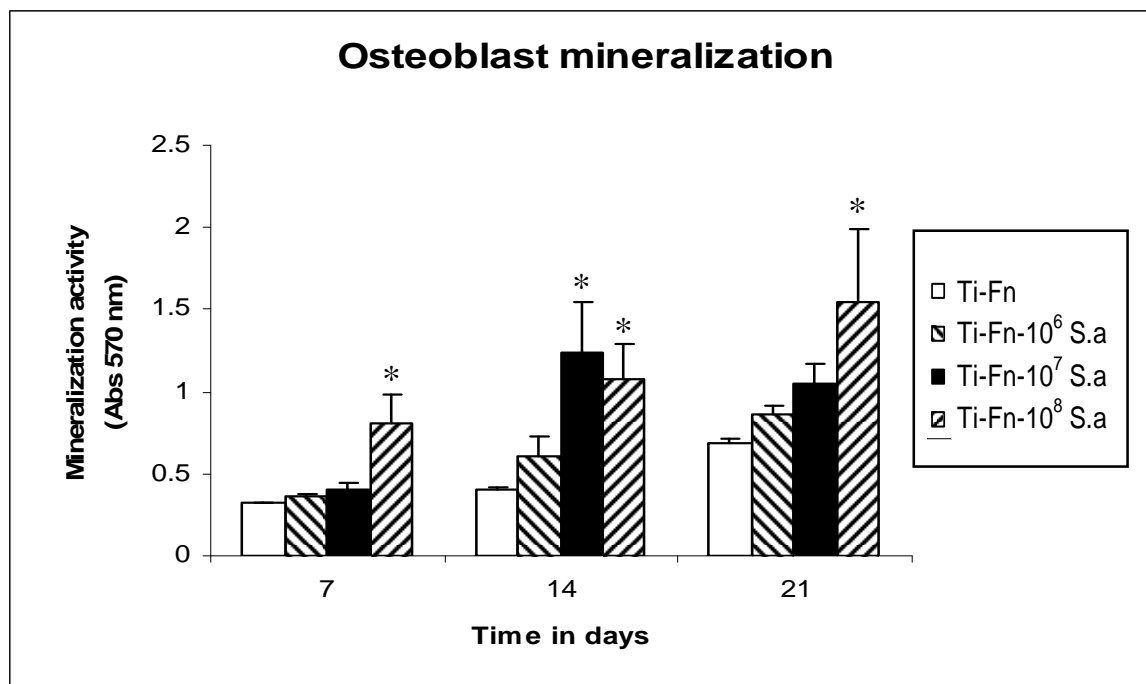



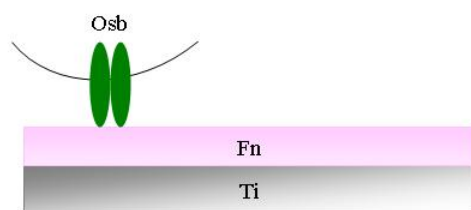


Figure 7. Osteoblast mineralization on Ti-Fn and Ti-Fn-*S. aureus*-coated culture dishes following 7, 14 and 21 days of incubation. Cells were cultured and stained with alizarin Red S to quantify the extent of mineralization. Alizarin red S was then eluted and measured spectrophotometrically at 570 nm. Results are expressed as means \pm SEM. The data are representative of three separate experiments performed in triplicate. * $p < 0.05$ compared to Ti-Fn at the respective time points.

a)

 - Fn binding proteins
 - Types of integrins
 - Other MSCRAMMs



b)

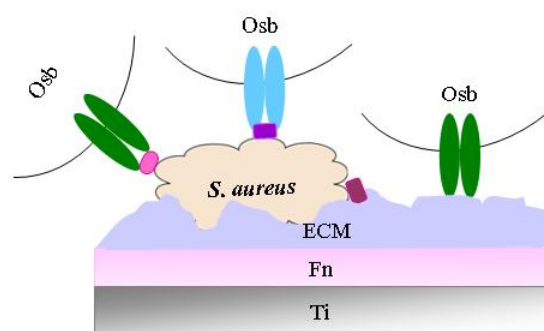


Figure 8. Schematic to describe binding interaction of osteoblasts on implant surfaces. a) Ti-Fn implant; b) Ti-Fn-SA implant, Titanium, Ti; Fibronectin, Fn; Osteoblast, Osb; Extracellular matrix, ECM.

CHAPTER 13: INTRODUCTION

Artificial joints and orthopedic implants are used to repair or restore function to damaged and diseased tissue. Following insertion, the host response to implants involves a series of events, both at a cellular and molecular level, which ideally should result in osseointegration. Depending on the surface properties and composition of the biomaterial, osseointegration has been defined either as direct bone apposition on the implant surface or indirectly, with a fibrous layer at the bone-implant surface (1, 33). The clinical success of such devices is dependent upon them fulfilling several criteria such as a) biocompatibility, b) intimate deposition of bone onto the implant surface, and c) dissipation of forces resulting from the load by the implant on to surrounding bone (32). In the long term, the newly formed bone may persist and undergo remodeling depending on the mechanical stresses it needs to transfer during load-bearing.

Of the various implant materials, titanium (Ti) and cobalt-chromium (Co-Cr) alloys as well as bioactive ceramics such as calcium phosphate, principally hydroxyapatite, and bioglass are most commonly used (32). However, Titanium alloys such as Ti-6Al-4V are the preferred material of choice for orthopedic applications as it offers excellent biocompatibility due to the interaction of its spontaneously formed oxide layer with biological fluids, resistance to corrosion and excellent mechanical properties (31, 32). However, a major disadvantage of titanium alloys as a biomaterial is that they are relatively bio-inert and do not facilitate or mediate sufficient bone growth or contact

around the implant. Considerable strategies have therefore been developed to generate either osteoconductive, providing a template for new bone growth, or osteoinductive, inducing bone formation, Ti-based biomaterials. Some of these strategies include modulating the implant surface by applying coatings of hydroxyapatite (HAP), bone sialoprotein (BSP), cell adhesion peptides; Arg-Gly-Asp (RGD) and osteotropic growth factors such as bone morphogenetic proteins: BMPs and transforming growth factor-beta; TGF- β (12, 14, 17, 34). Several studies have also examined the ability of surface textures (plasma spray coating, acid etching and sand blasting) to stimulate bone formation in vivo (30, 41, 44, 45). However, there are still long-term complications and limitations associated with these methods such as high temperatures needed for coating in case of HAP which in turn alters both mineral as well as metal structure and variable thickness of deposited coatings and their subsequent dissolution from the substrates (5, 6, 17, 41). In addition, the short half-life of osteoinductive growth factors along with their high concentrations locally can cause ectopic bone formation which is of concern in their applications. Lastly, not all of the above surface treatments involve biologically-specific receptor-mediated mechanisms.

Bone is an anisotropic and dynamic tissue consisting of cells (osteoblasts and osteoclasts), connective tissue (primarily type 1 collagen), and minerals (hydroxyapatite). Osteoblasts form a bone matrix (the osteoid) that later becomes mineralized. The extracellular matrix (ECM) secreted by osteoblasts is approximately 90% collagen and 10% non-collagenic proteins such as osteocalcin, osteonectin, sialoproteins, proteoglycans, osteopontin, and fibronectin (39). On a macroscopic scale, bone can be classified as dense areas with cavities called compact/cortical bone and areas with many

cavities called spongy/trabecular/cancellous bone. In long bones, such as the femur and tibia, the bulbous ends are comprised primarily of spongy bone surrounded by a thin layer of cortical bone. The central shaft region, the diaphysis, consists mostly of cortical bone around the bone marrow cavity. Microscopically, bone can exist as primary/immature/woven bone and secondary/mature/lamellar bone. Woven bone is temporarily formed either during embryonic development or during bone repair processes and is characterized by random deposition of collagen fibers. It is subsequently replaced by the lamellar bone which consists of organized deposition of collagen. Bone formation can also be divided into two categories: endochondral ossification, in which bone formation takes place by replacing pre-existing cartilage and intramembranous ossification, in which bone formation occurs by direct matrix deposition and subsequent mineralization by osteoblasts (35).

Staphylococcus aureus is a gram-positive bacterium capable of binding to and colonizing tissues via a collection of cell-surface adhesins referred to as microbial surface components recognizing adhesive matrix molecules (MSCRAMMs). MSCRAMMs recognizing collagen, bone sialoprotein, fibronectin, and fibrinogen mediate adherence of *S. aureus* to bone and biomaterials coated with host proteins (25). There is evidence that *S. aureus* can bind to cells (16, 37) and biomaterials (23, 24) directly. Interaction of *S. aureus* with host cells via MSCRAMMs can induce signal transduction, tyrosine kinase activity, and cytoskeletal rearrangement (15, 16). UV-killed *S. aureus* is also able to attach efficiently osteoblasts (26). Although viable *S. aureus* cells are potent inducers of immune modulator expression by osteoblasts, UV-killed *S. aureus* does not induce significant expression of such molecules (7-9). In summary, UV-killed *S. aureus* can

tenaciously bind biomaterials and effectively colonize bone which can initiate cell-signaling cascades that can potentiate osteogenesis. These are an intriguing combination of properties with respect to bone-implant interfaces and the current work addresses the efficacy of *S. aureus* as a novel osteoconductive coating for bone-associated biomaterials.

In the previous chapter, we investigated the in vitro effect of coating Ti surfaces with dead bacteria on osteoblast functions pertinent to new bone formation. Osteoblast differentiation on Ti-6Al-4V alloy coated with fibronectin (Ti-Fn) surfaces was compared to Ti-Fn surfaces coated with UV-killed *S. aureus* (Ti-Fn-SA). Fibronectin was chosen to pre-coat the polymer surface as it is pre-adsorbed on all biomaterials following insertion and is considered to be the model host protein that promotes *S. aureus* attachment to biomaterial surfaces (3, 43). Results of those studies, discussed in the preceeding chapter, demonstrate that compared to the Ti-Fn surface, osteoblast attachment and adhesion was enhanced on Ti-Fn surface coated with bacteria. On both substrates, cell proliferation was sustained at comparable levels while markers of osteoblast differentiation such as collagen, osteocalcin, alkaline phosphatase and mineralized nodule formation were increased on Ti-Fn-SA alloy compared to control surfaces. The present study was designed to evaluate the tissue response to Ti-Fn-SA implanted in rat femurs. The pilot data, from histological and electron microscopy studies, showed no significant inflammatory response and also demonstrated that the osteoconductivities of both surfaces, Ti-Fn and Ti-Fn-SA, are comparable at 8 weeks post-operation. Further studies to evaluate the mechanical strength of the implants are warranted.

CHAPTER 14: MATERIALS AND METHODS

Animals:

Sprague-Dawley male rats (Charles River Laboratories, MA) weighing approximately 450 g were used in this study. All the animals were housed in a temperature-controlled room and were given water and food *ad libitum* throughout the study. The IACUC of University of North Carolina at Charlotte approved the experimental protocol used in this study.

Implant material preparation:

Orthopedic implant grade Ti-6Al-4V wires were a generous gift from Perryman Company, PA. Ti wires were then trimmed to 15 mm in length and 1.64 mm in diameter and sterilized with 100% alcohol and stored until use. Wires were then treated with osteoblast growth medium (OBGM) supplemented with rat fibronectin (hereby abbreviated as Fn) (Affiland Company, Belgium) at a concentration of 2 µg/ml for 24 hr at 37° C. Following incubation, wires were rinsed with Hank's balanced salt solution (HBSS) to remove unbound Fn. Ti wires were incubated an additional 24 hr with 10⁸ UV-killed *S. aureus*. For all experiments, Ti-Fn coated wires with no bacteria (hereby abbreviated as Ti-Fn) served as controls for comparison with bacteria-coated surfaces (hereby abbreviated as Ti-Fn-SA). Following incubation, wires were rinsed with HBSS to remove unbound bacteria and implanted inside rat femurs during the surgical procedure.

Bacterial strain, growth conditions and UV-killing:

S. aureus strain UAMS-4 is a co-isogenic mutant of osteomyelitis-clinical isolate UAMS-1 (ATCC 49230) with an inactivated *agr* (accessory gene regulator) locus (18). The *agr* locus encodes a trans-activator of multiple *S. aureus* virulence-associated genes and is also responsible for growth-phase-dependent expression of cell surface and secreted virulence factors. The *agr* locus is inactive during exponential growth where cell surface adhesins are maximally expressed (36). Entry into stationary phase results in activation of *agr*, down-regulation of cell surface adhesins, and up-regulation of secreted proteins. Therefore, *agr* mutants retain the ability to colonize host tissue, but demonstrate decreased virulence (18, 36). UAMS-4 was grown overnight in 15 ml of tryptic soy broth (TSB) supplemented with erythromycin (5 µg/ml) (Em5) at 37°C with aeration. Ten ml of this overnight culture was then transferred to 1 liter of TSB-Em5 and grown for 3 hr in conditions as described above. Bacteria were harvested in the resulting exponential phase to ensure maximal expression of cell surface adhesions. Cells were harvested by centrifugation at 4300 x *g* at 4°C for 10 min and washed in HBSS. Bacteria were killed by exposure to short-wave (254 nm) ultraviolet radiation for 5 min and centrifuged at conditions described above. Subsequently, bacteria were suspended in OBGM to give the final concentration of 1 to 5 x 10⁸ colony-forming units (CFU/ml). To verify successful killing, aliquots of the cell suspension were plated on tryptic soy agar (TSA) supplemented with erythromycin (10 µg/ml) (Em10), followed by incubation for 24 h at 37°C.

Surgical procedure:

Thirty minutes prior to surgery, rats were given 0.05 mg/kg buprenorphine HCL (Reckitt and Colmant Pharmaceuticals Inc., VA) and 5 mg/kg Carprofen as analgesics. Animals were then anesthetized by utilizing isofluorane and the skin of the left femur was shaved and cleaned with 70% ethanol. Under aseptic conditions, the skin, muscle fascia and periosteum were retracted using an 18-gauge needle to gain access to the distal epiphysis. A Dremel drill with a 1.5 mm autoclaved bit was used to penetrate the cortical bone of the patellar groove to gain access to the femoral medullary canal. The canal was further reamed with a 16-gauge needle and the implants (Ti-Fn or Ti-Fn-SA) were press-fitted into the shaft of the femur. Some holes were left empty as controls which would constitute the 'reaming' only experimental group. One femur was operated per animal and the contralateral femur was utilized as the unoperated control. After insertion of the implant, the skin was sutured using autoclips. Postoperative analgesia was ensured by subcutaneous injection of buprenorphine HCL (Reckitt and Colmant Pharmaceuticals, Inc., VA) (0.05 mg/kg) every 12 h for 24 h. If the animals were weight-bearing on the operated leg and were ingesting rodent chow daily, buprenorphine were discontinued after the 24 h. The site of insertion was examined for 48 h following surgery, quantity of food consumed was monitored for a week following surgery to observe any signs of malaise and the animals were weighed weekly until the day of sacrifice. Any animal that demonstrated either hematoma formation at the wound site, lack of weightbearing on the operated leg after 24 hours or lack of appetite with associated weight loss were immediately euthanized.

Tissue harvesting:

Rat femurs, both operated and unoperated, were harvested 1, 4 and 8 weeks following implantation of the Ti wires. Animals were anesthetized with pentobarbital sodium administered intraperitoneally at the dose of 110 mg/kg and perfused via the cardiac aorta with 1X Phosphate buffered Saline (PBS) (for electron microscopy) or with 1X phosphate buffered saline (PBS) followed by buffered-formalin fixative (for Masson-Goldner and TRAP staining). The operated femurs were harvested with implants inside them and dissected free of soft tissue and muscle. The position of all implants was verified by radiological analysis and it was observed that none of the implants traversed past the mid-diaphysis region (Fig. 1). Those animals whose implants weren't inserted inside the femoral shaft were omitted for the purpose of experimental analysis. Based on the radiological location of the implant, a Dremel drill with a rotating bit was used to approximately generate three equal sized transverse fragments of the femoral region that encompassed the implant while the implant was simultaneously removed. For the purpose of analysis, the resulting fragments; A, B and C, were labeled progressing from the proximal end of the mid-shaft region towards the distal epiphysis. This systematic sectioning technique assured that the sectioned bone area was representative of the entire length of the inserted implant. Masson-goldner, toluidine blue followed by electron microscopy and TRAP staining were performed on bone specimens to examine the bone-implant interface and determine osteoclast numbers respectively.

Masson- Goldner trichrome staining:

Bone specimens A, B and C from each leg of each animal were fixed in 10% buffered formalin for 24 h at 4°C, were placed in 70% ethanol until dehydration, trimmed

at the ends, dehydrated and embedded in methyl methacrylate as described previously (22). Briefly, specimens were dehydrated in 95% and 100% ethanol and embedded in a final working solution of 85% methyl methacrylate, 10% glycol methacrylate, 5% dibutyl phthalate and 5% (w/v) polyethylene glycol. Undecalcified sections perpendicular to the long axis of the bone shaft were cut 5 μ m from the distal end of each embedded bone block using a Leica microtome, collected in tissue culture plates and stained as described previously (19). Sections were flattened using a drop of distilled water and stained for 7 min using a 1:1 Harris hematoxylin: Ferric chloride mixture solution (1.25 g of Hematoxylin in 100 ml of 25% Ethanol: 2.5 g Ferric Chloride in 1 ml of Concentrated HCl and 99 ml of distilled water). The stain was removed, sections rinsed twice with warm tap water and incubated in 2:1 Ponceau deoxylidine-acid fuchsin staining solution (1 g of Ponceau deoxylidine in 1 ml of glacial acetic acid in 100 ml of distilled water: 1 gm of acid fuchsin in 1 ml of glacial acetic acid in 100 ml of distilled water) for 5 min. The stain was removed and sections rinsed with 1% acetic acid. 1% Phosphomolybdic acid solution was applied for 6 min, stain removed and rinsed with 1% acetic acid. Sections were stained with light green staining solution (0.15 g Light Green Yellowish SF in 0.2 ml glacial acetic acid in 100 ml of distilled water) for 2 min, de-stained and rinsed twice with 1% acetic acid. Sections were dried on bibulous paper overnight, rinsed in 2% ethanol in xylene to clear and soften and mounted using Permount® solution. All reagents were obtained from Sigma Aldrich Co. The stained sections were evaluated and scored in a blinded manner for different parameters adapted from a previous report by Jansen et al. (28) (Table 1). Specifically, qualitative parameters related to bone reparative

process such as presence of inflammation, woven bone (immature), lamellar bone (mature) and soft tissue fibrosis were noted.

Tartrate- resistant acid phosphatase (TRAP) staining:

Bone specimens A, B and C from each leg of each animal were fixed in 10% buffered formalin for 24 h at 4°C, were placed in 70% ethanol until dehydration, trimmed at the ends, dehydrated and embedded in methyl methacrylate as described previously (22). Briefly, specimens were dehydrated in 95% and 100% ethanol and embedded in a final working solution of 85% methyl methacrylate, 10% glycol methacrylate, 5% dibutyl phthalate and 5% (w/v) polyethylene glycol. Undecalcified sections perpendicular to the long axis of the bone shaft were cut 5 µm from the distal end of each embedded bone block using a Leica microtome, collected in tissue culture plates and stained as described previously (21). 1 ml of pararosaniline solution was added to sodium nitrite solution (60 mg of sodium nitrite in 1 ml of water). Twenty five ml of sodium acetate working buffer was added to the above solution and pH was adjusted to 5.0 using NaOH. Naphthol AS-TR phosphate solution (1 mg of Naphthol AS-TR phosphate dissolved in 2 ml of N-N-dimethylformamide) was added to the former solution along with 1 ml of sodium tartrate and 10 drops of 10% MnCl₂ to make the substrate solution. Sections were stained with this substrate solution for 1 h at 37°C and rinsed with distilled water. Counterstaining was achieved by incubating sections for 1 min in the following solution: 1 part of 3.9 ml working thionin (5.5 mg thionin in 42 ml water) and 1.2 ml working methyl green (0.1 g Methyl green in 100 ml water) mixed with 13.5 ml 0.02 M citrate buffer (15 ml of solution A [4.2 g of citric acid in 1 L distilled water] and 85 ml of solution B [5.9 ml of sodium citrate in 1 L distilled water]) solution mixed with 4 parts of 0.02 M citrate

buffer). Sections were rinsed with distilled water, dried on bibulous paper overnight, rinsed in 2% ethanol in xylene to clear and soften and mounted using Permount® solution. All reagents were obtained from Sigma Aldrich Co. TRAP-positive cells on the bone surface were visualized via light microscopy as cells containing reddish pink dye deposits. The number of TRAP-positive cells was enumerated from different sections in a blinded manner by visualizing 5 random fields of view around the implant site with an original magnification of 40X objective.

Transmission electron microscopy:

Bone specimens A, B and C from each leg of each animal were fixed in Karnovsky's fixative (3% glutaraldehyde, 3% paraformaldehyde, 0.15% CaCl_2 in 0.2 mol/L sodium cacodylate buffer [pH 7.3]) at 4°C for 24 h and then decalcified in Rapid Bone Decalcifier solution (American MasterTech Scientific, CA) for 24-48 h (depending on the age of the animals). Following decalcification, bone fragments were trimmed at each end and three slices were cut from each end such that the interface is more maximally exposed compared to the outer cortical bone surface (Fig 1b). The bone sections were then rinsed twice in 0.2 M cacodylate buffer (pH 7.6) for 40 sec, post-fixed in 2% osmium tetroxide supplemented with 2% ruthenium red in 0.4 M cacodylate buffer (pH 7.6) for 6 min, again rinsed twice in 0.2 M cacodylate buffer (pH 7.6) for 40 sec, dehydrated in a series of ethanol (50, 70, 95, 100 and 100%) for 40 sec each and lastly embedded in Spurr's resin as described previously (38). To obtain representative sections for examination via electron microscopy, blocks were thick sectioned (0.9 μm) and then stained for 2-5 secs in 1% toluidine blue and 1% tetraborate. Following examination of the thickened sections via light microscopy, blocks were selected for thinning and ultra thin

sections (95 nm) of bone were cut with a diamond knife on an ultramicrotome. Sections were collected on thin-bar hexagonal, 200-mesh copper grids and stained for 15 min with 2% uranylacetate in 25% ethanol followed by 5 min in a modification of Sato's triple lead citrate (1% Pb nitrate, 1% Pb acetate, 1% Pb citrate, 2% Na citrate, 0.72% NaOH) and viewed at 60 KV on a Phillips CM10 transmission electron microscope (Phillips, Netherlands).

CHAPTER 15: RESULTS

Ti-Fn and Ti-Fn-SA wires were inserted inside the medullary cavity of rat femurs for 1, 4 and 8 weeks. Following reaming, some holes inside the femurs were left empty to examine the bone response in the absence of the biomaterial. One femur was operated on per animal and the contralateral leg was evaluated as an additional control. Following implantation, all animals ambulated normally within 12 h after surgery and were weight-bearing on the operated leg with no evidence of swelling at the insertion site. However, the reaming only animals all developed hematomas at the surgery site within 24 h after surgery and had to be euthanized. For the Ti-Fn and Ti-Fn-SA groups, X-rays taken on the day of the sacrifice revealed that the implants weren't inserted inside the majority of femurs and those which were implanted successfully were located inside the medullary space extending from the distal epiphysis towards the diaphysis (Fig. 1). Amongst the inserted implants, some were positioned more prominently in the distal epiphysis-metaphysis area while the others were lodged more proximally in the metaphysis-diaphysis area. As indicated in Fig. 1, fragments A, B and C were obtained from the length of the bone that approximately traverses the implant. Sections were obtained from each fragment as outlined in Fig. 1 and the interface was observed using Masson-Goldner (MG) stain, Toluidine blue (TB) stain and by transmission electron microscopy (TEM). Masson- Goldner discriminates mineralized bone matrix (stains green), immature

new matrix or osteoid (stains red), and osteoid seam, the layer between the newly deposited bone and mineralized tissue (stains magenta).

Data presented and discussed here onward are representative of fragment B only. Some of the implants that were lodged more distally were not found to be in contact within the region that encompasses fragment A and therefore results from this fragment were omitted for purpose of analysis. Data interpretation from fragment C, which was especially hard to decalcify, was complicated by the presence of native trabecular bone in the metaphysis area which couldn't be delineated from new bone formation in response to the implant. As shown in Fig. 1, this was more prominent a problem in TB and TEM data where transverse sections weren't obtained, which would have offered the advantage of an obvious implant insertion site; hence accurate estimation of new bone around the interface site wasn't possible in this region of bone. Therefore, for the purpose of predicting tissue response following implantation, the bone-implant interface was examined in fragment B only and the results are presented below.

A severe inflammatory reaction around the implant would have manifested as tissue swelling, exudate formation or redness around the wound site. However, none of the above signs were observed following surgery or at the time of sacrifice. In addition, radiological evidence of inflammation such as periosteal reaction wasn't detected in any of the implanted femurs either. Histologically, an increased influx of neutrophils and macrophages, which can be distinguished by multilobed nuclei and TRAP-positive cells outside the bone surface, respectively, can be indicative of an inflammatory environment. However, following examination of the implant interface in the Goldner-stained sections, such an exacerbated influx of inflammatory cells wasn't detected. The resident cells in

the implant interface appeared to be mostly fibroblasts, osteoblasts, osteocytes, osteoclasts or possibly, osteoprogenitor cells of mesenchymal origin (Figs. 2-6, 9).

1 week data:

By week 1, there was evidence of mineralized woven bone formation around the implant site in both Ti-Fn and Ti-Fn-SA groups as observed by Masson- Goldner stain (Fig. 2). These bone spicules consisted of mineralized matrix lined by osteoid seams which were in contact with cuboidal osteoblasts. The formation of bone in both cases proceeded from the endosteal cortex surface towards the center of the medullary cavity. Formation of a fibrous tissue layer interposed between the woven bone and the implant surface was also observed in both Ti-Fn and Ti-Fn-SA femurs, albeit thicker in the latter group. The toluidine blue stained sections along with TEM confirmed the presence of woven bony spicules as characterized by the extensive presence of both osteocyte lacunae and osteoblasts (Figs. 3 and 4). As demonstrated in Figs. 3b and 4b, fibrous tissue formation (1-3 spindle shaped elongated cell layers in thickness) was evident around the Ti-Fn insertion site, while a fibrotic 2-6 cell layer was observed in Ti-Fn-SA femurs, respectively. Goldner data obtained was representative from one animal per group while Toluidine blue/ electron microscopy data was representative of two animals per group.

4 week data:

After 4 weeks within a Ti-Fn implanted femur, more mature lamellar new bone formation was observed around the insertion site with an intervening connective fibrous tissue layer. However, in case of Ti-Fn-SA femur, extensive marrow fibrosis was observed in the area adjacent to the implant surface. Extensive new bone formation of woven character with thickened osteoid seams was observed adjacent to the fibrotic

tissue away from the implant insertion site (Fig. 5). The fibrotic tissue in the space between the implant and the woven bone was filled with a large number of oval or spindle shaped cells and lightly stained matrix.

8 week data:

After 8 weeks, trabeculae of mature lamellar bone were observed directly in contact with the implant insertion site without an intervening fibrous layer at the interface in both Ti-Fn and Ti-Fn-SA femurs. The extent of bone formation was similar in both groups (Fig. 6).

The toluidine blue and electron microscopy data following 4 and 8 weeks of implant insertion haven't been included for purpose of analysis. Some of the limitations associated with these sections were the presence of either necrotic fragments in the bone tissue that seemed to result from thermal necrosis while burring, lack of an intact implant interface due to method of sectioning employed (Fig. 1), or the presence of native trabecular bone which confounded the data interpretation.

Blinded qualitative evaluation of tissue reaction around the implant and bone implant interface of Masson- Goldner stained sections was performed using the scoring system as outlined in Table 1 and the results are represented graphically in Figs. 7 and 8, respectively. The numbers of TRAP-positive osteoclasts were measured in both Ti-Fn and Ti-Fn-SA femurs (Fig. 9). The number of osteoclasts was highest in both the implant groups following 1 week of implantation compared to 4 and 8 week time points. There was no discernable difference in osteoclast numbers between the two groups in histological sections obtained at 1 week. However, Ti-Fn-SA demonstrated a slight increase in the number of osteoclasts compared to Ti-Fn at both 4 and 8 weeks but a

statistically significant difference is hard to predict because of the small sample size in each group (n=1).

For all time points, histological sections of fragment B of contralateral unimplanted femurs demonstrated bone marrow next to the cortical bone as is the case in the diaphysis area of the long bones (data not shown). Although few TRAP-positive cells were observed inside the marrow cavity in the femurs, these cells weren't in contact with a bone surface and therefore weren't considered to be osteoclasts.

CHAPTER 16: DISCUSSION

The goal of osseointegration of implants is the achievement of a reliable and mechanically stable connection between the living bone and implant surface. For implant success, bone-bonding is a key factor which is established by direct formation of bone onto the implant surface. Bone formation on the implant interface involves a complex sequence of events that includes the recruitment of precursor cells, differentiation of bone cells, production of bone matrix and remodeling of the formed bone. Having demonstrated enhanced osteoblast functions on Ti-Fn-SA surfaces in vitro, we investigated the in vivo use of UV-killed *Staphylococcus aureus* as a bioactive-coating for implant materials in this study.

The portion of rat bone we have focused our results on is fragment B (Fig. 1), the midshaft region of the femur, as in this location any new bone formed would be in response to the implant only. The implant interface was observed histologically using Masson- Goldner trichrome, Toluidine blue staining and Transmission electron microscopy. TRAP staining was also done on the sections to determine osteoclast numbers. The histologic sections of the implant interface did not reveal any distinct signs of inflammation consistent with lack of any visible inflammatory signs at the implant insertion site. Particularly, apart from the cell types normally found in bone (osteoblasts, osteoclasts and osteocytes), no differences in extent of infiltrating inflammatory cells (neutrophils, macrophages) were observed between Ti-Fn and Ti-Fn-SA sections. At all

time points, we never detected cartilage and found evidence of new bone formation in fragment B (Figs. 2-6). Thus the bone healing seemed to occur exclusively through intramembraneous ossification which is believed to be the form of bone repair that occurs following implant fixation (11, 14, 40).

After 1 week, formation of both fibrous tissue and woven bone were prominent findings. The fibrous tissue was thicker in case of Ti-Fn-SA implants. The marrow cavity in both groups was filled with osteoid and mineralized matrix (Fig. 2). Toluidine blue and electron microscopy corroborated the results obtained from Goldner staining (Figs. 3, 4). The increased number of TRAP-positive osteoclasts along with woven bone observed within 1 week of implant insertion supports that bone resorption and formation occur concomitantly, which is consistent with the findings in other studies (27). Titanium is known to act as an inert yet well tolerated metal in bone and very often induces fibrous tissue formation around itself which is believed to limit the inflammatory response. After 4 weeks, a more extensive fibrous tissue layer (about 4-5 cell layer thick) was observed around Ti-Fn-SA implant compared to a thinner soft tissue layer next to the Ti-Fn implant surface. In addition, the bone formed around the Ti-Fn interface had a lamellar appearance compared to a more woven bone character with especially wide osteoid seams around the Ti-Fn-SA interface. The thick fibrous capsule around the Ti-Fn-SA implant may be especially rich in mesenchymal progenitor cells which could differentiate into either osteoblasts or fibroblasts. Cells surrounding the implant are believed to assume a fibroblastic phenotype if the space surrounding the implants consists of particles smaller than 125 μ m (10). It is possible that that while 'press-fitting' these implants, some bacteria, whose diameter would be in the order of microns, may have

been released into the surrounding site and favored the formation of the fibrous tissue immediate to the implant site. The high density of progenitor cells present inside the fibrous tissue or migrated from the endosteal surface explains the continued formation of woven bone in Ti-Fn-SA animal group following 4 weeks of insertion. While such hypercellularity can result in rapid deposition of osteoid, the rate of mineralization may not correlate with the former which could explain the occurrence of the wide osteoid seams in Ti-Fn-SA group at 4 weeks (Fig. 5). However, in case of Ti-Fn group, woven bone formed earlier appears to have been resorbed and replaced by lamellar bone (Fig. 6). After 8 weeks, both Ti-Fn and Ti-Fn-SA femora showed lamellar bone formation directly in contact with the implant surface. The osteoclast numbers at this time point had decreased, suggesting that bone formation and resorption had balanced sufficiently for the maintenance of normal bone structure. The phase between 1 and 8 weeks could be the healing period related to the removal of injured tissue at the interface and stabilizing the implant inside the bone.

A striking parallel exists between the phases of bone repair observed here and the cascade of events that occurs following marrow depletion injury inside long bones. In both, infiltration of mesenchymal cells, their differentiation into osteoblasts and osteoblast proliferation, formation of woven osteoid and calcification of this woven bone matrix, induction of lamellar bone formation in the marrow are observed. This is followed by a period of bone remodeling, during which bone resorption occurs before regeneration of bone marrow in case of marrow ablation, whereas in the case of implant insertion, some bone may still be left in contact with the implant following bone resorption (2, 4, 14, 27). The mechanical role of the residual bone is to transmit the load

from implant to the skeleton. The woven bone that appears in response to the injury is believed to be produced by endosteal osteoblasts or osteoblasts derived from progenitor stem cells inside the hematopoietic tissue (27). However, these events are influenced by the environment of the wound area and hence, also by the surface of the implant. Depending on the implant site, other environmental factors determine whether mesenchymal cells differentiate into fibroblasts, osteoblasts or chondrocytes. It is possible that the first osteoblasts to arrive at the biomaterial interface may secrete soluble or insoluble factors that can recruit more osteoblasts in the vicinity which can explain the intense proliferation observed. Some of these factors include local osteoinductive factors such as bone morphogenic protein (BMP) and other growth factors such as Transforming growth factor (TGF), Fibroblast growth factor (FGF), and insulin-like growth factor (IGF) which can stimulate osseous proliferation, differentiation and extracellular matrix synthesis (42).

Compared to our in vitro data which demonstrated increased osteoblast functions on Ti-Fn-SA versus Ti-Fn surfaces, we didn't observe as dramatic an effect following implant insertion in femurs. In vitro models are more static compared to the dynamic environment the implant is exposed to in vivo. Some of the additional variables in vivo include implant design, device load, interaction of different cell types, exposure to biological fluids such as serum etc. In addition, given the small sample sizes of our in vivo groups and other important considerations such as dose of bacteria in the coating and method of delivery, which may be critical but not easy to control, neutral findings associated with use of killed *S. aureus* need to be interpreted with caution before it is concluded that a given approach lacks utility. For instance, we propose that the available

surface area and therefore amount of adherent bacteria on the implant surfaces may account for the difference in trends between the in vitro and in vivo responses. The surface area of the implant available for bacterial binding was much less in vivo compared to in vitro. As a result, the implant surface on the thin Ti wire inserted inside the femur may not have been as saturated with bacteria as it was on the in vitro surface, whereby the initial adhesion step, which was much enhanced in vitro, may be compromised in vivo and may lead to decreased osteoblast binding and a subsequent decrease in bone apposition around the implant surface. When we enumerated the numbers of live bacteria bound on the implant surface coated under similar conditions as the UV-killed bacteria, we found almost a four-log drop in the numbers of bacteria compared to the highest possible dose of bound bacteria observed in vitro. Also, given that the implants were 'press-fitted' into the medullary cavity after reaming, the shear stress involved in inserting the implant may be more than sufficient to dislodge the bacteria from the implant and deposit them in the dead space between the implant and bone thereby initiating undesired responses. As a result, the bacteria were most likely engulfed by fibrous tissue to occlude it which can also explain the increased thickness of fibrous layer in Ti-Fn-SA implants compared to Ti-Fn only following 1 and 4 weeks of implantation. The dislodged bacteria may create an insulating barrier around the implant at 4 weeks which may prevent the direct apposition of bone around the implant. Assuming that bone deposition on implant entails that osteoblasts first be in the vicinity of implant surface, it is understandable that unless the insulating barrier of fibrous tissue be cleared, apposition of osteoblasts and subsequent bone deposition will not commence. We therefore conclude that the Ti-Fn-SA implants failed at the Ti-SA interface instead of

at bone-implant interface and postulate that a more appropriate presentation of bacteria on the prosthesis would result in improved direct bone-implant contact.

The qualitative examination of a few histological sections as reported in this study permits no assessment of osseointegration from a mechanical standpoint between the Ti-Fn and Ti-Fn-SA groups. Although the bone-implant contact isn't significantly different among the two groups, the pull out strength of the Ti-Fn-SA implant was much higher than Ti-Fn alone among three of the animals tested as evaluated in a blinded fashion. The results of some studies indicate that the percentage of surface coverage of implant with bone is not as sensitive an indicator of osseointegration as mechanical tests are (13, 45). Specifically, implants which had higher pull out strengths did not necessarily show increased bone coverage or bone-implant contact compared to groups that were less integrated in the tissue. This poor correlation between the effect of the coating and on bone-implant contact suggests that there may be other parameters that might be critical such as more bone ingrowth in the nanometric pits of the Ti-Fn surface coated with bacteria which could generate more potent bone interlocking at the implant interface (13). It is therefore likely that *S. aureus* coating did have a mechanical effect, but that it simply was not detectable as these pits are under the resolution power of the techniques utilized in this study. It is essential to conduct pull out tests in future studies so as to measure the mechanical fixation of the implant which is an important consideration to evaluate the functional competence of the regenerated bone.

The fact that there wasn't a marked difference in bone formation between the Ti-Fn and Ti-Fn-SA surfaces may also likely be due to our smooth implant model which doesn't offer as much surface area for bony interlock. This issue can be overcome in

future studies by either ‘roughening’ the surface texture by sandblasting/ acid etching the Ti surface or by using threaded implant designs before coating with bacteria. Increasing roughness creates more surface area for interdigitation of bone which leads to more pull out force.

In the course of this pilot study, we made other observations that would contribute towards an improved animal model in the future. For instance, in some toluidine blue stained sections, we observed tissue fragments that appeared to be an artifact as a result of thermal necrosis following high speed drilling (data not shown). Irrigating the medullary cavity with cold saline before implant insertion can reduce the thermal injury and also flush out bone debris generated during the drilling process itself. It is also crucial when making histologic and morphometric measurements in bone that the sampling sites are accurate in all groups and the sections be obtained in the appropriate plane with no obliquity.

In the chosen rodent model, bone activity changes in response to the implant were confounded greatly by bone formation associated with endochondral ossification that invariably accompanies growth cartilage activity in the epiphysis during normal elongation of long bones in rats. This observation was especially prevalent in fragment C and was therefore excluded for the purpose of data analysis. For future studies, we recommend using animal models with fused epiphysis as they would retain bone remodeling without bone elongation. In the case of rats, growth plate cartilages close earlier in females than in males, such that bone elongation ceases at an age where useful experimental time for implant studies still remains (29). Using animal models with fused epiphysis in conjunction with a fluorochrome label as a marker for bone formation will

clearly demonstrate the extent and rate of new bone deposition. In this regard, tetracycline labeling is a commonly used fluorochrome that binds to calcium exclusively on newly mineralizing bone surfaces. By administering different colored tetracyclines at various times during the duration of study and before sacrifice, rate of new bone formation can be measured (20).

In contrast to the implant groups, our reaming only group demonstrated hematoma formation at the surgery site and animals were moribund following surgery. It is possible that the access hole in the reaming groups may not have been small enough to enable the control of bleeding by mere closure of the skin incision and the debris resulting from the drilling may have potentiated the inflammatory response at the site. Preliminary data have indicated that it is possible to subvert this problem in the future by cauterizing the blood vessels in the medullary canal to stem the bleeding. In case of Ti-Fn and Ti-Fn-SA groups, the process of inserting the implant inside the drilled cavity may have eliminated some debris and also served to plug the influx of excess fluids. The contralateral unoperated leg showed no signs of bone remodeling in the diaphysis region at any times thus indicating that the factors released during injury on the operated leg had only local and not systemic effects.

In this context of an animal model with inherent limitations, the most remarkable in vivo observation of this pilot study was the stimulation of new bone formation around the Ti-Fn-SA implant, i.e, the osteoconductiveness of the implant. Clearly, more rigorous in vivo studies and mechanical testing with greater sample sizes must be carried out before recommending this material for hard tissue implant applications. In summary, this

preliminary study indicates that Ti-Fn-SA has the potential as a candidate implant coating.

FIGURES

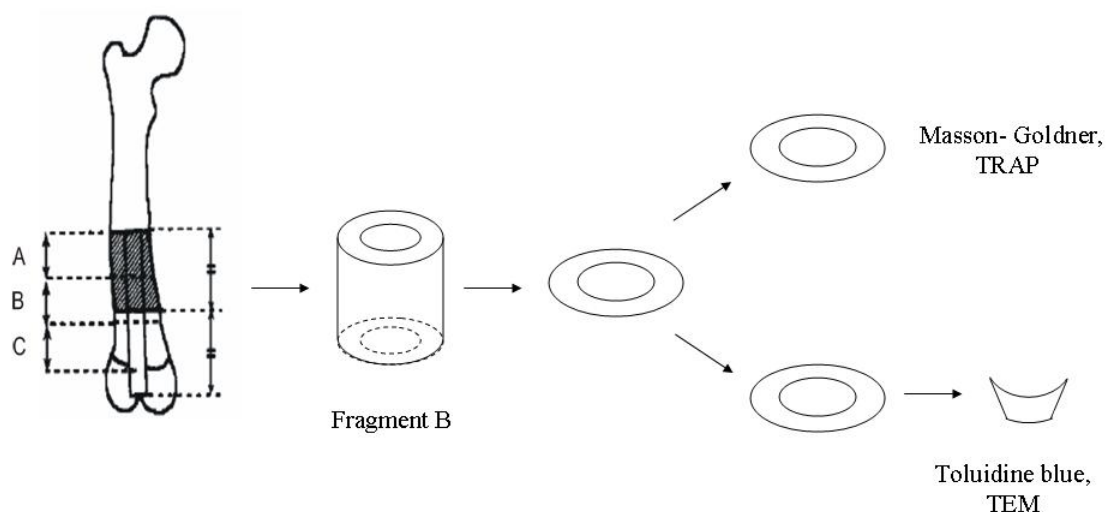


Figure 1. Schematic diagram of implant insertion and tissue sectioning for histological staining and electron microscopy analysis.

Reaction zone	Response	Score
Tissue reaction around the implant	Similar to original bone	5
	Lamellar or woven bone with bone forming activity	4
	Lamellar or woven bone with bone forming and osteoclastic activity	3
	Other tissue than bone (e.g., fibrous tissue)	2
	Inflammation	1
Bone- implant interface	Direct bone- implant contact without intervening soft tissue	5
	Remodelizing lacuna with osteoblasts and/or osteoclasts on surface	4
	Localized fibrous tissue not arranged as capsule	3
	Thick fibrous tissue capsule	2
	Inflammation	1

Table 1. Histologic scoring system for bone reaction around the implant and tissue formation at the implant interface as observed on Masson- Goldner stained sections following 1, 4 and 8 weeks of insertion.

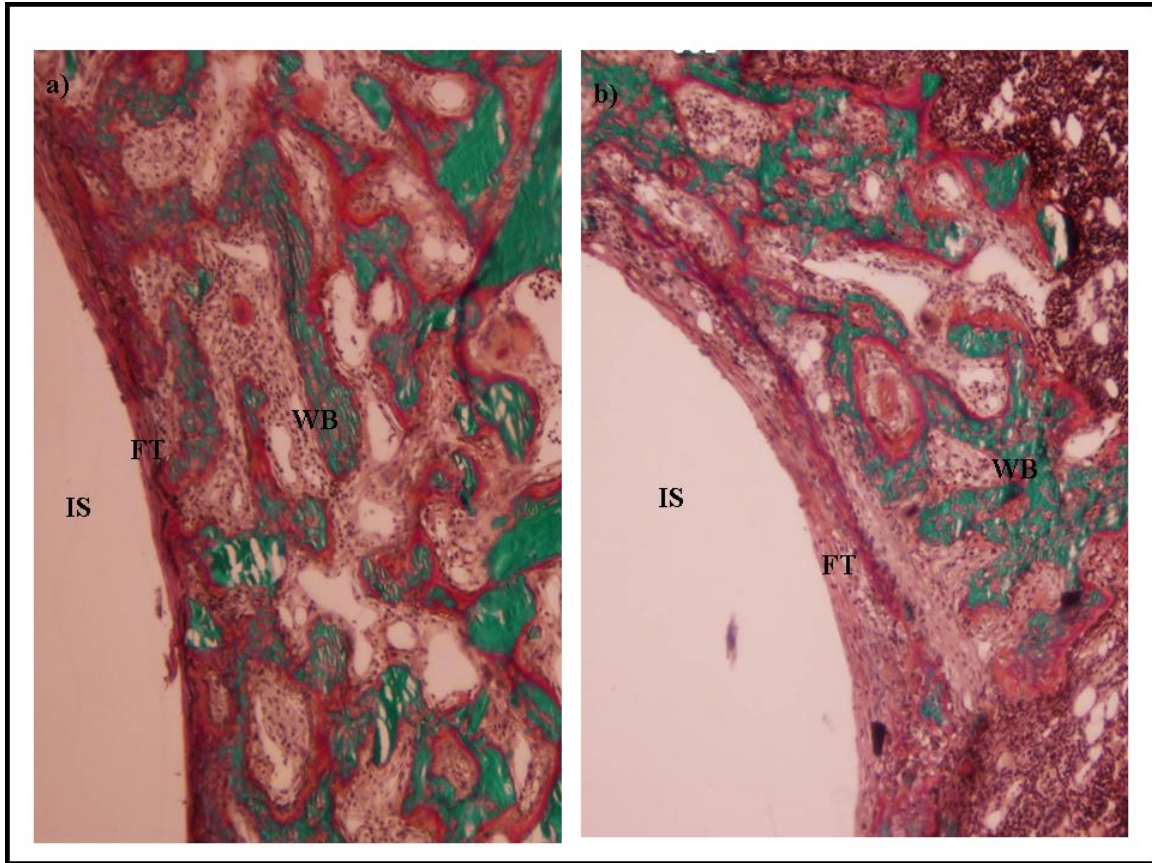


Figure 2. Masson- Goldner staining of bone surrounding the implant site following 1 week of insertion in the medullary cavity of rat femur (10X). a) Ti-Fn implant; b) Ti-Fn-SA implant; Implant site, IS; Fibrous tissue, FT; Woven bone, WB.

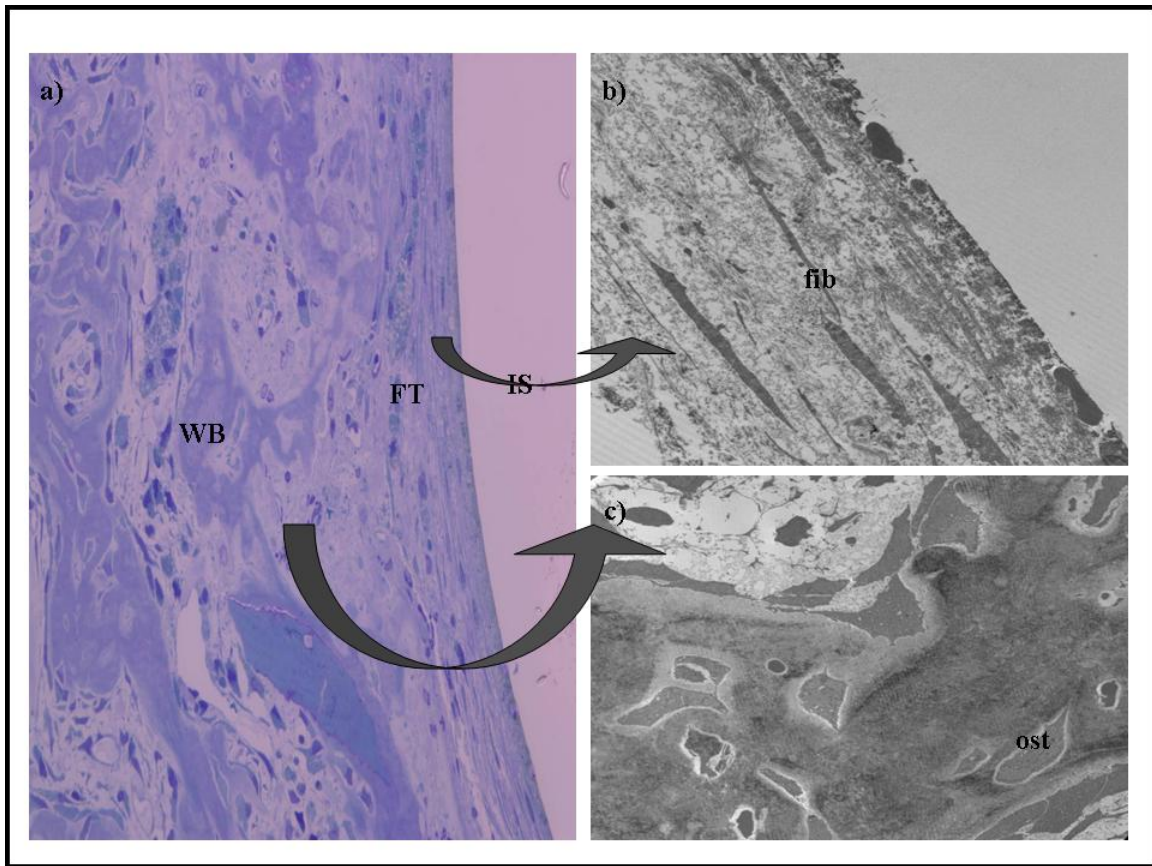


Figure 3. a) Toluidine blue staining of bone surrounding the Ti-Fn implant site following 4 weeks of insertion in the medullary cavity of rat femur (20X). b) Transmission electron micrograph of fibrous tissue observed at the implant interface (1950X) c) Transmission electron micrograph of woven bone observed around the implant (1950X). Implant site, IS; Fibrous tissue, FT; Woven bone, WB; Fibroblast, Fib; Osteocyte, Ost.

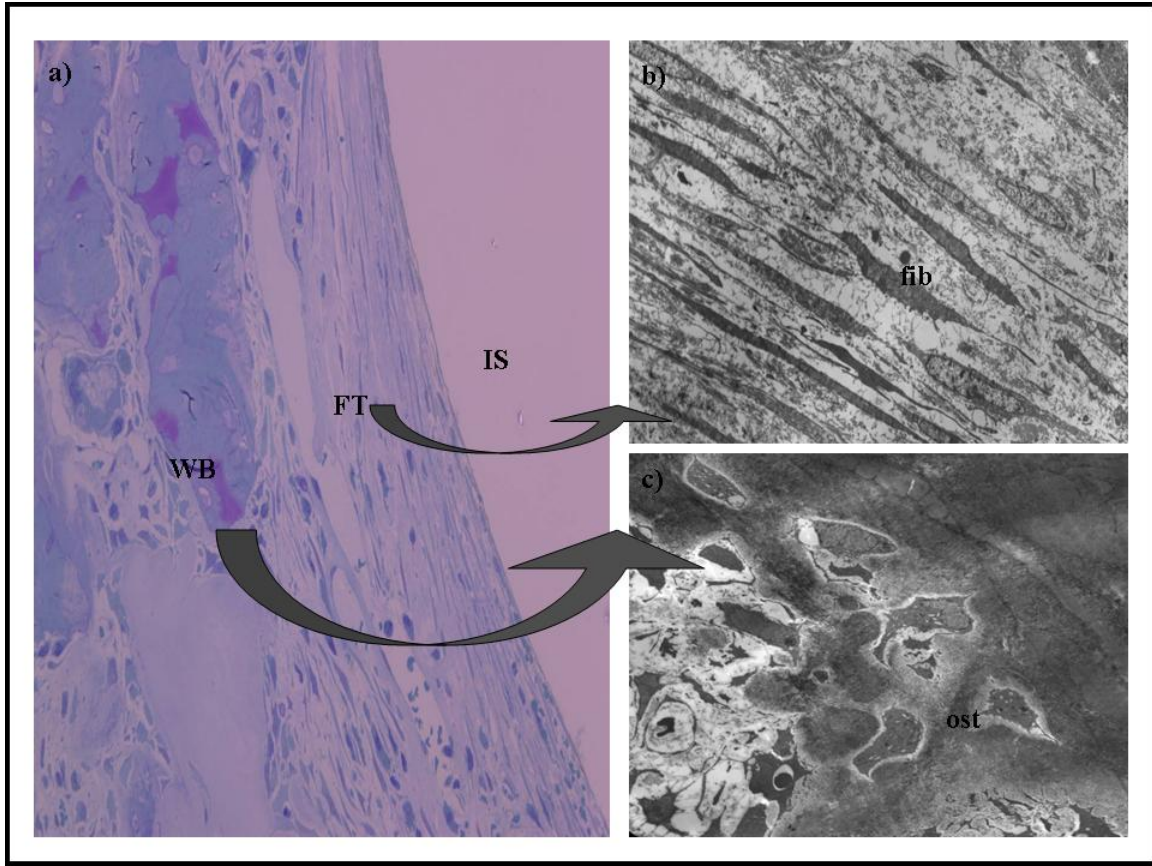


Figure 4. a) Toluidine blue staining of bone surrounding the Ti-Fn-SA implant site following 1 week of insertion in the medullary cavity of rat femur (20X). b) Transmission electron micrograph of fibrous tissue observed at the implant interface (1950X) c) Transmission electron micrograph of woven bone observed around the implant (1950X). Implant site, IS; Fibrous tissue, FT; Woven bone, WB; Fibroblast, Fib; Osteocyte, Ost.

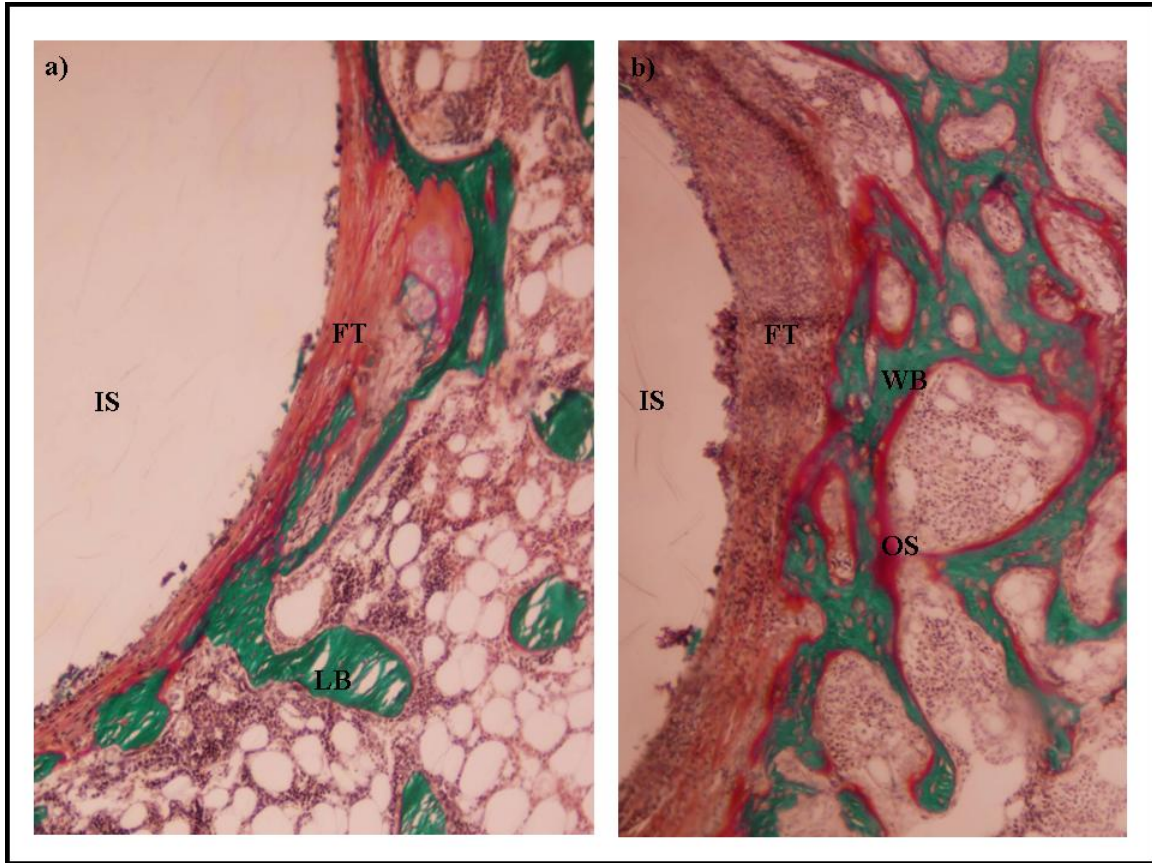


Figure 5. Masson- Goldner staining of bone surrounding the implant site following 4 weeks of insertion in the medullary cavity of rat femur (10X). a) Ti-Fn implant; b) Ti-Fn-SA; Implant site, IS; Fibrous tissue, FT; Woven bone, WB; Lamellar bone, LB; Osteoid seam, OS.

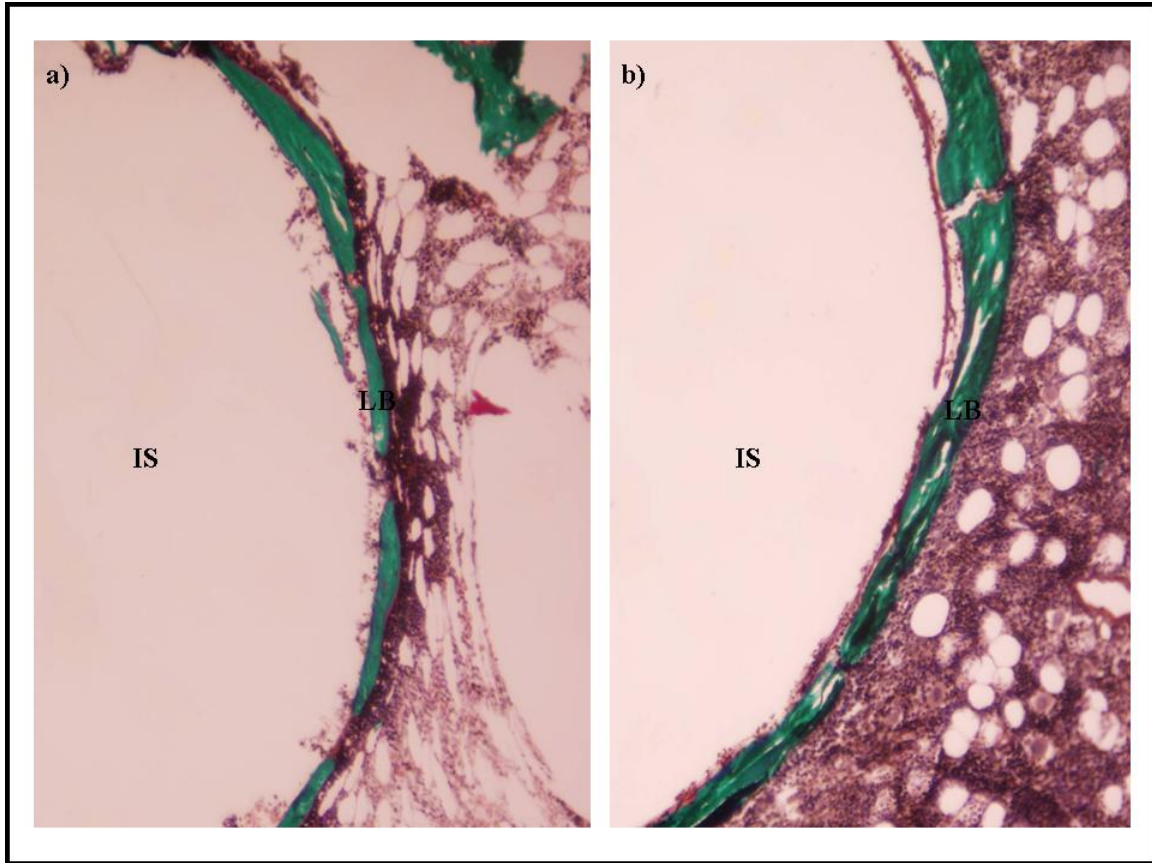


Figure 6. Masson- Goldner staining of bone surrounding the implant site following 8 weeks of insertion in the medullary cavity of rat femur (10X). a) Ti-Fn implant; b) Ti-Fn-SA Implant site, IS; Lamellar bone, LB.

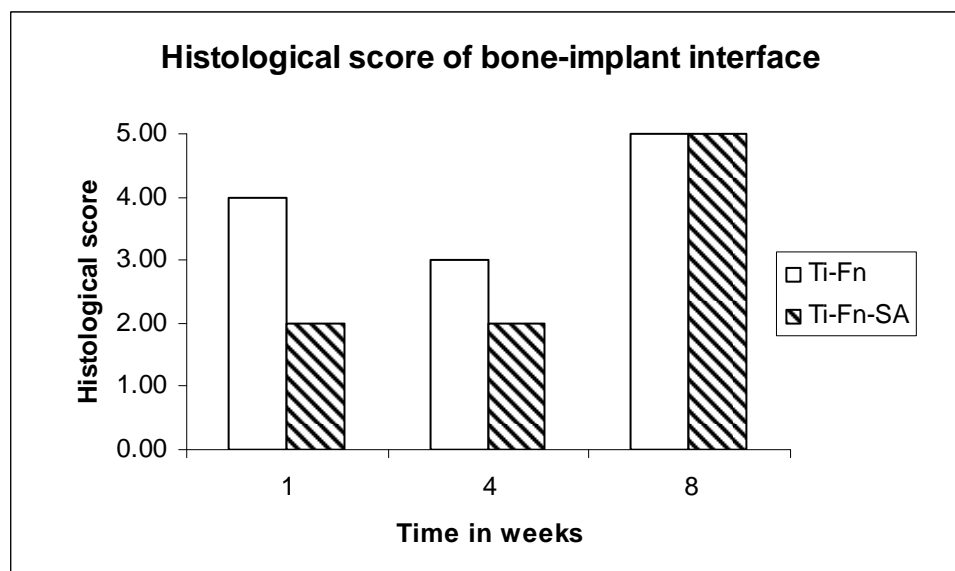


Figure 7. Histologic scoring system for bone reaction around Ti-Fn and Ti-Fn-SA implant surface as observed on Masson- Goldner stained sections following 1, 4 and 8 weeks of insertion.

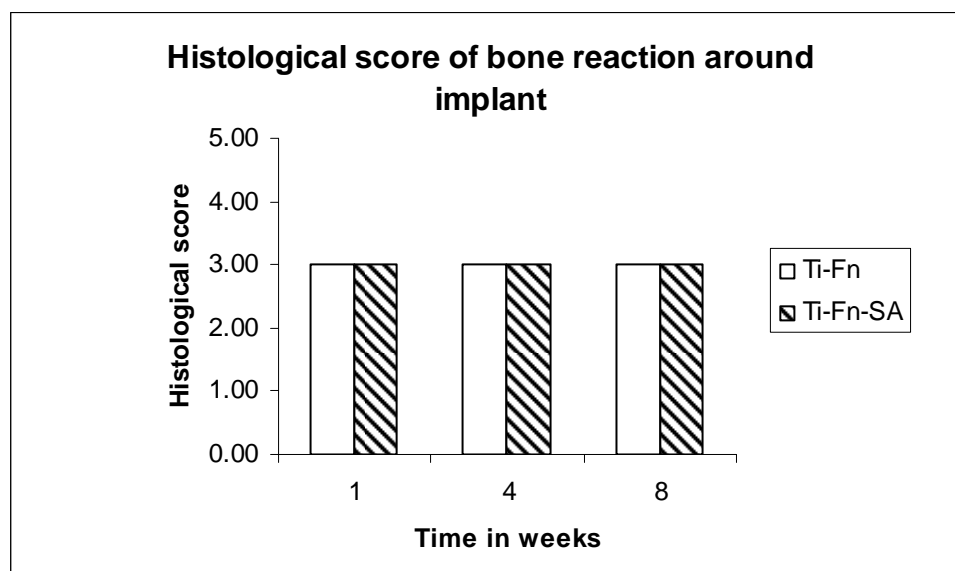


Figure 8. Histologic scoring system for tissue reaction around Ti-Fn and Ti-Fn-SA implant interface as observed on Masson- Goldner stained sections following 1, 4 and 8 weeks of insertion.

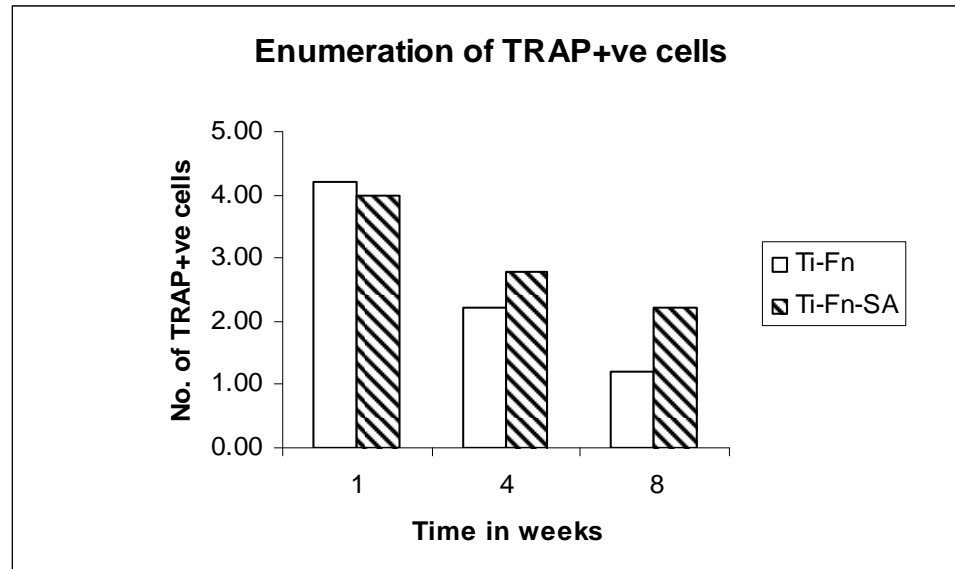


Figure 9. Tartrate-resistant acid phosphatase (TRAP) staining of osteoclasts in bone surrounding the implant site following 1, 4 and 8 weeks of insertion in the medullary cavity of rat femur.

SUMMARY

This dissertation is a compilation of experiments that investigated the responses of osteoblasts following *S. aureus* infection as well as the therapeutic use of nanoparticles loaded with antibiotic to target intracellular and extracellular bacteria. Finally we examined whether UV-killed *S. aureus* could act as an osteoconductive coating on bone-associated biomaterials.

By determining that RANK-L and PGE₂ are up-regulated in osteoblasts infected by *S. aureus*, we have identified possible key molecules involved in the bone destruction observed during osteomyelitis. We have also observed that there are PGE₂ - independent pathway(s) responsible for RANK-L induction in infected osteoblasts. Data demonstrate that all formulations of PLGA particles loaded with the antibiotic nafcillin either killed or significantly reduced all viable intracellular *S. aureus*. The use of the data obtained by this study and future investigations of the molecular pathways involved in *S. aureus*-induced osteomyelitis can result in more effective, alternative treatments for osteomyelitis. UV-killed *S. aureus* is indeed a bioactive coating on bone-associated biomaterials both in vivo and in vitro. Osteoblast attachment and adhesion were enhanced on titanium alloy surfaces coated with bacteria compared to uncoated surfaces. Cell proliferation was sustained at comparable levels in the presence and absence of *S. aureus* while markers of osteoblast differentiation such as collagen synthesis, osteocalcin synthesis, alkaline phosphatase activity and mineralized nodule formation were increased on Ti alloy coated with *S. aureus* compared to uncoated control surfaces. In vivo results showed no significant inflammatory response resulting from implants coated with *S.*

aureus and preliminary results suggest that the osteoconductivities of *S. aureus*-coated and uncoated implants were comparable at 8 weeks post-operation.

REFERENCES

INTRODUCTION:

1. **Akatsu, T., N. Takahashi, N. Udagawa, K. Imamura, A. Yamaguchi, K. Sato, N. Nagata, and T. Suda.** 1991. Role of prostaglandins in interleukin-1-induced bone resorption in mice in vitro. *J Bone Miner Res* **6**:183-189.
2. **Alexander, E. H., J. L. Bento, F. M. Hughes, Jr., I. Marriott, M. C. Hudson, and K. L. Bost.** 2001. Staphylococcus aureus and Salmonella enterica serovar Dublin induce tumor necrosis factor-related apoptosis-inducing ligand expression by normal mouse and human osteoblasts. *Infection and immunity* **69**:1581-1586.
3. **Alexander, E. H., and M. C. Hudson.** 2001. Factors influencing the internalization of Staphylococcus aureus and impacts on the course of infections in humans. *Applied microbiology and biotechnology* **56**:361-366.
4. **Alexander, E. H., F. A. Rivera, I. Marriott, J. Anguita, K. L. Bost, and M. C. Hudson.** 2003. Staphylococcus aureus - induced tumor necrosis factor - related apoptosis - inducing ligand expression mediates apoptosis and caspase-8 activation in infected osteoblasts. *BMC Microbiol* **3**:5.
5. **Anselme, K.** 2000. Osteoblast adhesion on biomaterials. *Biomaterials* **21**:667-681.
6. **Barton, L. L., L. M. Dunkle, and F. H. Habib.** 1987. Septic arthritis in childhood. A 13-year review. *Am J Dis Child* **141**:898-900.
7. **Bauer, T. W., and J. Schils.** 1999. The pathology of total joint arthroplasty.II. Mechanisms of implant failure. *Skeletal radiology* **28**:483-497.
8. **Bayles, K. W., C. A. Wesson, L. E. Liou, L. K. Fox, G. A. Bohach, and W. R. Trumble.** 1998. Intracellular Staphylococcus aureus escapes the endosome and induces apoptosis in epithelial cells. *Infection and immunity* **66**:336-342.
9. **Blair, J. M., H. Zhou, M. J. Seibel, and C. R. Dunstan.** 2006. Mechanisms of disease: roles of OPG, RANKL and RANK in the pathophysiology of skeletal metastasis. *Nature clinical practice* **3**:41-49.
10. **Bloebaum, R. D., D. Beeks, L. D. Dorr, C. G. Savory, J. A. DuPont, and A. A. Hofmann.** 1994. Complications with hydroxyapatite particulate separation in total hip arthroplasty. *Clinical orthopaedics and related research*:19-26.
11. **Bost, K. L., J. L. Bento, J. K. Ellington, I. Marriott, and M. C. Hudson.** 2000. Induction of colony-stimulating factor expression following Staphylococcus or

- Salmonella interaction with mouse or human osteoblasts. *Infection and immunity* **68**:5075-5083.
12. **Bost, K. L., J. L. Bento, C. C. Petty, L. W. Schrum, M. C. Hudson, and I. Marriott.** 2001. Monocyte chemoattractant protein-1 expression by osteoblasts following infection with *Staphylococcus aureus* or *Salmonella*. *J Interferon Cytokine Res* **21**:297-304.
 13. **Bost, K. L., W. K. Ramp, N. C. Nicholson, J. L. Bento, I. Marriott, and M. C. Hudson.** 1999. *Staphylococcus aureus* infection of mouse or human osteoblasts induces high levels of interleukin-6 and interleukin-12 production. *The Journal of infectious diseases* **180**:1912-1920.
 14. **Calhoun, J. H., and J. T. Mader.** 1997. Treatment of osteomyelitis with a biodegradable antibiotic implant. *Clinical orthopaedics and related research*:206-214.
 15. **Chen, Q. R., C. Miyaoura, S. Higashi, M. Murakami, I. Kudo, S. Saito, T. Hiraide, Y. Shibasaki, and T. Suda.** 1997. Activation of cytosolic phospholipase A2 by platelet-derived growth factor is essential for cyclooxygenase-2-dependent prostaglandin E2 synthesis in mouse osteoblasts cultured with interleukin-1. *The Journal of biological chemistry* **272**:5952-5958.
 16. **Clark, J. D., L. L. Lin, R. W. Kriz, C. S. Ramesha, L. A. Sultzman, A. Y. Lin, N. Milona, and J. L. Knopf.** 1991. A novel arachidonic acid-selective cytosolic PLA2 contains a Ca(2+)-dependent translocation domain with homology to PKC and GAP. *Cell* **65**:1043-1051.
 17. **Cook, S. D., K. A. Thomas, J. F. Kay, and M. Jarcho.** 1988. Hydroxyapatite-coated porous titanium for use as an orthopedic biologic attachment system. *Clinical orthopaedics and related research*:303-312.
 18. **Damsky, C. H.** 1999. Extracellular matrix-integrin interactions in osteoblast function and tissue remodeling. *Bone* **25**:95-96.
 19. **Darouiche, R. O., and R. J. Hamill.** 1994. Antibiotic penetration of and bactericidal activity within endothelial cells. *Antimicrobial agents and chemotherapy* **38**:1059-1064.
 20. **Davies, J. E., B. Lowenberg, and A. Shiga.** 1990. The bone-titanium interface in vitro. *Journal of biomedical materials research* **24**:1289-1306.
 21. **De Ranieri, A., A. S. Viridi, S. Kuroda, S. Shott, R. M. Leven, N. J. Hallab, and D. R. Sumner.** 2005. Local application of rhTGF-beta2 enhances peri-implant bone volume and bone-implant contact in a rat model. *Bone* **37**:55-62.

22. **Dubey, L., K. Krasinski, and M. Hernanz-Schulman.** 1988. Osteomyelitis secondary to trauma or infected contiguous soft tissue. *Pediatr Infect Dis J* **7**:26-34.
23. **Dziewanowska, K., A. R. Carson, J. M. Patti, C. F. Deobald, K. W. Bayles, and G. A. Bohach.** 2000. Staphylococcal fibronectin binding protein interacts with heat shock protein 60 and integrins: role in internalization by epithelial cells. *Infection and immunity* **68**:6321-6328.
24. **Dziewanowska, K., J. M. Patti, C. F. Deobald, K. W. Bayles, W. R. Trumble, and G. A. Bohach.** 1999. Fibronectin binding protein and host cell tyrosine kinase are required for internalization of *Staphylococcus aureus* by epithelial cells. *Infection and immunity* **67**:4673-4678.
25. **Ellington, J. K., A. Elhofy, K. L. Bost, and M. C. Hudson.** 2001. Involvement of mitogen-activated protein kinase pathways in *Staphylococcus aureus* invasion of normal osteoblasts. *Infection and immunity* **69**:5235-5242.
26. **Ellington, J. K., S. S. Reilly, W. K. Ramp, M. S. Smeltzer, J. F. Kellam, and M. C. Hudson.** 1999. Mechanisms of *Staphylococcus aureus* invasion of cultured osteoblasts. *Microbial pathogenesis* **26**:317-323.
27. **Ferris, D. M., G. D. Moodie, P. M. Dimond, C. W. Gioranni, M. G. Ehrlich, and R. F. Valentini.** 1999. RGD-coated titanium implants stimulate increased bone formation in vivo. *Biomaterials* **20**:2323-2331.
28. **Frank, A., S. Kumar Rath, F. Boey, and S. Venkatraman.** 2004. Study of the initial stages of drug release from a degradable matrix of poly(d,l-lactide-co-glycolide). *Biomaterials* **25**:813-821.
29. **Fukuzaki, H., M. Yoshida, M. Asano, M. Kumakura, T. Mashimo, H. Yuasa, K. Imai, and H. Yamanaka.** 1990. In vivo characteristics of low molecular weight copolymers composed of L-lactic acid and various DL-hydroxy acids as biodegradable carriers for drug delivery systems. *Biomaterials* **11**:441-446.
30. **Garcia, A. J., and D. Boettiger.** 1999. Integrin-fibronectin interactions at the cell-material interface: initial integrin binding and signaling. *Biomaterials* **20**:2427-2433.
31. **Gross, M., S. E. Cramton, F. Gotz, and A. Peschel.** 2001. Key role of teichoic acid net charge in *Staphylococcus aureus* colonization of artificial surfaces. *Infection and immunity* **69**:3423-3426.
32. **Gulyaeva, N., A. Zaslavsky, P. Lechner, A. Chait, and B. Zaslavsky.** 2000. Relative hydrophobicity of organic compounds measured by partitioning in aqueous two-phase systems. *Journal of chromatography* **743**:187-194.

33. **Haggar, A., M. Hussain, H. Lonnie, M. Herrmann, A. Norrby-Teglund, and J. I. Flock.** 2003. Extracellular adherence protein from *Staphylococcus aureus* enhances internalization into eukaryotic cells. *Infection and immunity* **71**:2310-2317.
34. **Hallab, N. J., K. J. Bundy, K. O'Connor, R. L. Moses, and J. J. Jacobs.** 2001. Evaluation of metallic and polymeric biomaterial surface energy and surface roughness characteristics for directed cell adhesion. *Tissue engineering* **7**:55-71.
35. **Harris, L. G., and R. G. Richards.** 2004. *Staphylococcus aureus* adhesion to different treated titanium surfaces. *Journal of materials science* **15**:311-314.
36. **Harris, L. G., S. Tosatti, M. Wieland, M. Textor, and R. G. Richards.** 2004. *Staphylococcus aureus* adhesion to titanium oxide surfaces coated with non-functionalized and peptide-functionalized poly(L-lysine)-grafted-poly(ethylene glycol) copolymers. *Biomaterials* **25**:4135-4148.
37. **Hofbauer, L. C., S. Khosla, C. R. Dunstan, D. L. Lacey, W. J. Boyle, and B. L. Riggs.** 2000. The roles of osteoprotegerin and osteoprotegerin ligand in the paracrine regulation of bone resorption. *J Bone Miner Res* **15**:2-12.
38. **Hofbauer, L. C., D. L. Lacey, C. R. Dunstan, T. C. Spelsberg, B. L. Riggs, and S. Khosla.** 1999. Interleukin-1 β and tumor necrosis factor- α , but not interleukin-6, stimulate osteoprotegerin ligand gene expression in human osteoblastic cells. *Bone* **25**:255-259.
39. **Hudson, M. C., W. K. Ramp, and K. P. Frankenburg.** 1999. *Staphylococcus aureus* adhesion to bone matrix and bone-associated biomaterials. *FEMS microbiology letters* **173**:279-284.
40. **Hudson, M. C., W. K. Ramp, N. C. Nicholson, A. S. Williams, and M. T. Nousiainen.** 1995. Internalization of *Staphylococcus aureus* by cultured osteoblasts. *Microbial pathogenesis* **19**:409-419.
41. **Jakobsson, P. J., S. Thoren, R. Morgenstern, and B. Samuelsson.** 1999. Identification of human prostaglandin E synthase: a microsomal, glutathione-dependent, inducible enzyme, constituting a potential novel drug target. *Proceedings of the National Academy of Sciences of the United States of America* **96**:7220-7225.
42. **Kaneda, T., T. Nojima, M. Nakagawa, A. Ogasawara, H. Kaneko, T. Sato, H. Mano, M. Kumegawa, and Y. Hakeda.** 2000. Endogenous production of TGF- β is essential for osteoclastogenesis induced by a combination of receptor activator of NF- κ B ligand and macrophage-colony-stimulating factor. *J Immunol* **165**:4254-4263.

43. **Kong, Y. Y., U. Feige, I. Sarosi, B. Bolon, A. Tafuri, S. Morony, C. Capparelli, J. Li, R. Elliott, S. McCabe, T. Wong, G. Campagnuolo, E. Moran, E. R. Bogoch, G. Van, L. T. Nguyen, P. S. Ohashi, D. L. Lacey, E. Fish, W. J. Boyle, and J. M. Penninger.** 1999. Activated T cells regulate bone loss and joint destruction in adjuvant arthritis through osteoprotegerin ligand. *Nature* **402**:304-309.
44. **Kong, Y. Y., H. Yoshida, I. Sarosi, H. L. Tan, E. Timms, C. Capparelli, S. Morony, A. J. Oliveira-dos-Santos, G. Van, A. Itie, W. Khoo, A. Wakeham, C. R. Dunstan, D. L. Lacey, T. W. Mak, W. J. Boyle, and J. M. Penninger.** 1999. OPGL is a key regulator of osteoclastogenesis, lymphocyte development and lymph-node organogenesis. *Nature* **397**:315-323.
45. **Kotake, S., N. Udagawa, N. Takahashi, K. Matsuzaki, K. Itoh, S. Ishiyama, S. Saito, K. Inoue, N. Kamatani, M. T. Gillespie, T. J. Martin, and T. Suda.** 1999. IL-17 in synovial fluids from patients with rheumatoid arthritis is a potent stimulator of osteoclastogenesis. *The Journal of clinical investigation* **103**:1345-1352.
46. **Kudo, I., M. Murakami, S. Hara, and K. Inoue.** 1993. Mammalian non-pancreatic phospholipases A2. *Biochimica et biophysica acta* **1170**:217-231.
47. **Kwon, B. S., S. Wang, N. Udagawa, V. Haridas, Z. H. Lee, K. K. Kim, K. O. Oh, J. Greene, Y. Li, J. Su, R. Gentz, B. B. Aggarwal, and J. Ni.** 1998. TR1, a new member of the tumor necrosis factor receptor superfamily, induces fibroblast proliferation and inhibits osteoclastogenesis and bone resorption. *Faseb J* **12**:845-854.
48. **LeBaron, R. G., and K. A. Athanasiou.** 2000. Extracellular matrix cell adhesion peptides: functional applications in orthopedic materials. *Tissue engineering* **6**:85-103.
49. **LeGeros, R. Z., and R. G. Craig.** 1993. Strategies to affect bone remodeling: osteointegration. *J Bone Miner Res* **8 Suppl 2**:S583-596.
50. **Lew, D. P., and F. A. Waldvogel.** 2004. Osteomyelitis. *Lancet* **364**:369-379.
51. **Lewis, R. T.** 1998. Soft tissue infections. *World journal of surgery* **22**:146-151.
52. **Long, M., and H. J. Rack.** 1998. Titanium alloys in total joint replacement--a materials science perspective. *Biomaterials* **19**:1621-1639.
53. **Mandal, T. K., L. A. Bostanian, R. A. Graves, and S. R. Chapman.** 2002. Poly(D,L-lactide-co-glycolide) encapsulated poly(vinyl alcohol) hydrogel as a drug delivery system. *Pharmaceutical research* **19**:1713-1719.

54. **Murakami, M., H. Naraba, T. Tanioka, N. Semmyo, Y. Nakatani, F. Kojima, T. Ikeda, M. Fueki, A. Ueno, S. Oh, and I. Kudo.** 2000. Regulation of prostaglandin E2 biosynthesis by inducible membrane-associated prostaglandin E2 synthase that acts in concert with cyclooxygenase-2. *The Journal of biological chemistry* **275**:32783-32792.
55. **O'Toole, G. C., E. Salih, C. Gallagher, D. FitzPatrick, N. O'Higgins, and S. K. O'Rourke.** 2004. Bone sialoprotein-coated femoral implants are osteoinductive but mechanically compromised. *J Orthop Res* **22**:641-646.
56. **Okahashi, N., A. Sakurai, I. Nakagawa, T. Fujiwara, S. Kawabata, A. Amano, and S. Hamada.** 2003. Infection by *Streptococcus pyogenes* induces the receptor activator of NF-kappaB ligand expression in mouse osteoblastic cells. *Infection and immunity* **71**:948-955.
57. **Olivier, S., M. Fillet, M. Malaise, J. Piette, V. Bours, M. P. Merville, and N. Franchimont.** 2005. Sodium nitroprusside-induced osteoblast apoptosis is mediated by long chain ceramide and is decreased by raloxifene. *Biochemical pharmacology* **69**:891-901.
58. **Raisz, L. G., J. Y. Vanderhoek, H. A. Simmons, B. E. Kream, and K. C. Nicolaou.** 1979. Prostaglandin synthesis by fetal rat bone in vitro: evidence for a role of prostacyclin. *Prostaglandins* **17**:905-914.
59. **Reilly, S. S., M. C. Hudson, J. F. Kellam, and W. K. Ramp.** 2000. In vivo internalization of *Staphylococcus aureus* by embryonic chick osteoblasts. *Bone* **26**:63-70.
60. **Robey, P. G., N. S. Fedarko, T. E. Hefferan, P. Bianco, U. K. Vetter, W. Grzesik, A. Friedenstein, G. Van der Pluijm, K. P. Mintz, M. F. Young, and et al.** 1993. Structure and molecular regulation of bone matrix proteins. *J Bone Miner Res* **8 Suppl 2**:S483-487.
61. **Sato, K., Y. Fujii, K. Kasono, M. Saji, T. Tsushima, and K. Shizume.** 1986. Stimulation of prostaglandin E2 and bone resorption by recombinant human interleukin 1 alpha in fetal mouse bones. *Biochemical and biophysical research communications* **138**:618-624.
62. **Shakoori, A. R., A. M. Oberdorf, T. A. Owen, L. A. Weber, E. Hickey, J. L. Stein, J. B. Lian, and G. S. Stein.** 1992. Expression of heat shock genes during differentiation of mammalian osteoblasts and promyelocytic leukemia cells. *Journal of cellular biochemistry* **48**:277-287.
63. **Sharp, J. D., D. L. White, X. G. Chiou, T. Goodson, G. C. Gamboa, D. McClure, S. Burgett, J. Hoskins, P. L. Skatrud, J. R. Sportsman, and et al.**

1991. Molecular cloning and expression of human Ca(2+)-sensitive cytosolic phospholipase A2. *The Journal of biological chemistry* **266**:14850-14853.
64. **Simonet, W. S., D. L. Lacey, C. R. Dunstan, M. Kelley, M. S. Chang, R. Luthy, H. Q. Nguyen, S. Wooden, L. Bennett, T. Boone, G. Shimamoto, M. DeRose, R. Elliott, A. Colombero, H. L. Tan, G. Trail, J. Sullivan, E. Davy, N. Bucay, L. Renshaw-Gegg, T. M. Hughes, D. Hill, W. Pattison, P. Campbell, S. Sander, G. Van, J. Tarpley, P. Derby, R. Lee, and W. J. Boyle.** 1997. Osteoprotegerin: a novel secreted protein involved in the regulation of bone density. *Cell* **89**:309-319.
 65. **Smith, W. L., R. M. Garavito, and D. L. DeWitt.** 1996. Prostaglandin endoperoxide H synthases (cyclooxygenases)-1 and -2. *The Journal of biological chemistry* **271**:33157-33160.
 66. **Song, C., V. Labhasetwar, X. Cui, T. Underwood, and R. J. Levy.** 1998. Arterial uptake of biodegradable nanoparticles for intravascular local drug delivery: results with an acute dog model. *J Control Release* **54**:201-211.
 67. **Soppimath, K. S., T. M. Aminabhavi, A. R. Kulkarni, and W. E. Rudzinski.** 2001. Biodegradable polymeric nanoparticles as drug delivery devices. *J Control Release* **70**:1-20.
 68. **Stein, G. S., J. B. Lian, and T. A. Owen.** 1990. Relationship of cell growth to the regulation of tissue-specific gene expression during osteoblast differentiation. *Faseb J* **4**:3111-3123.
 69. **Suda, K., N. Udagawa, N. Sato, M. Takami, K. Itoh, J. T. Woo, N. Takahashi, and K. Nagai.** 2004. Suppression of osteoprotegerin expression by prostaglandin E2 is crucially involved in lipopolysaccharide-induced osteoclast formation. *J Immunol* **172**:2504-2510.
 70. **Suda, T., N. Takahashi, and T. J. Martin.** 1992. Modulation of osteoclast differentiation. *Endocrine reviews* **13**:66-80.
 71. **Suzawa, T., C. Miyaara, M. Inada, T. Maruyama, Y. Sugimoto, F. Ushikubi, A. Ichikawa, S. Narumiya, and T. Suda.** 2000. The role of prostaglandin E receptor subtypes (EP1, EP2, EP3, and EP4) in bone resorption: an analysis using specific agonists for the respective EPs. *Endocrinology* **141**:1554-1559.
 72. **Sykaras, N., A. M. Iacopino, V. A. Marker, R. G. Triplett, and R. D. Woody.** 2000. Implant materials, designs, and surface topographies: their effect on osseointegration. A literature review. *The International journal of oral & maxillofacial implants* **15**:675-690.

73. **Tai, H., C. Miyaara, C. C. Pilbeam, T. Tamura, Y. Ohsugi, Y. Koishihara, N. Kubodera, H. Kawaguchi, L. G. Raisz, and T. Suda.** 1997. Transcriptional induction of cyclooxygenase-2 in osteoblasts is involved in interleukin-6-induced osteoclast formation. *Endocrinology* **138**:2372-2379.
74. **Takayanagi, H., K. Ogasawara, S. Hida, T. Chiba, S. Murata, K. Sato, A. Takaoka, T. Yokochi, H. Oda, K. Tanaka, K. Nakamura, and T. Taniguchi.** 2000. T-cell-mediated regulation of osteoclastogenesis by signalling cross-talk between RANKL and IFN-gamma. *Nature* **408**:600-605.
75. **Tanioka, T., Y. Nakatani, N. Semmyo, M. Murakami, and I. Kudo.** 2000. Molecular identification of cytosolic prostaglandin E2 synthase that is functionally coupled with cyclooxygenase-1 in immediate prostaglandin E2 biosynthesis. *The Journal of biological chemistry* **275**:32775-32782.
76. **Tarkowski, A., L. V. Collins, I. Gjertsson, O. H. Hultgren, I. M. Jonsson, E. Sakiniene, and M. Verdrengh.** 2001. Model systems: modeling human staphylococcal arthritis and sepsis in the mouse. *Trends in microbiology* **9**:321-326.
77. **Tsuda, E., M. Goto, S. Mochizuki, K. Yano, F. Kobayashi, T. Morinaga, and K. Higashio.** 1997. Isolation of a novel cytokine from human fibroblasts that specifically inhibits osteoclastogenesis. *Biochemical and biophysical research communications* **234**:137-142.
78. **Wada, T., T. Nakashima, N. Hiroshi, and J. M. Penninger.** 2006. RANKL-RANK signaling in osteoclastogenesis and bone disease. *Trends in molecular medicine* **12**:17-25.
79. **Waldvogel, F. A., G. Medoff, and M. N. Swartz.** 1970. Osteomyelitis: a review of clinical features, therapeutic considerations and unusual aspects. *The New England journal of medicine* **282**:198-206.
80. **Walsh, M. C., and Y. Choi.** 2003. Biology of the TRANCE axis. *Cytokine & growth factor reviews* **14**:251-263.
81. **Wong, M., J. Eulenberger, R. Schenk, and E. Hunziker.** 1995. Effect of surface topology on the osseointegration of implant materials in trabecular bone. *Journal of biomedical materials research* **29**:1567-1575.
82. **Xiao, G., D. Wang, M. D. Benson, G. Karsenty, and R. T. Franceschi.** 1998. Role of the alpha2-integrin in osteoblast-specific gene expression and activation of the Osf2 transcription factor. *J Biol Chem* **273**:32988-32994.
83. **Yasuda, H., N. Shima, N. Nakagawa, K. Yamaguchi, M. Kinosaki, S. Mochizuki, A. Tomoyasu, K. Yano, M. Goto, A. Murakami, E. Tsuda, T.**

Morinaga, K. Higashio, N. Udagawa, N. Takahashi, and T. Suda. 1998. Osteoclast differentiation factor is a ligand for osteoprotegerin/osteoclastogenesis-inhibitory factor and is identical to TRANCE/RANKL. *Proceedings of the National Academy of Sciences of the United States of America* **95**:3597-3602.

PROJECT I:

1. **Akatsu, T., N. Takahashi, N. Udagawa, K. Imamura, A. Yamaguchi, K. Sato, N. Nagata, and T. Suda.** 1991. Role of prostaglandins in interleukin-1-induced bone resorption in mice in vitro. *J Bone Miner Res* **6**:183-189.
2. **Alexander, E. H., J. L. Bento, F. M. Hughes, Jr., I. Marriott, M. C. Hudson, and K. L. Bost.** 2001. Staphylococcus aureus and Salmonella enterica serovar Dublin induce tumor necrosis factor-related apoptosis-inducing ligand expression by normal mouse and human osteoblasts. *Infection and immunity* **69**:1581-1586.
3. **Bost, K. L., J. L. Bento, J. K. Ellington, I. Marriott, and M. C. Hudson.** 2000. Induction of colony-stimulating factor expression following Staphylococcus or Salmonella interaction with mouse or human osteoblasts. *Infection and immunity* **68**:5075-5083.
4. **Bost, K. L., J. L. Bento, C. C. Petty, L. W. Schrum, M. C. Hudson, and I. Marriott.** 2001. Monocyte chemoattractant protein-1 expression by osteoblasts following infection with Staphylococcus aureus or Salmonella. *J Interferon Cytokine Res* **21**:297-304.
5. **Bost, K. L., W. K. Ramp, N. C. Nicholson, J. L. Bento, I. Marriott, and M. C. Hudson.** 1999. Staphylococcus aureus infection of mouse or human osteoblasts induces high levels of interleukin-6 and interleukin-12 production. *The Journal of infectious diseases* **180**:1912-1920.
6. **Chang, Y. C., P. C. Li, B. C. Chen, M. S. Chang, J. L. Wang, W. T. Chiu, and C. H. Lin.** 2006. Lipoteichoic acid-induced nitric oxide synthase expression in RAW 264.7 macrophages is mediated by cyclooxygenase-2, prostaglandin E2, protein kinase A, p38 MAPK, and nuclear factor-kappaB pathways. *Cell Signal* **18**:1235-1243.
7. **Chen, Q. R., C. Miyaura, S. Higashi, M. Murakami, I. Kudo, S. Saito, T. Hiraide, Y. Shibasaki, and T. Suda.** 1997. Activation of cytosolic phospholipase A2 by platelet-derived growth factor is essential for cyclooxygenase-2-dependent prostaglandin E2 synthesis in mouse osteoblasts cultured with interleukin-1. *J Biol Chem* **272**:5952-5958.
8. **Choi, B. K., S. Y. Moon, J. H. Cha, K. W. Kim, and Y. J. Yoo.** 2005. Prostaglandin E(2) is a main mediator in receptor activator of nuclear factor-kappaB ligand-dependent osteoclastogenesis induced by Porphyromonas

gingivalis, *Treponema denticola*, and *Treponema socranskii*. *J Periodontol* **76**:813-820.

9. **Clark, J. D., L. L. Lin, R. W. Kriz, C. S. Ramesha, L. A. Sultzman, A. Y. Lin, N. Milona, and J. L. Knopf.** 1991. A novel arachidonic acid-selective cytosolic PLA2 contains a Ca(2+)-dependent translocation domain with homology to PKC and GAP. *Cell* **65**:1043-1051.
10. **Darnay, B. G., J. Ni, P. A. Moore, and B. B. Aggarwal.** 1999. Activation of NF-kappaB by RANK requires tumor necrosis factor receptor-associated factor (TRAF) 6 and NF-kappaB-inducing kinase. Identification of a novel TRAF6 interaction motif. *J Biol Chem* **274**:7724-7731.
11. **Ellington, J. K., A. Elhofy, K. L. Bost, and M. C. Hudson.** 2001. Involvement of mitogen-activated protein kinase pathways in *Staphylococcus aureus* invasion of normal osteoblasts. *Infection and immunity* **69**:5235-5242.
12. **Ellington, J. K., S. S. Reilly, W. K. Ramp, M. S. Smeltzer, J. F. Kellam, and M. C. Hudson.** 1999. Mechanisms of *Staphylococcus aureus* invasion of cultured osteoblasts. *Microbial pathogenesis* **26**:317-323.
13. **Fujita, D., N. Yamashita, S. Iita, H. Amano, S. Yamada, and K. Sakamoto.** 2003. Prostaglandin E2 induced the differentiation of osteoclasts in mouse osteoblast-depleted bone marrow cells. *Prostaglandins Leukot Essent Fatty Acids* **68**:351-358.
14. **Gillaspy, A. F., S. G. Hickmon, R. A. Skinner, J. R. Thomas, C. L. Nelson, and M. S. Smeltzer.** 1995. Role of the accessory gene regulator (agr) in pathogenesis of staphylococcal osteomyelitis. *Infect Immun* **63**:3373-3380.
15. **Hofbauer, L. C., S. Khosla, C. R. Dunstan, D. L. Lacey, W. J. Boyle, and B. L. Riggs.** 2000. The roles of osteoprotegerin and osteoprotegerin ligand in the paracrine regulation of bone resorption. *J Bone Miner Res* **15**:2-12.
16. **Hofbauer, L. C., D. L. Lacey, C. R. Dunstan, T. C. Spelsberg, B. L. Riggs, and S. Khosla.** 1999. Interleukin-1beta and tumor necrosis factor-alpha, but not interleukin-6, stimulate osteoprotegerin ligand gene expression in human osteoblastic cells. *Bone* **25**:255-259.
17. **Hsu, H., D. L. Lacey, C. R. Dunstan, I. Solovyev, A. Colombero, E. Timms, H. L. Tan, G. Elliott, M. J. Kelley, I. Sarosi, L. Wang, X. Z. Xia, R. Elliott, L. Chiu, T. Black, S. Scully, C. Capparelli, S. Morony, G. Shimamoto, M. B. Bass, and W. J. Boyle.** 1999. Tumor necrosis factor receptor family member RANK mediates osteoclast differentiation and activation induced by osteoprotegerin ligand. *Proceedings of the National Academy of Sciences of the United States of America* **96**:3540-3545.

18. **Ishida, I., C. Kohda, Y. Yanagawa, H. Miyaoka, and T. Shimamura.** 2007. Epigallocatechin gallate suppresses expression of receptor activator of NF-kappaB ligand (RANKL) in *Staphylococcus aureus* infection in osteoblast-like NRG cells. *Journal of medical microbiology* **56**:1042-1046.
19. **Jakobsson, P. J., S. Thoren, R. Morgenstern, and B. Samuelsson.** 1999. Identification of human prostaglandin E synthase: a microsomal, glutathione-dependent, inducible enzyme, constituting a potential novel drug target. *Proc Natl Acad Sci U S A* **96**:7220-7225.
20. **Kaneda, T., T. Nojima, M. Nakagawa, A. Ogasawara, H. Kaneko, T. Sato, H. Mano, M. Kumegawa, and Y. Hakeda.** 2000. Endogenous production of TGF-beta is essential for osteoclastogenesis induced by a combination of receptor activator of NF-kappa B ligand and macrophage-colony-stimulating factor. *J Immunol* **165**:4254-4263.
21. **Kobayashi, Y., T. Mizoguchi, I. Take, S. Kurihara, N. Udagawa, and N. Takahashi.** 2005. Prostaglandin E2 enhances osteoclastic differentiation of precursor cells through protein kinase A-dependent phosphorylation of TAK1. *The Journal of biological chemistry* **280**:11395-11403.
22. **Kong, Y. Y., U. Feige, I. Sarosi, B. Bolon, A. Tafuri, S. Morony, C. Capparelli, J. Li, R. Elliott, S. McCabe, T. Wong, G. Campagnuolo, E. Moran, E. R. Bogoch, G. Van, L. T. Nguyen, P. S. Ohashi, D. L. Lacey, E. Fish, W. J. Boyle, and J. M. Penninger.** 1999. Activated T cells regulate bone loss and joint destruction in adjuvant arthritis through osteoprotegerin ligand. *Nature* **402**:304-309.
23. **Kong, Y. Y., H. Yoshida, I. Sarosi, H. L. Tan, E. Timms, C. Capparelli, S. Morony, A. J. Oliveira-dos-Santos, G. Van, A. Itie, W. Khoo, A. Wakeham, C. R. Dunstan, D. L. Lacey, T. W. Mak, W. J. Boyle, and J. M. Penninger.** 1999. OPGL is a key regulator of osteoclastogenesis, lymphocyte development and lymph-node organogenesis. *Nature* **397**:315-323.
24. **Kudo, I., M. Murakami, S. Hara, and K. Inoue.** 1993. Mammalian non-pancreatic phospholipases A2. *Biochim Biophys Acta* **1170**:217-231.
25. **Lew, D. P., and F. A. Waldvogel.** 2004. Osteomyelitis. *Lancet* **364**:369-379.
26. **Li, X., Y. Okada, C. C. Pilbeam, J. A. Lorenzo, C. R. Kennedy, R. M. Breyer, and L. G. Raisz.** 2000. Knockout of the murine prostaglandin EP2 receptor impairs osteoclastogenesis in vitro. *Endocrinology* **141**:2054-2061.
27. **Marriott, I., D. L. Gray, D. M. Rati, V. G. Fowler, Jr., M. E. Stryjewski, L. S. Levin, M. C. Hudson, and K. L. Bost.** 2005. Osteoblasts produce monocyte

chemoattractant protein-1 in a murine model of *Staphylococcus aureus* osteomyelitis and infected human bone tissue. *Bone* **37**:504-512.

28. **Marriott, I., D. L. Gray, S. L. Tranguch, V. G. Fowler, Jr., M. Stryjewski, L. Scott Levin, M. C. Hudson, and K. L. Bost.** 2004. Osteoblasts express the inflammatory cytokine interleukin-6 in a murine model of *Staphylococcus aureus* osteomyelitis and infected human bone tissue. *The American journal of pathology* **164**:1399-1406.
29. **Meghji, S., S. J. Crean, P. A. Hill, M. Sheikh, S. P. Nair, K. Heron, B. Henderson, E. B. Mawer, and M. Harris.** 1998. Surface-associated protein from *Staphylococcus aureus* stimulates osteoclastogenesis: possible role in *S. aureus*-induced bone pathology. *British journal of rheumatology* **37**:1095-1101.
30. **Miyaura, C., M. Inada, C. Matsumoto, T. Ohshiba, N. Uozumi, T. Shimizu, and A. Ito.** 2003. An essential role of cytosolic phospholipase A2alpha in prostaglandin E2-mediated bone resorption associated with inflammation. *J Exp Med* **197**:1303-1310.
31. **Montonen, M., T. F. Li, P. L. Lukinmaa, E. Sakai, M. Hukkanen, A. Sukura, and Y. T. Konttinen.** 2006. RANKL and cathepsin K in diffuse sclerosing osteomyelitis of the mandible. *J Oral Pathol Med* **35**:620-625.
32. **Murakami, M., H. Naraba, T. Tanioka, N. Semmyo, Y. Nakatani, F. Kojima, T. Ikeda, M. Fueki, A. Ueno, S. Oh, and I. Kudo.** 2000. Regulation of prostaglandin E2 biosynthesis by inducible membrane-associated prostaglandin E2 synthase that acts in concert with cyclooxygenase-2. *J Biol Chem* **275**:32783-32792.
33. **Nakagawa, N., M. Kinosaki, K. Yamaguchi, N. Shima, H. Yasuda, K. Yano, T. Morinaga, and K. Higashio.** 1998. RANK is the essential signaling receptor for osteoclast differentiation factor in osteoclastogenesis. *Biochem Biophys Res Commun* **253**:395-400.
34. **Okahashi, N., A. Sakurai, I. Nakagawa, T. Fujiwara, S. Kawabata, A. Amano, and S. Hamada.** 2003. Infection by *Streptococcus pyogenes* induces the receptor activator of NF-kappaB ligand expression in mouse osteoblastic cells. *Infect Immun* **71**:948-955.
35. **Raisz, L. G., J. Y. Vanderhoek, H. A. Simmons, B. E. Kream, and K. C. Nicolaou.** 1979. Prostaglandin synthesis by fetal rat bone in vitro: evidence for a role of prostacyclin. *Prostaglandins* **17**:905-914.
36. **Ramp, W. K., R. M. Dillaman, L. G. Lenz, D. M. Gay, R. D. Roer, and T. A. Ballard.** 1991. A serum substitute promotes osteoblast-like phenotypic expression in cultured cells from chick calvariae. *Bone Miner* **15**:1-17.

37. **Ramp, W. K., L. G. Lenz, and K. K. Kaysinger.** 1994. Medium pH modulates matrix, mineral, and energy metabolism in cultured chick bones and osteoblast-like cells. *Bone Miner* **24**:59-73.
38. **Ross, F. P.** 2000. RANKing the importance of measles virus in Paget's disease. *J Clin Invest* **105**:555-558.
39. **Sato, K., Y. Fujii, K. Kasono, M. Saji, T. Tsushima, and K. Shizume.** 1986. Stimulation of prostaglandin E2 and bone resorption by recombinant human interleukin 1 alpha in fetal mouse bones. *Biochem Biophys Res Commun* **138**:618-624.
40. **Sax, H., and D. Lew.** 1999. Osteomyelitis. *Curr Infect Dis Rep* **1**:261-266.
41. **Sharp, J. D., D. L. White, X. G. Chiou, T. Goodson, G. C. Gamboa, D. McClure, S. Burgett, J. Hoskins, P. L. Skatrud, J. R. Sportsman, and et al.** 1991. Molecular cloning and expression of human Ca(2+)-sensitive cytosolic phospholipase A2. *J Biol Chem* **266**:14850-14853.
42. **Simonet, W. S., D. L. Lacey, C. R. Dunstan, M. Kelley, M. S. Chang, R. Luthy, H. Q. Nguyen, S. Wooden, L. Bennett, T. Boone, G. Shimamoto, M. DeRose, R. Elliott, A. Colombero, H. L. Tan, G. Trail, J. Sullivan, E. Davy, N. Bucay, L. Renshaw-Gegg, T. M. Hughes, D. Hill, W. Pattison, P. Campbell, S. Sander, G. Van, J. Tarpley, P. Derby, R. Lee, and W. J. Boyle.** 1997. Osteoprotegerin: a novel secreted protein involved in the regulation of bone density. *Cell* **89**:309-319.
43. **Smith, W. L., R. M. Garavito, and D. L. DeWitt.** 1996. Prostaglandin endoperoxide H synthases (cyclooxygenases)-1 and -2. *J Biol Chem* **271**:33157-33160.
44. **Suda, K., N. Udagawa, N. Sato, M. Takami, K. Itoh, J. T. Woo, N. Takahashi, and K. Nagai.** 2004. Suppression of osteoprotegerin expression by prostaglandin E2 is crucially involved in lipopolysaccharide-induced osteoclast formation. *J Immunol* **172**:2504-2510.
45. **Suda, T., N. Takahashi, N. Udagawa, E. Jimi, M. T. Gillespie, and T. J. Martin.** 1999. Modulation of osteoclast differentiation and function by the new members of the tumor necrosis factor receptor and ligand families. *Endocr Rev* **20**:345-357.
46. **Suzawa, T., C. Miyaara, M. Inada, T. Maruyama, Y. Sugimoto, F. Ushikubi, A. Ichikawa, S. Narumiya, and T. Suda.** 2000. The role of prostaglandin E receptor subtypes (EP1, EP2, EP3, and EP4) in bone resorption: an analysis using specific agonists for the respective EPs. *Endocrinology* **141**:1554-1559.

47. **Tai, H., C. Miyaara, C. C. Pilbeam, T. Tamura, Y. Ohsugi, Y. Koishihara, N. Kubodera, H. Kawaguchi, L. G. Raisz, and T. Suda.** 1997. Transcriptional induction of cyclooxygenase-2 in osteoblasts is involved in interleukin-6-induced osteoclast formation. *Endocrinology* **138**:2372-2379.
48. **Takayanagi, H., K. Ogasawara, S. Hida, T. Chiba, S. Murata, K. Sato, A. Takaoka, T. Yokochi, H. Oda, K. Tanaka, K. Nakamura, and T. Taniguchi.** 2000. T-cell-mediated regulation of osteoclastogenesis by signalling cross-talk between RANKL and IFN-gamma. *Nature* **408**:600-605.
49. **Tanioka, T., Y. Nakatani, N. Semmyo, M. Murakami, and I. Kudo.** 2000. Molecular identification of cytosolic prostaglandin E2 synthase that is functionally coupled with cyclooxygenase-1 in immediate prostaglandin E2 biosynthesis. *J Biol Chem* **275**:32775-32782.
50. **Tintut, Y., F. Parhami, A. Tsingotjidou, S. Tetradis, M. Territo, and L. L. Demer.** 2002. 8-Isoprostaglandin E2 enhances receptor-activated NFkappa B ligand (RANKL)-dependent osteoclastic potential of marrow hematopoietic precursors via the cAMP pathway. *J Biol Chem* **277**:14221-14226.
51. **Tomita, M., X. Li, Y. Okada, F. N. Woodiel, R. N. Young, C. C. Pilbeam, and L. G. Raisz.** 2002. Effects of selective prostaglandin EP4 receptor antagonist on osteoclast formation and bone resorption in vitro. *Bone* **30**:159-163.
52. **Wada, T., T. Nakashima, N. Hiroshi, and J. M. Penninger.** 2006. RANKL-RANK signaling in osteoclastogenesis and bone disease. *Trends in molecular medicine* **12**:17-25.
53. **Walsh, M. C., and Y. Choi.** 2003. Biology of the TRANCE axis. *Cytokine Growth Factor Rev* **14**:251-263.
54. **Wani, M. R., K. Fuller, N. S. Kim, Y. Choi, and T. Chambers.** 1999. Prostaglandin E2 cooperates with TRANCE in osteoclast induction from hemopoietic precursors: synergistic activation of differentiation, cell spreading, and fusion. *Endocrinology* **140**:1927-1935.
55. **Wong, B. R., R. Josien, S. Y. Lee, M. Vologodskaya, R. M. Steinman, and Y. Choi.** 1998. The TRAF family of signal transducers mediates NF-kappaB activation by the TRANCE receptor. *J Biol Chem* **273**:28355-28359.
56. **Yasuda, H., N. Shima, N. Nakagawa, K. Yamaguchi, M. Kinosaki, S. Mochizuki, A. Tomoyasu, K. Yano, M. Goto, A. Murakami, E. Tsuda, T. Morinaga, K. Higashio, N. Udagawa, N. Takahashi, and T. Suda.** 1998. Osteoclast differentiation factor is a ligand for osteoprotegerin/osteoclastogenesis-inhibitory factor and is identical to TRANCE/RANKL. *Proc Natl Acad Sci U S A* **95**:3597-3602.

57. **Yongchaitrakul, T., K. Lertsirirangson, and P. Pavasant.** 2006. Human periodontal ligament cells secrete macrophage colony-stimulating factor in response to tumor necrosis factor-alpha in vitro. *J Periodontol* **77**:955-962.

PROJECT II:

1. **Alexander, E. H., F. A. Rivera, I. Marriott, J. Anguita, K. L. Bost, and M. C. Hudson.** 2003. Staphylococcus aureus - induced tumor necrosis factor - related apoptosis - inducing ligand expression mediates apoptosis and caspase-8 activation in infected osteoblasts. *BMC microbiology* **3**:5.
2. **Alexis, F., E. Pridgen, L. K. Molnar, and O. C. Farokhzad.** 2008. Factors affecting the clearance and biodistribution of polymeric nanoparticles. *Molecular pharmaceutics* **5**:505-515.
3. **Astete, C. E., and C. M. Sabliov.** 2006. Synthesis and characterization of PLGA nanoparticles. *Journal of biomaterials science* **17**:247-289.
4. **Bruchez, M. P.** 2005. Turning all the lights on: quantum dots in cellular assays. *Current opinion in chemical biology* **9**:533-537.
5. **Burton, K. W., M. Shameem, B. C. Thanoo, and P. P. DeLuca.** 2000. Extended release peptide delivery systems through the use of PLGA microsphere combinations. *Journal of biomaterials science* **11**:715-729.
6. **Calhoun, J. H., and J. T. Mader.** 1997. Treatment of osteomyelitis with a biodegradable antibiotic implant. *Clinical orthopaedics and related research*:206-214.
7. **Darouiche, R. O., and R. J. Hamill.** 1994. Antibiotic penetration of and bactericidal activity within endothelial cells. *Antimicrobial agents and chemotherapy* **38**:1059-1064.
8. **Ellington, J. K., M. Harris, L. Webb, B. Smith, T. Smith, K. Tan, and M. Hudson.** 2003. Intracellular Staphylococcus aureus. A mechanism for the indolence of osteomyelitis. *The Journal of bone and joint surgery* **85**:918-921.
9. **Ellington, J. K., S. S. Reilly, W. K. Ramp, M. S. Smeltzer, J. F. Kellam, and M. C. Hudson.** 1999. Mechanisms of Staphylococcus aureus invasion of cultured osteoblasts. *Microbial pathogenesis* **26**:317-323.
10. **Frank, A., S. Kumar Rath, F. Boey, and S. Venkatraman.** 2004. Study of the initial stages of drug release from a degradable matrix of poly(d,l-lactide-co-glycolide). *Biomaterials* **25**:813-821.

11. **Fukuzaki, H., M. Yoshida, M. Asano, M. Kumakura, T. Mashimo, H. Yuasa, K. Imai, and H. Yamanaka.** 1990. In vivo characteristics of low molecular weight copolymers composed of L-lactic acid and various DL-hydroxy acids as biodegradable carriers for drug delivery systems. *Biomaterials* **11**:441-446.
12. **Gonsalves, K. E., S. Jin, and M. I. Baraton.** 1998. Synthesis and surface characterization of functionalized polylactide copolymer microparticles. *Biomaterials* **19**:1501-1505.
13. **Gulyaeva, N., A. Zaslavsky, P. Lechner, A. Chait, and B. Zaslavsky.** 2000. Relative hydrophobicity of organic compounds measured by partitioning in aqueous two-phase systems. *Journal of chromatography* **743**:187-194.
14. **Hudson, M. C., W. K. Ramp, N. C. Nicholson, A. S. Williams, and M. T. Nousiainen.** 1995. Internalization of *Staphylococcus aureus* by cultured osteoblasts. *Microbial pathogenesis* **19**:409-419.
15. **Jaiswal, J., S. K. Gupta, and J. Kreuter.** 2004. Preparation of biodegradable cyclosporine nanoparticles by high-pressure emulsification-solvent evaporation process. *J Control Release* **96**:169-178.
16. **Jaiswal, J. K., H. Mattoussi, J. M. Mauro, and S. M. Simon.** 2003. Long-term multiple color imaging of live cells using quantum dot bioconjugates. *Nature biotechnology* **21**:47-51.
17. **Lamprecht, A., N. Ubrich, M. Hombreiro Perez, C. Lehr, M. Hoffman, and P. Maincent.** 1999. Biodegradable monodispersed nanoparticles prepared by pressure homogenization-emulsification. *International journal of pharmaceutics* **184**:97-105.
18. **Leroux, J. C., P. Gravel, L. Balant, B. Volet, B. M. Anner, E. Allemann, E. Doelker, and R. Gurny.** 1994. Internalization of poly(D,L-lactic acid) nanoparticles by isolated human leukocytes and analysis of plasma proteins adsorbed onto the particles. *J Biomed Mater Res* **28**:471-481.
19. **Lu, L., C. A. Garcia, and A. G. Mikos.** 1999. In vitro degradation of thin poly(DL-lactic-co-glycolic acid) films. *J Biomed Mater Res* **46**:236-244.
20. **Lucke, M., G. Schmidmaier, S. Sadoni, B. Wildemann, R. Schiller, A. Stemberger, N. P. Haas, and M. Raschke.** 2003. A new model of implant-related osteomyelitis in rats. *J Biomed Mater Res B Appl Biomater* **67**:593-602.
21. **Mandal, T. K., L. A. Bostanian, R. A. Graves, and S. R. Chapman.** 2002. Poly(D,L-lactide-co-glycolide) encapsulated poly(vinyl alcohol) hydrogel as a drug delivery system. *Pharmaceutical research* **19**:1713-1719.

22. **Markou, C. P., E. M. Lutostansky, D. N. Ku, and S. R. Hanson.** 1998. A novel method for efficient drug delivery. *Annals of biomedical engineering* **26**:502-511.
23. **Meghji, S., S. J. Crean, P. A. Hill, M. Sheikh, S. P. Nair, K. Heron, B. Henderson, E. B. Mawer, and M. Harris.** 1998. Surface-associated protein from *Staphylococcus aureus* stimulates osteoclastogenesis: possible role in *S. aureus*-induced bone pathology. *British journal of rheumatology* **37**:1095-1101.
24. **Meinel, L., O. E. Illi, J. Zapf, M. Malfanti, H. Peter Merkle, and B. Gander.** 2001. Stabilizing insulin-like growth factor-I in poly(D,L-lactide-co-glycolide) microspheres. *J Control Release* **70**:193-202.
25. **Nair, S., Y. Song, S. Meghji, K. Reddi, M. Harris, A. Ross, S. Poole, M. Wilson, and B. Henderson.** 1995. Surface-associated proteins from *Staphylococcus aureus* demonstrate potent bone resorbing activity. *J Bone Miner Res* **10**:726-734.
26. **Panyam, J., and V. Labhasetwar.** 2003. Biodegradable nanoparticles for drug and gene delivery to cells and tissue. *Advanced drug delivery reviews* **55**:329-347.
27. **Pillai, R. R., S. N. Somayaji, M. Rabinovich, M. C. Hudson, and K. E. Gonsalves.** 2008. Nafcillin-loaded PLGA nanoparticles for treatment of osteomyelitis. *Biomedical materials (Bristol, England)* **3**:034114.
28. **Qian, F., A. Szymanski, and J. Gao.** 2001. Fabrication and characterization of controlled release poly(D,L-lactide-co-glycolide) millirods. *J Biomed Mater Res* **55**:512-522.
29. **Rabinovich, M. M., S. N Somayaji, R. R. Pillai, M. C. Hudson, J. K. Ellington, M. Bosse, J. Horton, and K. E. Gonsalves.** 2007. Active Polymer Nanoparticles: Delivery of Antibiotics. *Mater. Res. Soc. Symp. Proc.* **1019**.
30. **Ramp, W. K., R. M. Dillaman, L. G. Lenz, D. M. Gay, R. D. Roer, and T. A. Ballard.** 1991. A serum substitute promotes osteoblast-like phenotypic expression in cultured cells from chick calvariae. *Bone and mineral* **15**:1-17.
31. **Ramp, W. K., L. G. Lenz, and K. K. Kaysinger.** 1994. Medium pH modulates matrix, mineral, and energy metabolism in cultured chick bones and osteoblast-like cells. *Bone Miner* **24**:59-73.
32. **Ravi Kumar, M. N., U. Bakowsky, and C. M. Lehr.** 2004. Preparation and characterization of cationic PLGA nanospheres as DNA carriers. *Biomaterials* **25**:1771-1777.

33. **Rosenthal, S. J., I. Tomlinson, E. M. Adkins, S. Schroeter, S. Adams, L. Swafford, J. McBride, Y. Wang, L. J. DeFelice, and R. D. Blakely.** 2002. Targeting cell surface receptors with ligand-conjugated nanocrystals. *Journal of the American Chemical Society* **124**:4586-4594.
34. **Siepmann, J., and A. Gopferich.** 2001. Mathematical modeling of bioerodible, polymeric drug delivery systems. *Advanced drug delivery reviews* **48**:229-247.
35. **Song, C., V. Labhasetwar, X. Cui, T. Underwood, and R. J. Levy.** 1998. Arterial uptake of biodegradable nanoparticles for intravascular local drug delivery: results with an acute dog model. *J Control Release* **54**:201-211.
36. **Soppimath, K. S., T. M. Aminabhavi, A. R. Kulkarni, and W. E. Rudzinski.** 2001. Biodegradable polymeric nanoparticles as drug delivery devices. *J Control Release* **70**:1-20.
37. **Tan, A. K., and A. L. Fink.** 1992. Identification of the site of covalent attachment of nafcillin, a reversible suicide inhibitor of beta-lactamase. *The Biochemical journal* **281** (Pt 1):191-196.
38. **Zweers, M. L., G. H. Engbers, D. W. Grijpma, and J. Feijen.** 2006. Release of anti-restenosis drugs from poly(ethylene oxide)-poly(DL-lactic-co-glycolic acid) nanoparticles. *J Control Release* **114**:317-324.

PROJECT III:

1. **Abe, T., S. Nomura, R. Nakagawa, M. Fujimoto, I. Kawase, and T. Naka.** 2006. Osteoblast differentiation is impaired in SOCS-1-deficient mice. *J Bone Miner Metab* **24**:283-290.
2. **Anselme, K.** 2000. Osteoblast adhesion on biomaterials. *Biomaterials* **21**:667-681.
3. **Bellows, C. G., J. E. Aubin, and J. N. Heersche.** 1991. Initiation and progression of mineralization of bone nodules formed in vitro: the role of alkaline phosphatase and organic phosphate. *Bone Miner* **14**:27-40.
4. **Bost, K. L., J. L. Bento, J. K. Ellington, I. Marriott, and M. C. Hudson.** 2000. Induction of colony-stimulating factor expression following *Staphylococcus* or *Salmonella* interaction with mouse or human osteoblasts. *Infection and immunity* **68**:5075-5083.
5. **Bost, K. L., J. L. Bento, C. C. Petty, L. W. Schrum, M. C. Hudson, and I. Marriott.** 2001. Monocyte chemoattractant protein-1 expression by osteoblasts following infection with *Staphylococcus aureus* or *Salmonella*. *J Interferon Cytokine Res* **21**:297-304.

6. **Bost, K. L., W. K. Ramp, N. C. Nicholson, J. L. Bento, I. Marriott, and M. C. Hudson.** 1999. Staphylococcus aureus infection of mouse or human osteoblasts induces high levels of interleukin-6 and interleukin-12 production. *The Journal of infectious diseases* **180**:1912-1920.
7. **Bowers, K. T., J. C. Keller, B. A. Randolph, D. G. Wick, and C. M. Michaels.** 1992. Optimization of surface micromorphology for enhanced osteoblast responses in vitro. *The International journal of oral & maxillofacial implants* **7**:302-310.
8. **Boyan, B. D., L. F. Bonewald, E. P. Paschalis, C. H. Lohmann, J. Rosser, D. L. Cochran, D. D. Dean, Z. Schwartz, and A. L. Boskey.** 2002. Osteoblast-mediated mineral deposition in culture is dependent on surface microtopography. *Calcified tissue international* **71**:519-529.
9. **Boyan, B. D., T. W. Hummert, D. D. Dean, and Z. Schwartz.** 1996. Role of material surfaces in regulating bone and cartilage cell response. *Biomaterials* **17**:137-146.
10. **Dalton, B. A., M. Dziegielewski, G. Johnson, P. A. Underwood, and J. G. Steele.** 1996. Measurement of cell adhesion and migration using phosphor-screen autoradiography. *Biotechniques* **21**:298-303.
11. **Davies, J. E., B. Lowenberg, and A. Shiga.** 1990. The bone-titanium interface in vitro. *J Biomed Mater Res* **24**:1289-1306.
12. **Dee, K. C., D. C. Rueger, T. T. Andersen, and R. Bizios.** 1996. Conditions which promote mineralization at the bone-implant interface: a model in vitro study. *Biomaterials* **17**:209-215.
13. **Degasne, I., M. F. Basle, V. Demais, G. Hure, M. Lesourd, B. Grolleau, L. Mercier, and D. Chappard.** 1999. Effects of roughness, fibronectin and vitronectin on attachment, spreading, and proliferation of human osteoblast-like cells (Saos-2) on titanium surfaces. *Calcified tissue international* **64**:499-507.
14. **Ducy, P., R. Zhang, V. Geoffroy, A. L. Ridall, and G. Karsenty.** 1997. *Osf2/Cbfa1*: a transcriptional activator of osteoblast differentiation. *Cell* **89**:747-754.
15. **Dziewanowska, K., A. R. Carson, J. M. Patti, C. F. Deobald, K. W. Bayles, and G. A. Bohach.** 2000. Staphylococcal fibronectin binding protein interacts with heat shock protein 60 and integrins: role in internalization by epithelial cells. *Infection and immunity* **68**:6321-6328.

16. **Dziewanowska, K., J. M. Patti, C. F. Deobald, K. W. Bayles, W. R. Trumble, and G. A. Bohach.** 1999. Fibronectin binding protein and host cell tyrosine kinase are required for internalization of *Staphylococcus aureus* by epithelial cells. *Infection and immunity* **67**:4673-4678.
17. **Effah Kaufmann, E. A., P. Ducheyne, and I. M. Shapiro.** 2000. Evaluation of osteoblast response to porous bioactive glass (45S5) substrates by RT-PCR analysis. *Tissue engineering* **6**:19-28.
18. **Foppiano, S., S. J. Marshall, G. W. Marshall, E. Saiz, and A. P. Tomsia.** 2004. The influence of novel bioactive glasses on in vitro osteoblast behavior. *Journal of biomedical materials research* **71**:242-249.
19. **Galante, J. O., and J. Jacobs.** 1992. Clinical performances of ingrowth surfaces. *Clin Orthop Relat Res*:41-49.
20. **Gillaspy, A. F., S. G. Hickmon, R. A. Skinner, J. R. Thomas, C. L. Nelson, and M. S. Smeltzer.** 1995. Role of the accessory gene regulator (agr) in pathogenesis of staphylococcal osteomyelitis. *Infection and immunity* **63**:3373-3380.
21. **Gronthos, S., K. Stewart, S. E. Graves, S. Hay, and P. J. Simmons.** 1997. Integrin expression and function on human osteoblast-like cells. *J Bone Miner Res* **12**:1189-1197.
22. **Gross, M., S. E. Cramton, F. Gotz, and A. Peschel.** 2001. Key role of teichoic acid net charge in *Staphylococcus aureus* colonization of artificial surfaces. *Infection and immunity* **69**:3423-3426.
23. **Gumbiner, B. M.** 1996. Cell adhesion: the molecular basis of tissue architecture and morphogenesis. *Cell* **84**:345-357.
24. **Hallab, N. J., K. J. Bundy, K. O'Connor, R. L. Moses, and J. J. Jacobs.** 2001. Evaluation of metallic and polymeric biomaterial surface energy and surface roughness characteristics for directed cell adhesion. *Tissue engineering* **7**:55-71.
25. **Harris, L. G., and R. G. Richards.** 2004. *Staphylococcus aureus* adhesion to different treated titanium surfaces. *Journal of materials science* **15**:311-314.
26. **Harris, L. G., S. Tosatti, M. Wieland, M. Textor, and R. G. Richards.** 2004. *Staphylococcus aureus* adhesion to titanium oxide surfaces coated with non-functionalized and peptide-functionalized poly(L-lysine)-grafted-poly(ethylene glycol) copolymers. *Biomaterials* **25**:4135-4148.

27. **Hogt, A. H., J. Dankert, and J. Feijen.** 1985. Adhesion of *Staphylococcus epidermidis* and *Staphylococcus saprophyticus* to a hydrophobic biomaterial. *Journal of general microbiology* **131**:2485-2491.
28. **Hudson, M. C., W. K. Ramp, and K. P. Frankenburg.** 1999. *Staphylococcus aureus* adhesion to bone matrix and bone-associated biomaterials. *FEMS Microbiol Lett* **173**:279-284.
29. **Hudson, M. C., W. K. Ramp, N. C. Nicholson, A. S. Williams, and M. T. Nousiainen.** 1995. Internalization of *Staphylococcus aureus* by cultured osteoblasts. *Microbial pathogenesis* **19**:409-419.
30. **Kim, M. J., C. W. Kim, Y. J. Lim, and S. J. Heo.** 2006. Microrough titanium surface affects biologic response in MG63 osteoblast-like cells. *Journal of biomedical materials research* **79**:1023-1032.
31. **Kornu, R., W. J. Maloney, M. A. Kelly, and R. L. Smith.** 1996. Osteoblast adhesion to orthopaedic implant alloys: effects of cell adhesion molecules and diamond-like carbon coating. *J Orthop Res* **14**:871-877.
32. **LeBaron, R. G., and K. A. Athanasiou.** 2000. Extracellular matrix cell adhesion peptides: functional applications in orthopedic materials. *Tissue engineering* **6**:85-103.
33. **Lee, D. A., E. Assoku, and V. Doyle.** 1998. A specific quantitative assay for collagen synthesis by cells seeded in collagen-based biomaterials using sirius red F3B precipitation. *Journal of materials science* **9**:47-51.
34. **Long, M., and H. J. Rack.** 1998. Titanium alloys in total joint replacement--a materials science perspective. *Biomaterials* **19**:1621-1639.
35. **Lopez-Sastre, S., J. M. Gonzalo-Orden, J. A. Altonaga, J. R. Altonaga, and M. A. Orden.** 1998. Coating titanium implants with bioglass and with hydroxyapatite. A comparative study in sheep. *Int Orthop* **22**:380-383.
36. **Lowry, O. H., N. R. Roberts, M. L. Wu, W. S. Hixon, and E. J. Crawford.** 1954. The quantitative histochemistry of brain. II. Enzyme measurements. *The Journal of biological chemistry* **207**:19-37.
37. **Moursi, A. M., R. K. Globus, and C. H. Damsky.** 1997. Interactions between integrin receptors and fibronectin are required for calvarial osteoblast differentiation in vitro. *J Cell Sci* **110 (Pt 18)**:2187-2196.
38. **Papakyriacou, H., D. Vaz, A. Simor, M. Louie, and M. J. McGavin.** 2000. Molecular analysis of the accessory gene regulator (agr) locus and balance of

- virulence factor expression in epidemic methicillin-resistant *Staphylococcus aureus*. *The Journal of infectious diseases* **181**:990-1000.
39. **Prigodich, R. V., and M. R. Vesely.** 1997. Characterization of the complex between bovine osteocalcin and type I collagen. *Arch Biochem Biophys* **345**:339-341.
 40. **Puleo, D. A., L. A. Holleran, R. H. Doremus, and R. Bizios.** 1991. Osteoblast responses to orthopedic implant materials in vitro. *J Biomed Mater Res* **25**:711-723.
 41. **Puleo, D. A., and A. Nanci.** 1999. Understanding and controlling the bone-implant interface. *Biomaterials* **20**:2311-2321.
 42. **Ramp, W. K., R. M. Dillaman, L. G. Lenz, D. M. Gay, R. D. Roer, and T. A. Ballard.** 1991. A serum substitute promotes osteoblast-like phenotypic expression in cultured cells from chick calvariae. *Bone Miner* **15**:1-17.
 43. **Ramp, W. K., L. G. Lenz, and K. K. Kaysinger.** 1994. Medium pH modulates matrix, mineral, and energy metabolism in cultured chick bones and osteoblast-like cells. *Bone Miner* **24**:59-73.
 44. **Saldana, L., J. L. Gonzalez-Carrasco, M. Rodriguez, L. Munuera, and N. Vilaboa.** 2006. Osteoblast response to plasma-spray porous Ti6Al4V coating on substrates of identical alloy. *Journal of biomedical materials research* **77**:608-617.
 45. **Schneider, G. B., H. Perinpanayagam, M. Clegg, R. Zaharias, D. Seabold, J. Keller, and C. Stanford.** 2003. Implant surface roughness affects osteoblast gene expression. *Journal of dental research* **82**:372-376.
 46. **Schneider, G. B., R. Zaharias, D. Seabold, J. Keller, and C. Stanford.** 2004. Differentiation of preosteoblasts is affected by implant surface microtopographies. *Journal of biomedical materials research* **69**:462-468.
 47. **Schneider, G. B., R. Zaharias, and C. Stanford.** 2001. Osteoblast integrin adhesion and signaling regulate mineralization. *Journal of dental research* **80**:1540-1544.
 48. **Shakoori, A. R., A. M. Oberdorf, T. A. Owen, L. A. Weber, E. Hickey, J. L. Stein, J. B. Lian, and G. S. Stein.** 1992. Expression of heat shock genes during differentiation of mammalian osteoblasts and promyelocytic leukemia cells. *J Cell Biochem* **48**:277-287.
 49. **Sheng, M. H., K. H. Lau, S. Mohan, D. J. Baylink, and J. E. Wergedal.** 2006. High osteoblastic activity in C3H/HeJ mice compared to C57BL/6J mice is

associated with low apoptosis in C3H/HeJ osteoblasts. *Calcified tissue international* **78**:293-301.

50. **Stein, G. S., J. B. Lian, and T. A. Owen.** 1990. Relationship of cell growth to the regulation of tissue-specific gene expression during osteoblast differentiation. *Faseb J* **4**:3111-3123.
51. **Tullberg-Reinert, H., and G. Jundt.** 1999. In situ measurement of collagen synthesis by human bone cells with a sirius red-based colorimetric microassay: effects of transforming growth factor beta2 and ascorbic acid 2-phosphate. *Histochemistry and cell biology* **112**:271-276.
52. **Vaudaux, P., R. Suzuki, F. A. Waldvogel, J. J. Morgenthaler, and U. E. Nydegger.** 1984. Foreign body infection: role of fibronectin as a ligand for the adherence of *Staphylococcus aureus*. *The Journal of infectious diseases* **150**:546-553.
53. **Wenstrup, R. J., J. L. Fowlkes, D. P. Witte, and J. B. Florer.** 1996. Discordant expression of osteoblast markers in MC3T3-E1 cells that synthesize a high turnover matrix. *The Journal of biological chemistry* **271**:10271-10276.
54. **Wong, M., J. Eulenberger, R. Schenk, and E. Hunziker.** 1995. Effect of surface topology on the osseointegration of implant materials in trabecular bone. *J Biomed Mater Res* **29**:1567-1575.
55. **Xiao, G., D. Wang, M. D. Benson, G. Karsenty, and R. T. Franceschi.** 1998. Role of the alpha2-integrin in osteoblast-specific gene expression and activation of the Osf2 transcription factor. *The Journal of biological chemistry* **273**:32988-32994.
56. **Zhao, G., Z. Schwartz, M. Wieland, F. Rupp, J. Geis-Gerstorfer, D. L. Cochran, and B. D. Boyan.** 2005. High surface energy enhances cell response to titanium substrate microstructure. *Journal of biomedical materials research* **74**:49-58.

PROJECT IV:

1. **Albrektsson, T., P. I. Branemark, H. A. Hansson, and J. Lindstrom.** 1981. Osseointegrated titanium implants. Requirements for ensuring a long-lasting, direct bone-to-implant anchorage in man. *Acta orthopaedica Scandinavica* **52**:155-170.
2. **Amsel, S., A. Maniatis, M. Tavassoli, and W. H. Crosby.** 1969. The significance of intramedullary cancellous bone formation in the repair of bone marrow tissue. *The Anatomical record* **164**:101-111.

3. **Anselme, K.** 2000. Osteoblast adhesion on biomaterials. *Biomaterials* **21**:667-681.
4. **Bab, I. A.** 1995. Postablation bone marrow regeneration: an in vivo model to study differential regulation of bone formation and resorption. *Bone* **17**:437S-441S.
5. **Bauer, T. W., and J. Schils.** 1999. The pathology of total joint arthroplasty.II. Mechanisms of implant failure. *Skeletal radiology* **28**:483-497.
6. **Bloebaum, R. D., D. Beeks, L. D. Dorr, C. G. Savory, J. A. DuPont, and A. A. Hofmann.** 1994. Complications with hydroxyapatite particulate separation in total hip arthroplasty. *Clinical orthopaedics and related research*:19-26.
7. **Bost, K. L., J. L. Bento, J. K. Ellington, I. Marriott, and M. C. Hudson.** 2000. Induction of colony-stimulating factor expression following Staphylococcus or Salmonella interaction with mouse or human osteoblasts. *Infection and immunity* **68**:5075-5083.
8. **Bost, K. L., J. L. Bento, C. C. Petty, L. W. Schrum, M. C. Hudson, and I. Marriott.** 2001. Monocyte chemoattractant protein-1 expression by osteoblasts following infection with Staphylococcus aureus or Salmonella. *J Interferon Cytokine Res* **21**:297-304.
9. **Bost, K. L., W. K. Ramp, N. C. Nicholson, J. L. Bento, I. Marriott, and M. C. Hudson.** 1999. Staphylococcus aureus infection of mouse or human osteoblasts induces high levels of interleukin-6 and interleukin-12 production. *The Journal of infectious diseases* **180**:1912-1920.
10. **Boyan, B. D., T. W. Hummert, D. D. Dean, and Z. Schwartz.** 1996. Role of material surfaces in regulating bone and cartilage cell response. *Biomaterials* **17**:137-146.
11. **Colnot, C., D. M. Romero, S. Huang, J. Rahman, J. A. Currey, A. Nanci, J. B. Brunski, and J. A. Helms.** 2007. Molecular analysis of healing at a bone-implant interface. *Journal of dental research* **86**:862-867.
12. **Cook, S. D., K. A. Thomas, J. F. Kay, and M. Jarcho.** 1988. Hydroxyapatite-coated porous titanium for use as an orthopedic biologic attachment system. *Clinical orthopaedics and related research*:303-312.
13. **Dayer, R., I. Badoud, R. Rizzoli, and P. Ammann.** 2007. Defective implant osseointegration under protein undernutrition: prevention by PTH or pamidronate. *J Bone Miner Res* **22**:1526-1533.

14. **De Ranieri, A., A. S. Viridi, S. Kuroda, S. Shott, R. M. Leven, N. J. Hallab, and D. R. Sumner.** 2005. Local application of rhTGF-beta2 enhances peri-implant bone volume and bone-implant contact in a rat model. *Bone* **37**:55-62.
15. **Dziewanowska, K., A. R. Carson, J. M. Patti, C. F. Deobald, K. W. Bayles, and G. A. Bohach.** 2000. Staphylococcal fibronectin binding protein interacts with heat shock protein 60 and integrins: role in internalization by epithelial cells. *Infection and immunity* **68**:6321-6328.
16. **Dziewanowska, K., J. M. Patti, C. F. Deobald, K. W. Bayles, W. R. Trumble, and G. A. Bohach.** 1999. Fibronectin binding protein and host cell tyrosine kinase are required for internalization of *Staphylococcus aureus* by epithelial cells. *Infection and immunity* **67**:4673-4678.
17. **Ferris, D. M., G. D. Moodie, P. M. Dimond, C. W. Gioranni, M. G. Ehrlich, and R. F. Valentini.** 1999. RGD-coated titanium implants stimulate increased bone formation in vivo. *Biomaterials* **20**:2323-2331.
18. **Gillaspy, A. F., S. G. Hickmon, R. A. Skinner, J. R. Thomas, C. L. Nelson, and M. S. Smeltzer.** 1995. Role of the accessory gene regulator (agr) in pathogenesis of staphylococcal osteomyelitis. *Infection and immunity* **63**:3373-3380.
19. **Gruber, H. E.** 1992. Adaptations of Goldner's Masson trichrome stain for the study of undecalcified plastic embedded bone. *Biotech Histochem* **67**:30-34.
20. **Gruber, H. E.** 1993. In vitro tetracycline labelling and bone cell survival in human trabecular bone explants. *Bone* **14**:531-535.
21. **Gruber, H. E., J. L. Ivey, E. R. Thompson, C. H. Chesnut, 3rd, and D. J. Baylink.** 1986. Osteoblast and osteoclast cell number and cell activity in postmenopausal osteoporosis. *Mineral and electrolyte metabolism* **12**:246-254.
22. **Gruber, H. E., G. J. Marshall, L. M. Nolasco, M. E. Kirchen, and D. L. Rimoim.** 1988. Alkaline and acid phosphatase demonstration in human bone and cartilage: effects of fixation interval and methacrylate embedments. *Stain technology* **63**:299-306.
23. **Harris, L. G., and R. G. Richards.** 2004. *Staphylococcus aureus* adhesion to different treated titanium surfaces. *Journal of materials science* **15**:311-314.
24. **Harris, L. G., S. Tosatti, M. Wieland, M. Textor, and R. G. Richards.** 2004. *Staphylococcus aureus* adhesion to titanium oxide surfaces coated with non-functionalized and peptide-functionalized poly(L-lysine)-grafted-poly(ethylene glycol) copolymers. *Biomaterials* **25**:4135-4148.

25. **Hudson, M. C., W. K. Ramp, and K. P. Frankenburg.** 1999. Staphylococcus aureus adhesion to bone matrix and bone-associated biomaterials. *FEMS Microbiol Lett* **173**:279-284.
26. **Hudson, M. C., W. K. Ramp, N. C. Nicholson, A. S. Williams, and M. T. Nousiainen.** 1995. Internalization of Staphylococcus aureus by cultured osteoblasts. *Microb Pathog* **19**:409-419.
27. **Ishizaka, M., T. Tanizawa, M. Sofue, Y. Dohmae, N. Endo, and H. E. Takahashi.** 1996. Bone particles disturb new bone formation on the interface of the titanium implant after reaming of the marrow cavity. *Bone* **19**:589-594.
28. **Jansen, J. A., W. J. Dhert, J. P. van der Waerden, and A. F. von Recum.** 1994. Semi-quantitative and qualitative histologic analysis method for the evaluation of implant biocompatibility. *J Invest Surg* **7**:123-134.
29. **Kimmel, D.** 1991. Quantitative histologic changes in the proximal tibial growth cartilage of aged female rats. *Cells and Materials Supplement* **1**:11-18.
30. **Klokkevold, P. R., R. D. Nishimura, M. Adachi, and A. Caputo.** 1997. Osseointegration enhanced by chemical etching of the titanium surface. A torque removal study in the rabbit. *Clinical oral implants research* **8**:442-447.
31. **Lautenschlager, E. P., and P. Monaghan.** 1993. Titanium and titanium alloys as dental materials. *International dental journal* **43**:245-253.
32. **LeGeros, R. Z., and R. G. Craig.** 1993. Strategies to affect bone remodeling: osteointegration. *J Bone Miner Res* **8 Suppl 2**:S583-596.
33. **Linder, L., T. Albrektsson, P. I. Branemark, H. A. Hansson, B. Ivarsson, U. Jonsson, and I. Lundstrom.** 1983. Electron microscopic analysis of the bone-titanium interface. *Acta orthopaedica Scandinavica* **54**:45-52.
34. **O'Toole, G. C., E. Salih, C. Gallagher, D. FitzPatrick, N. O'Higgins, and S. K. O'Rourke.** 2004. Bone sialoprotein-coated femoral implants are osteoinductive but mechanically compromised. *J Orthop Res* **22**:641-646.
35. **Opperman, L. A.** 2000. Cranial sutures as intramembranous bone growth sites. *Dev Dyn* **219**:472-485.
36. **Papakyriacou, H., D. Vaz, A. Simor, M. Louie, and M. J. McGavin.** 2000. Molecular analysis of the accessory gene regulator (agr) locus and balance of virulence factor expression in epidemic methicillin-resistant Staphylococcus aureus. *The Journal of infectious diseases* **181**:990-1000.

37. **Shakoori, A. R., A. M. Oberdorf, T. A. Owen, L. A. Weber, E. Hickey, J. L. Stein, J. B. Lian, and G. S. Stein.** 1992. Expression of heat shock genes during differentiation of mammalian osteoblasts and promyelocytic leukemia cells. *J Cell Biochem* **48**:277-287.
38. **Spurr, A. R.** 1969. A low-viscosity epoxy resin embedding medium for electron microscopy. *Journal of ultrastructure research* **26**:31-43.
39. **Stein, G. S., J. B. Lian, and T. A. Owen.** 1990. Relationship of cell growth to the regulation of tissue-specific gene expression during osteoblast differentiation. *Faseb J* **4**:3111-3123.
40. **Sumner, D. R., T. M. Turner, R. M. Urban, A. S. Viridi, and N. Inoue.** 2006. Additive enhancement of implant fixation following combined treatment with rhTGF-beta2 and rhBMP-2 in a canine model. *The Journal of bone and joint surgery* **88**:806-817.
41. **Sykaras, N., A. M. Iacopino, V. A. Marker, R. G. Triplett, and R. D. Woody.** 2000. Implant materials, designs, and surface topographies: their effect on osseointegration. A literature review. *The International journal of oral & maxillofacial implants* **15**:675-690.
42. **Urist, M. R.** 1965. Bone: formation by autoinduction. *Science (New York, N.Y)* **150**:893-899.
43. **Vaudaux, P., R. Suzuki, F. A. Waldvogel, J. J. Morgenthaler, and U. E. Nydegger.** 1984. Foreign body infection: role of fibronectin as a ligand for the adherence of *Staphylococcus aureus*. *The Journal of infectious diseases* **150**:546-553.
44. **Wennerberg, A., T. Albrektsson, and B. Andersson.** 1993. Design and surface characteristics of 13 commercially available oral implant systems. *The International journal of oral & maxillofacial implants* **8**:622-633.
45. **Wong, M., J. Eulenberger, R. Schenk, and E. Hunziker.** 1995. Effect of surface topology on the osseointegration of implant materials in trabecular bone. *Journal of biomedical materials research* **29**:1567-1575.